Exploiting gene regulation as an approach to identify, analyze and utilize the biosynthetic pathways of the glycopeptide ristomycin A and the zincophore [*S,S*]-EDDS in *Amycolatopsis japonicum*

DISSERTATION

der Mathematisch-Naturwissenschaftlichen Fakultät
der Eberhard Karls Universität Tübingen
zur Erlangung des Grades eines
Doktors der Naturwissenschaften
(Dr. rer. nat.)

vorgelegt von
Marius Steffen Spohn
aus Tettnang

Tübingen
2015

Exploiting gene regulation as an approach to identify, analyze and utilize the biosynthetic pathways of the glycopeptide ristomycin A and the zincophore [*S,S*]-EDDS in *Amycolatopsis japonicum*

DISSERTATION

der Mathematisch-Naturwissenschaftlichen Fakultät
der Eberhard Karls Universität Tübingen
zur Erlangung des Grades eines
Doktors der Naturwissenschaften
(Dr. rer. nat.)

vorgelegt von
Marius Steffen Spohn
aus Tettnang

Tübingen
2015

Tag der mündlichen Qualifikation:	27.01.2016
Dekan:	Prof. Dr. Wolfgang Rosenstiel
1. Berichterstatter:	PD Dr. Evi Stegmann
2. Berichterstatter:	Prof. Dr. Karl Forchhammer
3. Berichterstatter:	Prof. Dr. Christian Hertweck

Erklärung

Ich erkläre hiermit, dass ich die zur Promotion eingereichte Arbeit selbständig verfasst, nur die angegebenen Quellen und Hilfsmittel benutzt und Stellen, die wörtlich oder inhaltlich nach den Werken anderer Autoren entnommen sind, als solche gekennzeichnet habe. Eine detaillierte Abgrenzung meiner eigenen Leistungen von den Beiträgen meiner Kooperationspartner habe ich im Anhang vorgenommen.

.....

Unterschrift

Tübingen, den 30.11.2015

Table of content

Zusammenfassung

Der mikrobielle Sekundärmetabolismus ist eine reichhaltige Quelle für Naturstoffe, von denen viele klinische beziehungsweise industrielle Anwendung gefunden haben. Die Gattung *Amycolatopsis* ist für die Synthese vieler Naturstoffe bekannt. Beispielsweise werden viele Glykopeptid-Antibiotika, wie das klinisch relevante Vancomycin oder das Balhimycin, von Stämmen dieser Gattung produziert. Im Gegensatz dazu wurde der Stamm *Amycolatopsis japonicum* nie als Produzent einer biologisch aktiven Substanz beschrieben. Dieser Stamm produziert jedoch unter Zinkmangelbedingungen das EDTA-Isomer Ethylendiamindisuccinat ([*S,S*]-EDDS). Diese zinkabhängige [*S,S*]-EDDS Produktion lässt darauf schließen, dass [*S,S*]-EDDS ein Zinkophor ist, das an der Zinkaufnahme beteiligt ist.

[*S,S*]-EDDS weist Komplexbildungseigenschaften auf, die mit denen von EDTA vergleichbar sind. Im Gegensatz zu EDTA ist [*S,S*]-EDDS jedoch biologisch abbaubar. Die weitverbreitete industrielle Anwendung von EDTA in Kombination mit dessen Unzugänglichkeit für biologische Abbauprozesse führt zu einer umweltgefährdenden EDTA-Persistenz in aquatischen Lebensräumen. Der Naturstoff [*S,S*]-EDDS ist deshalb ein nachhaltiger EDTA Ersatz mit einem verbesserten ökologischen Fingerabdruck.

In dieser Arbeit wurden zwei molekulargenetische Strategien entwickelt, um die Biosynthese des Glykopeptid-Antibiotikums Ristomycin A zu aktivieren und um die [*S,S*]-EDDS-Biosynthese-Gene in *A. japonicum* zu identifizieren.

Untersuchungen des genetischen Potenzials der Gattung *Amycolatopsis* ließen vermuten, dass auch *A. japonicum* die Fähigkeit besitzt, ein Glykopeptid-Antibiotikum zu synthetisieren. Um dieses nicht exprimierte, sogenannte „stille Gencluster“ zu aktivieren, wurde ein molekulargenetischer Ansatz verwendet, bei dem der Biosynthese-spezifische Aktivator Bbr heterolog in *A. japonicum* exprimiert wurde. Bbr reguliert die Balhimycin-Biosynthese in *Amycolatopsis balhimycina*. In *A. japonicum* induzierte dessen Expression die Produktion von Ristomycin A, was durch HPLC-DAD, MS, MS/MS, HR-MS, und NMR-Analysen bestätigt werden konnte. Ristomycin A ist ein vielfach glykosyliertes Heptapeptid, das als Hauptwirkstoff in Diagnoseverfahren zur Bestimmung von angeborenen und weitverbreiteten Blutgerinnungsstörungen verwendet wird. Die Sequenzierung des *A. japonicum* Genoms und dessen computergestützte Auswertung führten zur Identifizierung des Biosynthese-Genclusters, das für die Synthese von Ristomycin A verantwortlich ist.

Solche computergestützten Genomanalysen mittels verschiedenster bioinformatischen Plattformen werden heutzutage standardmäßig zur Identifizierung von Sekundärmetabolit-Gencluster angewandt, die bekannten Synthesemechanismen zugeordnet werden können. Allerdings konnten die [*S,S*]-EDDS-Biosynthese-Gene mit diesen Tools nicht entdeckt werden, was auf einen bislang nicht bekannten Biosynthesemechanismus hindeutet. Um diesen zu identifizieren, wurde ein neuer Ansatz entwickelt, der auf der Annahme beruht, dass die Zink-reprimierte [*S,S*]-EDDS-Biosynthese durch

einen Zink-sensitiven Regulator gewährleistet wird. Die bakterielle Zink-Homöostase wird meistens durch den globalen Zink-spezifische Transkriptionsregulator Zur reguliert. Das Zur Protein von *A. japonicum* wurde identifiziert und detailliert charakterisiert. Es konnten gezeigt werden, dass Zur_{Aj} die Transkription des hoch affinen Zinkaufnahmesystems $ZnuABC_{Aj}$ durch seine Zink-abhängige Bindung an spezifische DNA Bindesequenzen reguliert. Diese Zur-Bindesequenzen wurden verwendet, um das *A. japonicum* Genom nach weiteren, Zur_{Aj} regulierten, Genen zu durchsuchen. Dies führte zur Auffindung des *aesA-D* Operons. Umfangreiche Transkriptions-Untersuchungen ergaben, dass *aesA-D* Zink-abhängig von Zur_{Aj} reguliert wird. Die Beteiligung von *aesA-D* an der [*S,S*]-EDDS konnte durch Inaktivierungsversuche nachgewiesen werden. Zusätzlich führte die Deletion des Zinkregulators Zur_{Aj} (*A. japonicum* Δ*zur*) dazu, dass auch in Gegenwart von hohen Zink-Konzentrationen [*S,S*]-EDDS in hohen Mengen produziert wird.

A. japonicum Δ*zur* ist eine erfolgversprechende Ausgangsbasis, um einen nachhaltigen und wirtschaftlich verwertbaren [*S,S*]-EDDS Produktionsprozess zu entwickeln, der keiner Limitierung durch negative Einflüsse von Zink unterliegt.

Die Strategie, ein vorhergesagtes, stilles Gencluster durch die Expression eines spezifischen Regulators zu aktivieren, sowie auch die Strategie, neue Biosynthese-Gene durch die Charakterisierung eines globalen Regulators, der spezifische Umweltsignale wahrnimmt, zu identifizieren, ermöglichte die Charakterisierung neuer Naturstoffsynthesewege in *A. japonicum*. Beide Ansätze nutzen Erkenntnisse über regulatorische Mechanismen und besitzen das Potenzial zukünftig angewendet zu werden, um neue Naturstoffe und neue Synthesewege zu identifizieren.

Abstract

The microbial secondary metabolism is a rich source for valuable products that have found their way into various clinical and industrial applications. A particularly productive bacterial genus for the discovery of natural products is *Amycolatopsis*. The most frequently reported type of secondary metabolites produced by this genus are glycopeptide antibiotics like balhimycin or the medically relevant vancomycin. In contrast to most other members of the *Amycolatopsis* genus, *Amycolatopsis japonicum* was never described to produce any product with antibacterial activity. This strain however is known to synthesize the chelating agent ethylenediamine-disuccinate ([*S,S*]-EDDS), a biodegradable EDTA isomer in response to zinc deficiency. This zinc responsive repression of [*S,S*]-EDDS production indicates a possible contribution of [*S,S*]-EDDS to zinc uptake and that it might belong to the rarely described physiological group of zincophores. Combining excellent chelating properties with the accessibility to biodegradation, [*S,S*]-EDDS is considered as a sustainable chelating agent, possessing the potential to replace EDTA and other environmentally threatening chelating agents in various applications.

In this study, two distinct molecular genetic strategies were developed and implemented to activate the biosynthesis of the glycopeptide antibiotic ristomycin A and to identify the [*S,S*]-EDDS biosynthetic genes in *Amycolatopsis japonicum*.

Genetic evaluation of the *Amycolatopsis* antibiotic biosynthetic potential indicated that *A. japonicum* might has the capability to produce a glycopeptide antibiotic. Since the biosynthesis of the predicted glycopeptide was not detected by altering the culture conditions, a molecular genetic approach was employed to activate its production. Heterologous expression of the characterized pathway specific activator Bbr, naturally inducing the balhimycin biosynthesis in *A. balhimycina*, induced the synthesis of a bioactive substance in *A. japonicum*. The bioactivity could be assigned to the production of ristomycin A, a highly glycosylated peptide antibiotic which is used in diagnostic kits to detect widespread hereditary coagulation disorders. Full sequencing of the *A. japonicum* genome and its computational analysis led to the identification of the corresponding biosynthetic gene cluster which is directing the biosynthesis of ristomycin A.

Such computational genome analyses by various bioinformatic tools are nowadays standardized applied strategies to identify secondary metabolite gene clusters. These approaches however failed to detect the [*S,S*]-EDDS biosynthetic genes. This required the development of a new approach which relies on the assumption that the zinc repressed biosynthesis of [*S,S*]-EDDS is regulated by a zinc responsive regulatory element. Therefore, the major zinc responsive transcriptional regulator of *A. japonicum* (Zur) was characterized in detail. Zur regulates the expression of the high affinity zinc uptake system ZnuABC by binding to a specific DNA binding sequence. The screening of the *A. japonicum* genome for further Zur regulated genes by using this deduced Zur binding sequence led to

the identification of the operon *aesA-D*. Extensive transcriptional analyses and band shift assays revealed that *aesA-D* is zinc responsively regulated by Zur and involved in [*S,S*]-EDDS biosynthesis, as shown by inactivation studies. The [*S,S*]-EDDS biosynthesis was uncoupled from zinc repression by deleting *zur*. This mutant sets the stage to establish a sustainable [*S,S*]-EDDS production process without limits formerly imposed by zinc repression.

The strategy to awake predicted silent gene clusters by using a characterized regulator as well as the strategy to identify new biosynthetic genes by characterizing an environmental signal-sensing regulator enabled the isolation of novel biosynthetic pathways in *A. japonicum*. Both approaches follow the joint concept to exploit knowledge of regulatory pathways and have the prospect to be generally applicable in order to guide future detection of new natural products.

List of publications

Publication 1

Spohn, M., Kirchner, N., Kulik, A., Jochim, A., Wolf, F., Münzer, P., Borst, O., Gross, H., Wohlleben, W., and Stegmann, E. (2014) Overproduction of ristomycin A by activation of a silent gene cluster in *Amycolatopsis japonicum* MG417-CF17. *Antimicrobial Agents and Chemotherapy* **58**, 6185-6196.

Publication 2

Stegmann, E., Albersmeier, A., **Spohn, M.**, Gert, H., Weber, T., Wohlleben, W., Kalinowski, J., and Rückert, C. (2014) Complete genome sequence of the actinobacterium *Amycolatopsis japonica* MG417-CF17 (=DSM 44213T) producing (S,S)-N,N'-ethylenediaminedisuccinic acid. *Journal of Biotechnology* **189**C, 46-47.

Publication 3

Spohn, M., Wohlleben, W., and Stegmann, E. (2016) Elucidation of the zinc dependent regulation in *Amycolatopsis japonicum* enabled the identification of the ethylenediamine-disuccinate ([*S,S*]-EDDS) genes. *Environmental Microbiology* **18**, 1249-1263.

Contributions

In publication 1 (Spohn *et al.*, 2014), I overexpressed the proteins, performed transcriptional analysis and the fermentative production process. Also the analytical analyses by HPLC-DAD, MS and MS/MS were performed by me. Furthermore, I designed most of the experiments, analyzed and interpreted the data and wrote most of the manuscript. For the fermentation and the analytic I was assisted by A. Kulik. I supervised F. Wolf during his initial attempt to overexpress *bbr* and during the computational analysis of the gene cluster. A. Jochim cloned *ajrR* and overexpressed it under my supervision. N. Kirchner and H. Gross isolated ristomycin A from the culture broth and determined its structure by NMR, HR-MS and CD-spectroscopy. H. Gross also wrote the corresponding paragraph for the manuscript. P. Münzer and O. Borst performed the platelet aggregation assay and wrote the corresponding paragraph for the manuscript. E. Stegmann and W. Wohlleben supervised the project, took part in designing the experiments and revised the manuscript.

In publication 2 (Stegmann *et al.*, 2014), I contributed to manual gene annotation and performed the computational analysis of the *A. japonicum* potential to produce secondary metabolites. I also took part in editing the manuscript.

In publication 3 (Spohn *et al.*, 2016), all the experiments were designed and performed by me. I analyzed and interpreted the data and wrote the manuscript. E. Stegmann and W. Wohlleben supervised the project, took part in designing the experiments and revised the manuscript.

Abbreviations

A	Adenine
A.	*Amycolatopsis*
Ala	Alanine
B.	*Bacillus*
bp	Base pair
C.	*Corynebacterium*
Dae	1,2-diaminoethane
Dap	2,3-diaminopropionic acid
Dpg	3,5-dihydroxyphenylglycine
E.	*Escherichia*
G	Guanine
GUS	β-glucuronidase
Hpg	*p*-hydroxyphenylglycine
M.	*Mycobacterium*
NIS	Non-ribosomal peptide-synthetase idependent siderophore
NRPS	Non-ribosomal peptide-synthetase
PCR	Polymerase chain reaction
PKS	Polyketide synthase
S.	*Streptomyces*
S. aureus	*Staphylococcus aureus*
S. typhimurium	*Salmonella typhimurium*
SB	Staphyloferrin B
T	Thymine
UV	Ultraviolet
β-Ht	β-hydroxytyrosine

1. Introduction

1.1 The genus *Amycolatopsis*: a valuable source of secondary metabolites

Secondary metabolites are natural products which are considered to be not essential for vegetative growth, development or reproduction of an organism but rather function in increasing the evolutionary fitness and survivability under certain specialized growth conditions. Many microbial secondary metabolites either function as growth inhibitors, having antibacterial, antifungal or antiviral activity or, as growth promoters by e.g. enhancing the uptake of scarce nutrient sources. Natural compounds have the potential to be developed into drug substances which can be used as antiinfective or anticancer therapeutic agents for clinical application or for agricultural use as fungicides, insecticides, herbicides or fertilizers.

A known bacterial genus producing valuable compounds which already found medical application is the genus *Amycolatopsis*. The medically most relevant antibacterial agents are rifamycin, the lead drug of rifampicin, and vancomycin, a glycopeptide antibiotic. Members of this genus however are described to produce many further secondary metabolites of various structural classes, reflecting its particularly high potential as sources for valuable compounds.

The polyketide rifamycin was first identified as a product of *A. mediterranei* in 1959 (Sensi *et al.*, 1959). Its derivatives are important antibiotics for the treatment of infectious disease caused by *Mycobacterium tuberculosis*. Other *Amycolatopsis* polyketide synthase (PKS) derived antibiotics are chelocardin, produced by *A. sulphurea*, a broad-spectrum tetracyclic antibiotic exhibiting potent bacteriolytic activity (Lukezic *et al.*, 2013) and ECO-0501, a polyene which was identified in *A. orientalis* ATCC 43491 (Banskota *et al.*, 2006). ECO-0501 possesses strong activity against gram-positive bacteria, including methicillin-resistant *Staphylococcus aureus* (MRSA) and vancomycin-resistant enterococci (VRE).

The most frequently reported type of secondary metabolites produced by the genus *Amycolatopsis*, however, are glycopeptide antibiotics. In addition to the actually known glycopeptide producing *Amycolatopsis* species, PCR screening indicated the genetic potential of several further strains to also produce glycopeptides (Everest and Meyers, 2011). This biosynthetic potential however is not a common feature of the entire *Amycolatopsis* genus but rather of a certain phylogenetic clade.

Vancomycin, which was isolated from *A. orientalis* (Brigham and Pittenger, 1956) finds clinical application as antibiotic to treat severe infections with enterococci and MRSA strains. Besides vancomycin, several other glycopeptides were identified as *Amycolatopsis* products. Balhimycin and chloroeremomycin, isolated from *A. balhimycina* (Nadkarni *et al.*, 1994) and an *A. orientalis* strain (van Wageningen *et al.*, 1998), respectively share an identical heptapeptide backbone with vancomycin and differ only in the glycosylation pattern. *A. orientalis* CPCC200066 produces norvancomycin, whose chemical structure is almost the same as that of vancomycin, except for an

absent methyl group at the N-terminus (Lei *et al.*, 2015). Avoparcin is a product of *A. coloradensis* (Kunstmann *et al.*, 1968) and has been used as growth-promoting feed additive in agricultural applications (Labeda, 1995). This glycopeptide slightly differs from the vancomycin-like gylcopeptides in the composition of the heptapeptide backbone. Ristomycin A (also called ristocetin A), which is produced by *A. lurida* (Grundy *et al.*, 1956) causes thrombocytopenia and platelet agglutination and is therefore no longer used for the treatment of human staphylococcal infections. These therapeutically unfavorable functions however are nowadays exploited to detect widespread hereditary genetic disorders in coagulation such as the von Willebrand disease and the Bernard-Soulier syndrome by utilizing ristomycin A as an *in vitro* diagnosis compound (Sarji *et al.*, 1974).

To compete with other soil-dwelling microorganisms, *Amycolatopsis* strains do not only produce compounds with antimicrobial activity but also chelating compounds (ionophores) to monopolize scarce metal ion resources. To solubilize and to facilitate the uptake of iron under iron deficient growth conditions microbes secrete siderophores. Siderophores are small molecular weight compounds which exhibit high iron chelating affinity. Such secreted chelating agents are described from *Amycolatopsis* sp. AA4 (amychelin) (Seyedsayamdost *et al.*, 2011) and *A. alba* (albachelin) (Kodani *et al.*, 2015). Both structurally related molecules are composed of six siderophore characteristic amino acids, while amychelin is additionally decorated with a hydroxybenzoyl group. Other iron chelating agents are the siderochelins produced by *Amycolatopsis* sp. LZ149 (Liu *et al.*, 1981). The siderochelins which show anti-mycobacterial activities were isolated by a bioassay-guided fractionation. This activities however are rather due to their ion chelating properties than due to a direct target interaction in means of classical antimicrobial chemotherapy (Liu *et al.*, 1981; Lu *et al.*, 2015). A different kind of chelating agent is ethylenediamine-disuccinate (EDDS), which is synthesized by the strain *Amycolatopsis japonicum* MG417-CF17 in the [*S,S*]-configuration (Nishikiori *et al.*, 1984). [*S,S*]-EDDS production does not occur in response to iron deficiency but in response to zinc deficiency (Cebulla, 1995; Zwicker *et al.*, 1997). This indicates that the ionophore EDDS contributes to zinc uptake and that it belongs to the rarely described physiological group of the zincophores (Hantke, 2001a; Zhao *et al.*, 2012).

The broad variety of *Amycolatopsis* secondary metabolites with respect to physiological function as active defense or in competition for resources and with respect to biosynthesis and biochemistry described so far indicates the broad potential of this genus to synthesize valuable substances.

1.2 Glycopeptide antibiotics

The glycopeptide heptapeptide backbone is predominantly assembled by the nonproteinogenic aromatic amino acids 3,5-dihydroxyphenylglycine (Dpg), *p*-hydroxyphenylglycine (Hpg) and β-hydroxytyrosine (β-Ht). These aromatic amino acid side chains are oxidatively cross-linked with each

other to form a rigid cup shaped structure (Bischoff *et al.*, 2005) required for the interaction with their molecular target, the D-alanyl–D-alanine (D-Ala-D-Ala) terminus of bacterial cell wall precursors (Reynolds, 1989). This binding interferes with the bacterial cell wall biosynthesis and thus leads to cell death.

1.2.1 Structural categorization of glycopeptides

The structural diversity of glycopeptides arises from the variation of incorporated amino acids and from the variable decoration of the heptapeptide backbone by glycosylic moieties, methyl groups, chlorine atoms and fatty acid residues, respectively. Based on the incorporated amino acids, the level of side chain cross-linking and the decoration with a fatty acid residue, glycopeptides can be categorized into distinct classes. The type I glycopeptides are characterized by two aliphatic amino acids at position 1 and 3 of the heptapeptide backbone. This class comprises e.g. vancomycin, norvancomycin, balhimycin and chloroeremomycin. Avoparcin is exemplifying the type II glycopeptides with incorporated aromatic amino acids also at position 1 and 3. These amino acids however do not undergo an oxidative cross-linking in contrast to the type III glycopeptides, characterized by a fully cross-linked heptapeptide backbone. The model type III glycopeptide is the highly glycosylated ristomycin A.

The glycopeptide biosynthesis pathway follows three distinct steps: the precursor supply by specific biosynthesis pathways, the assembly of this specific building blocks and the final modification of the heptapeptide backbone by various tailoring reactions (Stegmann *et al.*, 2010).

1.2.2 Glycopeptide antibiotics biosynthesis: precursor supply

The nonproteinogenic aromatic amino acids which are incorporated into glycopetides have to be specifically supplied. All genes required for the synthesis of Dpg, Hpg and β-Ht are located within the corresponding gene clusters (Donadio *et al.*, 2005).

For the synthesis of Hpg and Dpg seven genes are required in total. Hpg derives from hydroxyphenylpyruvate, the direct precursor of tyrosine. Hydroxyphenylpyruvate is converted into the Hpg precursor *p*-hydroxyphenylglyoxylate by the enzymatic activities of a *p*-hydroxymandelate synthase and a *p*-hydroxymandelate oxidase (Hubbard *et al.*, 2000; Kastner *et al.*, 2012). Dpg is not derived from a proteinogenic amino acid but from four malonyl-CoA subunits and synthesized by a polyketide synthase mechanism (Pfeifer *et al.*, 2001). The concerted enzymatic catalysis of DpgA-D leads to the Dpg precursor 3,5-dihydroxyphenylglyoxylate. The transamination of both, *p*-hydroxyphenylglyoxylate and 3,5-dihydroxyphenylglyoxylate to yield the end products Hpg and Dpg is catalyzed by the same tyrosine dependent aminotransferase (Pfeifer *et al.*, 2001).

β-Ht is formed by the activity of three gene products, a nonribosomal peptide synthetase homologue, a P450 monooxygenase and a perhydrolase. The conversion of the precursor tyrosine to β-Ht is performed by loading tyrosine onto a peptide synthase module and its hydroxylation at the β-position by a P450 monooxygenase (Puk *et al.*, 2004). Finally, a perhydrolase catalyzes the release of β-Ht from the peptide synthase module by cleaving the thioester bond (Mulyani *et al.*, 2010). In the biosynthesis of lipoglycopeptides like dalbavancin and teicoplanin however, hydroxylation of tyrosine is catalyzed by a β-hydroxylase after its activation by the NRPS (Stinchi *et al.*, 2006).

Tyrosine and its precursor 4-hydroxyphenylpyruvate are required for the biosynthesis of Dpg, Hpg and β-Ht, either as direct precursor or as amino donor. The supply of tyrosine is therefore a rate controlling factor in glycopeptide biosynthesis. In order to ensure adequate precursor supply for glycopeptide production the corresponding gene clusters encode a prephenate dehydrogenase (Pdh) as a common feature and in many cases also a 3-deoxy-D-arabino-heptulosonate-7-phosphate (DAHP) synthase (Donadio *et al.*, 2005) as a specific metabolic adaptation to channel the metabolic flux in the direction of tyrosine. The DAHP synthase and the Pdh are key enzymes of the shikimate pathway, the metabolic pathway for the biosynthesis of aromatic compounds such as the amino acids phenylalanine, tyrosine, and tryptophan. The DAHP synthase is catalyzing the preliminary step of the shikimate pathway, the formation of DAHP by a condensation reaction of the pentose phosphate pathway intermediate D-erythrose 4-phosphate and the glycolytic pathway intermediate phosphoenolpyruvate. Further downstream in the shikimate pathway the Pdh directs the flux towards tyrosine at the branching point of tyrosine and phenylalanine by converting prephenate to 4-hydroxyphenylpyruvate (Stegmann *et al.*, 2010).

1.2.3 Glycopeptide antibiotics biosynthesis: assembly of the heptapeptide

The predominant composition of the heptapeptide from nonproteinogenic amino acids necessitates its assembly by nonribosomal peptide synthetases (NRPSs). NRPSs are multimodular enzymes with each module responsible for the recognition, incorporation and optionally for the epimerization of one specific amino acid into the assembling oligopeptide (Marahiel, 1997). Therefore, each module is organized by an adenylation (A) domain, responsible for substrate recognition and activation, a thiolation (T) domain, covalently binding the cognate amino acid and the nascent peptide via a thioesther bond and the condensation (C) domain, for catalyzing peptide bond formation. The optionally occurring epimerization (E) domain is required in modules converting L-amino acids into their D-forms. Several of these multimodular NRPSs are interacting as multienzyme complexes to assemble the heptapeptide backbone of glycopeptides. The last module in the assembly line is terminated by a thioestherase (TE) domain. The TE domain is hydrolyzing the thioester bond which links the mature heptapeptide to the NRPS.

The released heptapeptide is an aglycon with already oxidatively cross-linked amino acid side chains due to the activity of P450 monooxygenases whose substrates are not free biosynthetic precursors but rather NRPS bound intermediates (Stegmann *et al.*, 2010). Glycopeptide gene clusters encode three or four P450 monooxygenases in addition to the one required for β-Ht synthesis. Gene clusters containing only three *oxy* genes encode the synthesis of type I and type II glycopeptides which are characterized by two ether links (between amino acid 2-4 and 4-6) and one C-C link (between amino acid 5-7) (Stegmann *et al.*, 2006). Glycopeptides of the type III and IV however have a fully cyclized heptapeptide backbone due to the activity of a fourth P450 monooxygenases catalyzing the formation of an additional ether link between amino acid 1 and 3 of the heptapeptide (Hadatsch *et al.*, 2007).

1.2.4 Glycopeptide antibiotics biosynthesis: modification of the heptapeptide

All described glycopetides besides ristomycin A exhibit at least one chlorination. These chlorine atoms are attached by cluster encoded $FADH_2$-dependent halogenases (Puk *et al.*, 2002). It is assumed that the chlorination time point is most likely during heptapeptide synthesis, occurring at NRPS bound intermediates (Puk *et al.*, 2004). Further tailoring reactions occur at a late stage of glycopeptide biosynthesis at the free, already cross-linked and halogenated aglycon in the cytoplasm and comprise methylation and glycosylation. These reactions are catalyzed by a set of various methyl- and glycosyltransferases.

1.2.5 Transcriptional regulation of glycopeptide biosynthesis

Glycopeptide gene clusters contain enzymes required for the biosynthesis of the end product and its export, often genes conferring self-resistance to the producer strain and genes encoding regulatory functions. One mutual feature of all described glycopeptide gene cluster is the presence of a pathway-specific StrR-like transcriptional regulator (Donadio *et al.*, 2005). StrR was initially described in *Streptomyces griseus* (Retzlaff and Distler, 1995) and *Streptomyces glausescens* (Beyer *et al.*, 1996). StrR is an essential transcriptional activator for the streptomycin biosynthesis, required to activate the expression of all streptomycin biosynthetic genes but not for the expression of the gene conferring self-resistance (Tomono *et al.*, 2005). In the case of glycopeptide biosynthesis, it was shown that the StrR-like regulator Bbr of the balhimycin gene cluster is essential for glycopeptide production (Stegmann *et al.*, 2010). Specific Bbr binding to promoter regions of several biosynthetic genes within the balhimycin gene cluster initiates their transcription (Shawky *et al.*, 2007).

1.3 Ionophores: naturally occurring chelating agents

Bioavailability of iron is very low due to its predominant occurrence as ferric ions in aerobic environments, which form insoluble complexes that cannot be assimilated by microorganisms (Challis, 2005). The biosynthesis and excretion of siderophores is a common strategy to address this problem. Siderophores scavenge and solubilize ferric ions in order to enhance specific iron uptake. This functionally class of iron acquiring chelating compounds is widely described and a common feature of many microorganisms. However, chelating agents, which function in acquisition of transition metals other than iron, have been disregarded for long time. Examples described so far are e.g. the zincophore coelibactin from the actinomycete *Streptomyces coelicolor* (Kallifidas *et al.*, 2010) whose NRPS gene cluster is zinc responsively transcribed and chalkophores from methane oxidizing bacteria (Kim *et al.*, 2004) termed methanobactins which are uptaken as copper-loaded complex.

1.3.1 Siderophore biosynthesis

Most of the described ionophores can be classified into catecholates, hydroxamates or carboxylates according to the functional groups coordinating the binding of the metal ion. Catecholate ionophores contain a hydroxylated aryl moiety deriving from the 2,3-dihydroxybenzoic acid. Many ionophores are polypeptides that are synthesized by NRPS systems (Crosa and Walsh, 2002). Also most aryl group containing ionophores are NRPS assembled. An exemplary NRPS derived siderophore is the enterobactin (also called enterochelin) of various enterobacteriaceae like *Escherichia coli* (O'Brien and Gibson, 1970; Gehring *et al.*, 1998) or *Salmonella typhimurium* (Pollack and Neilands, 1970).
Several other bacterial ionophores however are no polypeptides, but instead assembled by alternating dicarboxylic acid and diamine or amino alcohol building blocks which nevertheless derive from amino acids (Challis, 2005). These kind of ionophores are usually synthesized by the second main pathways for siderophore biosynthesis, the NRPS-independent siderophore (NIS) pathway. This pathway depends on an adenylating enzyme family of synthetases (NIS synthetases) that characteristically mediate the formation of amide or ester bonds between a substrate amine and a carboxylic acid substrate (Oves-Costales *et al.*, 2009). Aerobactin is an example of a siderophore produced by the NRPS independent pathway (de Lorenzo and Neilands, 1986).

1.3.2 Metal responsive regulation of ionophore biosynthesis

An efficient uptake of iron and other metal ions is essential for all living cells. However, highly concentrated metal ions are toxic to cells by e.g. creating reactive oxygen species or inhibiting physiological functions of proteins by blocking important thiols or by competing with other metal ions for binding sites. Hence, all cells have to adjust to this bivalent nature of metal ions and maintain metal homeostasis optimal for cell survival. In prokaryotes this precise balance is mainly maintained

by using metal-responsive transcriptional factors, which sense metal deficiency and metal excess, respectively and regulate genes encoding e.g. metal uptake or metal export, storage and detoxification functions. Genes encoding metal uptake functions are usually controlled by repressor proteins which are active in their metal bound form when the cytoplasmatic metal concentration increases above the homeostasis level.

1.3.2.1 The ferric uptake regulator (Fur)

The major iron dependent regulator in gram-negative and low-GC gram-positive bacteria is the ferric uptake regulator (Fur) (Hantke, 1981; Bagg and Neilands, 1987). Besides the iron sensing Fur there is a huge diversity in metal selectivity and biological function within the Fur protein family of transcriptional regulators, including sensors of zinc (Zur) (Patzer and Hantke, 1998), manganese (Mur) (Diaz-Mireles *et al.*, 2004) and nickel (Nur) (Ahn *et al.*, 2006). Other family members use metal catalyzed oxidation reactions to sense peroxide-stress (PerR) (Bsat *et al.*, 1998) or the availability of heme (Irr) (Qi *et al.*, 1999).
Fur proteins are typically transcriptional repressors. In their cognate metal ion bound form (holoFur protein) they specifically bind to corresponding palindromic A/T-rich sequences found in the promoters of their DNA targets (Fillat, 2014). Thereby they prevent the access of the RNA polymerase to the promoter region resulting in the repression of downstream genes. The metal free proteins (apoFur protein) possess low or negligible affinity for the operator sequence leading to a derepression of the target genes.
This Fur mediated iron dependent transcriptional regulation is also utilized to restrict the biosynthesis of siderophores to iron depleted conditions. Already one of the very first studies on the genetic background of iron regulation in *S. typhimurium* described the iron dependent biosynthesis of the NRPS derived enterobactin by an at that time not yet identified factor which was already termed *fur* (iron uptake regulation) (Ernst *et al.*, 1978). Later on it was shown that also the NIS directed biosynthesis of the *E. coli* aerobactin is tightly repressed by Fur and its ferrous ion corepressor (Bagg and Neilands, 1987).

1.3.2.2 The iron dependent DtxR protein family

The DtxR family of metalloregulatory proteins includes two major subfamilies, the iron sensing and the manganese sensing ones. The members of the iron sensing subfamily have been either termed DtxR (diphtheria toxin repressor) or IdeR (iron dependent regulator) and are described to fulfill their iron regulatory function in high-GC gram-positive bacteria like e.g. in *Corynebacterium* spp. (Pohl *et al.*, 1999a), *Mycobacterium* spp. (Pohl *et al.*, 1999b) and *Streptomyces* spp. (Günter-Seeboth and Schupp, 1995). Due to their overlapping regulon, the iron sensing DtxR subfamily is considered to be

the functional orthologue of Fur in most high-GC gram-positive bacteria (Hantke, 2001b). Although there is no sequence similarity between the two major iron sensing transcriptional repressors Fur and DtxR, they do share some similar structural features.

The iron dependent transcriptional regulation of siderophore biosynthesis by IdeR was shown e.g. in *Mycobacterium smegmatis* for the extracellular siderophore exochelin and the cell-wall-associated siderophore mycobatin (Dussurget *et al.*, 1998; Dussurget *et al.*, 1999). Also the synthesis of the NIS derived hydroxamate siderophores of the desferrioxamine group, which are secreted by many *Streptomyces* species, is iron dependently regulated by a DtxR family protein (Tunca *et al.*, 2007).

1.3.2.3 The zinc uptake regulator (Zur)

The major prokaryotic factor regulating the expression of genes encoding zinc uptake and mobilization functions is Zur (zinc uptake regulator) initially described in *Bacillus subtilis* and *E. coli* (Gaballa and Helmann, 1998; Patzer and Hantke, 1998). Zur proteins are present in a diversity of bacterial clades and have been functionally characterized in gram-negative bacteria as well as in low and high-GC gram-positive bacteria (Fillat, 2014).

Regulons under the control of Zur proteins include genes encoding e.g. high affinity zinc uptake systems (*znuABC*), putative zincophors and zinc free paralogues of ribosomal proteins. These genes are repressed by binding of the zinc bound holoZur proteins under zinc-replete conditions and derepressed by dissociation of the zinc free apoZur protein from the DNA.

The zinc responsive Zur of the actinomycete *S. coelicolor* controls the expression of a ZnuABC uptake system, of an alternative zinc free set of ribosomal proteins and also of an NRPS gene cluster (Kallifidas *et al.*, 2010). Though no product was yet assigned to this cluster it was predicted to direct the synthesis of a compound (termed coelibactin) with siderophore-characteristic structural features. Due to the zinc dependent transcription of the corresponding genes coelibactin is predicted to serves as zincophore which is synthesized in order to satisfy the zinc demand of *S. coelicolor* (Zhao *et al.*, 2012).

1.4 Ethylenediamine-disuccinate (EDDS)

The aminopolycarboxylic acid EDDS contains a central diaminoethane moiety. EDDS is a structural isomer of the synthetic compound ethylenediamine-tetra-acetate (EDTA). Both chelating agents form typical sixfold coordinated complexes with transient metal ions (Chen *et al.*, 2010). In contrast to EDTA, EDDS exhibits two asymmetric C-atoms allowing the formation of four optical stereoisomers, [*S,S*]-, [*R,R*]- and the meso-isomers [*R,S*]- and [*S,R*]-EDDS. Exclusively the *S,S*-configuration is readily biodegradable until complete mineralization (Schowanek *et al.*, 1997; Takahashi *et al.*, 1997). On a commercial scale, [*S,S*]-EDDS is chemically produced by Innospec Inc. UK and commercialized under

the trade name Envioment™ as an alternative to its widespread industrially applied isomer EDTA, which strongly resists biodegradation. Combining excellent chelating properties with the accessibility to biodegradation, [*S,S*]-EDDS is considered as a sustainable chelating agent with a favorable environmental profile, possessing the potential to replace EDTA and other environmentally threatening chelating agents in various applications. Chelating agents are used in industrial processes to remove perturbing metal ions or to keep the metal concentration constant. They are widely implemented as antioxidants in paper, textile and laundry industry but also as cosmetic, food and medical additives. In consumer applications, chelating agents are used to sequester trace elements to prevent catalytic reactions leading to rancidity, loss of flavor and discoloration. Chelating agents further found application as crop fertilizers and to remediate contaminated soils.

EDDS was chemically synthesized (Kezerian and Ramsey, 1964; Neal and Rose, 1968) prior to its identification as a natural product of the bacterial strain *A. japonicum* during a screening for phospholipase C inhibitors (Nishikiori *et al.*, 1984). [*S,S*]-EDDS exerts its inhibitory effect by complexing zinc ions, which are essential cofactors of this zinc-metalloenzyme (Hough *et al.*, 1989). *A. japonicum* sets the stage to establish a fermentative [*S,S*]-EDDS production process as alternative to today's chemical production. A sustainable biotechnological [*S,S*]-EDDS production would even further improve the environmental finger print of this chelating agent by using renewable educts instead of fossil ones. The fermentation process was already optimized by growing *A. japonicum* in defined minimal medium characterized by very low zinc concentration. Under this conditions a final yield of up to 20 g L^{-1} [*S,S*]-EDDS was obtained using a long term fed batch cultivation strategy (Zwicker *et al.*, 1997). However, the biosynthesis of [*S,S*]-EDDS under zinc deficiency prevents the scale up of the fermentative production due to the ubiquitous presence of zinc in large industrial metal fermenters. To circumvent this problem and to achieve an economically efficient biotechnological process, a zinc deregulated high performance production strain is required.

1.5 Genome mining: an empirical strategy to discover new natural products

During the golden era of natural product screening the process of compound discovery almost exclusively relied on the detection of bioactivity in extracts from large quantities of natural sources and the activity guided isolation of the corresponding substances. This massive screening effort provided the vast majority of secondary metabolites know today. Due to frequent reisolation of already known natural compounds concerns emerged regarding the limits of natural product discovery. However, one major progress in the scientific field of natural product discovery was the observation that one microorganism has the potential to produce a variety of different compounds when grown under variable culture conditions and the henceforth established one strain/many compounds (OSMAC) paradigm (Bode *et al.*, 2002).

Genome sequencing projects finally revealed the genetic basis for this observation. Secondary metabolite producing bacteria like e.g. members of the order actinomycetales show a genetic potential to manufacture small molecules that exceeds their observed chemistry by far. These observations highlighted that a large proportion of structurally novel natural products remained to be isolated and it was assumed that there are compounds which have escaped detection during massive screening programs.

These not detected compounds can be categorized into two distinct groups: In principle detectable molecules which are produced by the microorganisms and escaped the classical screening approaches due to e.g. limits in analytics or proper evaluation of the data and into the group of natural products which are not produced under classical applied cultivation conditions and which are thus analytically neither detectable. The corresponding gene clusters of the produced but not detected metabolites are referred to as cryptic or orphan gene clusters, while the gene clusters which are very poorly expressed or not expressed at all are referred to as silent gene clusters.

These fundamental findings led to the development of alternative methods to discovery natural compounds. The new methodology relies on the evaluation of the genetic information as the base for rational hunting for new metabolites (Monciardini *et al.*, 2014). A strategy to get access to this enormous genetic potential by exploiting these cryptic or silent gene clusters is the Genome Mining approach. The crucial points of Genome Mining are the confidential evaluation of the genetic information, the subsequent activation and final exploitation of these cryptic gene clusters. However, due to the biochemical heterogeneity of structures, the presence of unknown enzymes and the dispersed nature of the secondary metabolite gene clusters and end products, the identification, categorization and interpretation of the enormous information has been extremely challenging. To get an idea of the synthetic potential of a certain strain, a rapidly and reliably working bioinformatical tool (antiSMASH) has been developed (Weber *et al.*, 2015). antiSMASH is the first comprehensive pipeline capable of identifying and categorizing biosynthetic loci covering the whole range of described secondary metabolite compound classes.

To eventually use these available genetic informations to get access to putative valuable compounds several distinct genome mining techniques were developed and successfully implemented. In certain cases the bioinformatical analyses can lead to a confidential prediction of characteristic structural features of the product and thus to a prediction of the physicochemical properties (Zerikly and Challis, 2009). These predicted properties can then in turn be targeted by adapted analytical methods, facilitating the identification of the corresponding metabolic product. The identification of salinilactam A is exemplifying this strategy (Udwary *et al.*, 2007). Analysis of a polyketide gene cluster in the marine actinomycete *Salinispora tropica* suggested that it codes for a novel lysine-primed polyene macrolactam polyketide. The rational evaluation of a fermentative broth for compounds

with characteristic UV chromophores associated with polyene units, successfully led to the isolation of salinilactam A (Udwary *et al.*, 2007). An advantage of this approach is that genetic manipulation of the producing bacteria is not needed. However, for cases that prediction of physicochemical properties deduced from the genetic cluster information cannot be done with sufficient accuracy and confidence more generic approaches have to be applied. One strategy relies on the inactivation of essential biosynthetic genes and the subsequent comparative analysis of the wild type and the mutant metabolomes in order to identify a compound whose synthesis is directed by the inactivated cluster. This strategy however requires an established genetic manipulation system of the producing strain, which can be a limiting factor. One of the first examples in which this strategy was successfully applied was the identification of the *S. coelicolor* siderophore coelichelin (Lautru *et al.*, 2005). Coelichelin was identified after the inactivation of the NRPS encoding gene *cchH* and the subsequently performed comparative metabolic profiling.

These approaches however have one common limitation; they are not suitable to yield new compounds of not expressed, silent gene clusters. Thus, empirical approaches that exploit knowledge in the field of transcriptional gene regulation were developed to awake these silent secondary metabolite gene clusters in order to make their corresponding product accessible for detection and isolation. In the hierarchically arranged regulatory cascades of secondary metabolite biosynthesis regulation, the gene cluster associated regulatory genes do form the lowest level (Fedorenko *et al.*, 2015). Targeted strategies directly attack these low level pathway specific regulators and rely on their uncoupling from their natural regulatory system and therefore generating a synthetic regulatory state. Overexpression of positive pathway specific regulators mainly enhances or even induces the transcription of structural genes and thus is a commonly used strategy for either improving production yield or for awakening silent gene clusters (Fedorenko *et al.*, 2015).

Such a pathway specific activator targeting approach was applied in *Streptomyces ambofaciens* to induce the expression of a silent PKS gene cluster (Laureti *et al.*, 2011). The constitutive expression of a cluster associated positive regulator gene triggered the expression of the corresponding biosynthetic genes and led to the identification of the stambomycins, glycosylated macrolides with promising antitumor activity.

However, regulation of a gene cluster by a transcriptional repressor does necessitate its deletion instead of its overexpression to induce cluster expression. This strategy was followed to regulatory uncouple the jadomycin B PKS gene cluster of *Streptomyces venezuelae* (Yang *et al.*, 1995). Inactivation of a cluster adjacent repressive gene led to constitutive production of jadomycin B, without the requirement of a stress treatment procedure, essential prior to production in the wild type strain. This is one of the first successfully applied approaches of deleting a repressive regulatory

gene within a cryptic gene cluster to enhance the production of related secondary metabolites and thus make them detectable.

The empirical approach to manipulate regulatory genes enables the access to a further and deeper level of secondary metabolite discovery. Rational exploitation of knowledge in regulation of secondary metabolite biosynthesis however can not only help to assign a molecule to a known gene cluster but also in turn to assign unknown genes to the biosynthesis of a known molecule.

Moreover, the evaluation and the consideration of mechanisms of biosynthetic cluster regulation, including superior triggers and regulatory cascades can further contribute to the fundamental understanding of the physiological functions of natural products and also to address the question what fore do certain microorganisms possess such a well-equipped tool box of natural products.

1.6 Aim of the work

Aim of this study was to develop and to implement empirical regulatory approaches to specifically investigate selected aspects of *A. japonicum* secondary metabolism.

Therefore the following questions had to be answered:

- Does *A. japonicum* possess the genetic potential to produce a glycopeptide, which can be specifically activated?
- Can we gain knowledge in the field of zinc regulation and exploit it to identify the [*S,S*]-EDDS biosynthetic genes?

2. Results

2.1 Activation of a silent glycopeptide gene cluster in *A. japonicum*

Strains of the genus *Amycolatopsis* are known glycopeptide antibiotic producers. Although *A. japonicum* has been intensively studied for many years, no product with antibacterial activity could be identified so far. However, in previous works, it was shown that *A. japonicum* produces glycopeptide resistant cell wall precursors (Schäberle *et al.*, 2011) and that the genome contains an *oxyB* gene, encoding a P450 monooxygenase, which is essential for the production of glycopeptides (Everest and Meyers, 2011). From these results it was assumed that *A. japonicum* has the potential to produce a glycopeptide. To test whether *A. japonicum* genome contains such a silent glycopeptide gene cluster the knowledge of its transcriptional regulation was exploited.

2.1.1 *A. japonicum* encodes a silent glycopeptide gene cluster

All known glycopeptide clusters are transcriptionally controlled by a pathway-specific StrR-like regulator (Donadio *et al.*, 2005). Hence, we applied a cluster activation strategy, by overexpressing the gene encoding the characterized pathway-specific transcriptional regulator of the balhimycin gene cluster, bbr_{Aba} (Shawky *et al.*, 2007), in *A. japonicum* with the aim to awake the suggested silent glycopeptide gene cluster. The recombinant strain overexpressing bbr_{Aba} and the *A. japonicum* wild type strain were grown in a medium suitable for glycopeptide production and the supernatants were screened for production of an antibiotically active product by a growth inhibition assay combined with comparative metabolic profiling. Whereas the supernatant from *A. japonicum* wild type did not contain any biological active compound, the culture supernatant from the recombinant strain strongly inhibited growth of an indicator strain (Fig. 1, publication 1). The comparative metabolic profiling approach using HPLC-DAD revealed a peak in the supernatant of the recombinant *A. japonicum* strain overexpressing bbr_{Aba} which was absent in the chromatogram of the *A. japonicum* wild type supernatant (Fig. 2, publication 1). The detected peak revealed specific DAD spectra with high similarity to spectra of other described glycopeptides.

2.1.2 Genome sequencing and Genome mining revealed a glycopeptide gene cluster

In order to identify the gene cluster for the biosynthesis of the glycopeptide the genome *of A. japonicum* was sequenced. The genome consists of two replicons: the chromosome (8,961,318 bp) and the plasmid pAmyja1 (92,539 bp), encoding a total of 8422 protein coding genes (Table 1, Publication 2). Genome analysis revealed the presence of a type III PKS/NRPS hybrid gene cluster which showed high similarity to already described glycopeptide gene clusters. This cluster consists of 39 distinct open reading frames (Fig. 3, publication 1) with a total size of almost 69 kb. It is predicted

to encode enzymes responsible for assembly and export of the glycopeptide, self-resistance and gene regulation. In the last two decades considerable progress has been made in understanding the genetics and biochemistry of glycopeptide biosynthesis. Therefore, the putative functions of all 39 gene products could be deduced by comparative amino acid sequence analysis with homologues from known glycopeptide clusters (Table 1, publication 1). The profound knowledge of the individual enzymes participating in glycopeptide biosynthesis makes it possible to almost completely predict the structure of the final product. The *in silico* data strongly suggested that the final product of the identified gene cluster is a six-fold glycosylated, twice methylated, non-halogenated and fully cross-linked glycopeptide. The genetic organization and domain composition of the NRPS specifies a heptapeptide with the amino acid sequence L-Hpg^{1}-D-β-Ht^{2}-L-Dpg^{3}-D-Hpg^{4}-D-Hpg^{5}-L-β-Ht^{6}-L-Dpg^{7} (Dpg = 3,5-dihydroxyphenylglycine, Hpg = *p*-hydroxyphenylglycine, β-Ht = β-hydroxytyrosine). The incorporation of aromatic amino acids at position 1 and 3 together with the predicted complete cyclized heptapeptide implies that this gene cluster directs the synthesis of a type III glycopeptide (Fig. 4, publication 1).

2.1.3 The cluster encoded transcriptional activator AjrR is functional

The newly identified gene cluster harbours a gene whose deduced product (AjrR) exhibits high similarity to the StrR-like transcriptional activator of the balhimycin gene cluster (Bbr_{Aba}). However, Bbr_{Aba} initiates the transcription of the glycopeptide gene cluster in *A. balhimycina* while the *A. japonicum* gene cluster is of silent nature under identical growth conditions. To evaluate its *in vivo* functionality, AjrR was expressed under the control of a constitutive promoter in *A. japonicum*. The supernatant of the recombinant *A. japonicum* strain, constitutively expressing *ajrR*, inhibited growth of an indicator strain as shown for the heterologous expression of bbr_{Aba} (Fig. 1, publication 1). HPLC-DAD analyses confirmed the biosynthesis of the glycopeptide. To investigate the influence of the StrR-like transcriptional activators on gene expression of the identified glycopeptide gene cluster the transcriptional pattern of representative cluster genes were determined in the *A. japonicum* wild type and in the two recombinant strains expressing bbr_{Aba} and *ajrR*, respectively. No transcript of *ajrR* and neither of any other analyzed structural gene was detected in *A. japonicum* wild type (Fig. 5, publication 1). However, overexpression of both bbr_{Aba} and *ajrR* induced the transcription of all investigated structural genes. In contrast, transcription of the *vanHAX*-like glycopeptide resistance cassette was detected in *A. japonicum* wild type without the requirement of a specific transcriptional initiation by *ajrR*.

2.1.4 Structure elucidation revealed ristomycin A as product of *A. japonicum*

In order to determine the chemical structure of the glycopeptide, *A. japonicum* overexpressing the pathway specific regulator Bbr_{Aba} was grown in a 20 L fermenter prior to purification procedure. Glycopeptide production was detected after 24 h of growth and reached a maximum amount up to 200 mg L^{-1} (Fig. 7, publication 1). Activity guided isolation was performed via an adsorbent resin and subsequent reversed phase preparative HPLC. The purified compound was analyzed by various analytical methods (HPLC-ESI-MS, ESI-MS/MS, HR-MS, ^{1}H and ^{13}C NMR, CD-spectroscopy) to determine its chemical structure. The structure elucidation revealed that the identified gene cluster is directing the production of ristomycin A. Ristomycin A is a type III glycopeptide with a four time oxidatively cross-linked amino acid backbone consisting of Hpg-β-Ht-Dpg-Hpg-Hpg-β-Ht-Dpg which is decorated by six glycosidic residues and two methylations (Fig. 4, publication 1).

2.1.5 *A. japonicum* ristomycin A induces *in vitro* platelet aggregation

Ristomycin A causes thrombocytopenia and platelet agglutination. Thus it is applied to assay those therapeutically unfavorable functions *in vitro* as a diagnostic compound to detect widespread hereditary genetic disorders such as von Willebrand disease and Bernard-Soulier syndrome (Sarji *et al.*, 1974). Activity of the von Willebrand factor is measurable by the ristomycin-platelet-induced agglutination method. In a platelet aggregation assay it was demonstrated that ristomycin A isolated from *A. japonicum* has the same *in vitro* function as the commercial reference ristomycin A (Fig. 8, publication 1).

2.2 Identification of the [*S,S*]-EDDS biosynthetic genes by exploiting knowledge of zinc dependent transcriptional regulation

A. japonicum was described as the producer of [*S,S*]-EDDS in 1984 (Nishikiori *et al.*, 1984). However, the enzymes required for EDDS biosynthesis have not been identified during the pregenomic era. Different classical approaches such as heterologous expression of an *A. japonicum* cosmid library in a non-producer strain, comparative proteomics of cells growing in the presence and in the absence of zinc or screening for predicted biosynthetic enzymes or regulatory elements with degenerative primers have been applied unsuccessfully in order to identify the [*S,S*]-EDDS biosynthetic genes (Stegmann, 1999; Moll, 2006; Frasch, 2008). The access to the *A. japonicum* genome sequence allowed the *in silico* data analysis to evaluate the biosynthetic potential of *A. japonicum*. This *in silico* analysis revealed the presence of various putative gene clusters encoding the synthesis of natural products in *A. japonicum* (Table S1, publication 1).

However, the characteristic structural features of [*S,S*]-EDDS could not be assigned to any of the predicted assembly mechanisms encoded by the identified clusters. Therefore, the development of an alternative strategy for the identification of the [*S,S*]-EDDS biosynthetic genes was required.

The key assumption of the established approach is that the zinc repressed biosynthesis of [*S,S*]-EDDS is mediated by a zinc responsive regulatory element. The molecular genetic analysis of the zinc regulation and the subsequent computational screening for zinc repressed genes were conducted to investigate [*S,S*]-EDDS biosynthesis.

2.2.1 The zinc responsive zinc uptake regulator Zur controls the [*S,S*]-EDDS biosynthesis

The major zinc responsive transcriptional regulator which is regulating the expression of genes encoding zinc uptake and zinc mobilization functions in prokaryotes is the zinc uptake regulator Zur (Fillat, 2014). Blast analysis of the *A. japonicum* genome using the *S. coelicolor* Zur protein (Owen *et al.*, 2007) as query revealed a gene whose proposed gene product exhibits high similarity. In support of its potential role as major zinc regulator, computational amino acid sequence analyses showed that the amino acids described to be involved in zinc binding are highly conserved (Fig. S1, publication 3). The coding region of *A. japonicum zur* was deleted (*A. japonicum* Δ*zur*) to investigate its role as regulator of the [*S,S*]-EDDS biosynthesis. In order to study the effect of the deletion, the mutant strain and the *A. japonicum* wild type strain were grown in synthetic medium in presence of increasing zinc concentrations. At zinc concentrations ≥ 2 µM [*S,S*]-EDDS production was inhibited in the *A. japonicum* wild type (Fig. 2, publication 3). In contrast, zinc independent and constant [*S,S*]-EDDS biosynthesis was observed in *A. japonicum* Δ*zur* over the total range of the applied zinc gradient (Fig. 2, publication 3). The production of [*S,S*]-EDDS in this mutant in presence of zinc suggested that the deleted gene encodes the zinc sensing regulator Zur indeed and that the [*S,S*]-EDDS biosynthetic genes are under its zinc responsive control. In addition to the zinc independent [*S,S*]-EDDS production, the deletion of *zur* led to a significantly increased total [*S,S*]-EDDS yield compared to the wild type strain.

2.2.2 Zur controls the high affinity zinc uptake system ZnuABC

Zur regulons characterized so far usually comprise 10-30 genes with different functions often related to zinc homeostasis. In particular the high affinity zinc uptake system ZnuABC has been identified as Zur regulated in many bacteria and is widely distributed throughout the bacterial kingdom (Patzer and Hantke, 1998; Campoy *et al.*, 2002; Lucarelli *et al.*, 2007; Shin *et al.*, 2007; Pawlik *et al.*, 2012). Blast analyses using the previously described ZnuABC system of *S. coelicolor* (Shin *et al.*, 2007) revealed the presence of two putative ABC transporters, whose deduced protein sequences show high levels of similarity to ZnuABC of *S. coelicolor* (Fig. 3B, publication 3). To elucidate which ABC transporter system is physiologically connected to zinc uptake in *A. japonicum*, their transcriptional patterns were investigated with respect to the presence of various divalent metal ions. The transcription of one ABC uptake system was specifically repressed by manganese while the second one was specifically repressed by zinc (Fig. 3C, publication 3). Therefore the physiological functions of high affinity zinc and manganese uptake were assigned to the corresponding ABC uptake systems.

To evaluate the zinc regulatory function of Zur for *znuABC* transcription, *znuB* transcription was analyzed in *A. japonicum* Δ*zur*. In contrast to the wild type, where *znuB* transcription is absolutely repressed by zinc concentrations ≥ 2.0 µM, its transcription occurred zinc independently in *A. japonicum* Δ*zur*, with detectable expression even at highly elevated zinc concentrations (Fig. 4, publication 3). To analyze whether Zur binds to the *znu* promoter region in a zinc dependent manner, electrophoretic mobility shift assays (EMSA) were performed. This revealed a zinc dependent and specific binding of purified Zur protein to the *znu* promoter region (Fig. 5, publication 3).

2.2.3 The rational screening of the *A. japonicum* Zur regulon revealed putative [*S,S*]-EDDS biosynthetic genes

The zinc dependent binding of Zur to the *znu* promoter region suggested the presence of a specific Zur binding sequence. To identify this motif a computational alignment of the *znu* promoter region to previously described Zur binding sequences of other, high-GC gram-positive bacteria was performed. This alignment revealed an A/T-rich palindromic sequence within the *znu* promoter region, exhibiting high similarity to the previously described motifs. The newly identified sequence was used to deduce a more specific *A. japonicum* Zur binding sequence (Fig. 6, publication 3).

This motif was then used to screen the *A. japonicum* genome to identify further Zur regulated genes, in particular the [*S,S*]-EDDS biosynthetic genes for molecular biological evaluation. This screening

revealed a putative binding motif between two genes transcribed in diverse directions (*aesE* and *aesA*) (Fig. 6C and 7A, publication 3). *aesE* encodes a protein belonging to the amidase signature family, while *aesA* is the first gene of an operon (*aesA-D*). The proposed gene products of *aesA*, *aesB* and *aesC* share significant similarity to enzymes involved in the synthesis of staphyloferrin B (SB) (Fig. 6B, publication 3), a NIS derived siderophore of *S. aureus* (Cheung *et al.*, 2009). The concerted enzymatic activities of the three AesA-C homologous of *S. aureus* lead to the generation of a central 1,2-diaminoethane (Dae) moiety present in SB (Fig. 7C, publication 3). Also the [*S,S*]-EDDS structure is characterized by such a central Dae moiety. Accordingly, the generation of the central Dae moiety in [*S,S*]-EDDS biosynthesis is suggested to occur in a similar way as in SB biosynthesis. However, a NIS dependent stepwise assembly of the single building blocks has to be excluded for [*S,S*]-EDDS biosynthesis since no NIS synthetase is encoded in the *A. japonicum* genome at all.

2.2.4 The transcription of the *aesA-D* operon is zinc responsively regulated by Zur

Since [*S,S*]-EDDS is only produced under zinc limiting conditions, the transcription of the identified candidate genes *aesA-D* was analysed to possibly detect any collinearity between zinc inhibitory effects on [*S,S*]-EDDS productivity and gene transcription. The transcription pattern of *aesA* was determined after growth of *A. japonicum* in presence of various zinc concentrations. An inverse correlated transcription level of *aesA* to increased zinc concentration was observed whereby no transcript was detected for zinc concentrations above 2 µM (Fig. 4, publication 3). The zinc inhibitory effect was also seen for the genes *aesB-D* (Fig. S4, publication 3). In *A. japonicum Δzur* however, *aesA-D* expression was zinc independent (Fig. S4, publication 3). *aesA*, which was used as probe representing the entire operon, exhibited a constitutive transcription over the whole range of applied zinc gradient in the *Δzur* background (Fig. 4, publication 3).

To further verify the Zur mediated zinc dependent repression of *aesA-D*, gel shift assays using purified Zur and the 5' upstream region of *aesA* were performed. Purified Zur bound specifically to the DNA probe in presence of zinc, while no binding occurred in the absence of zinc (Fig. 5, publication 3).

To quantitatively determine the transcriptional level of *aesA-D* in a zinc dependent manner, a transcriptional fusion of the *aesA* promoter region with the reporter gene *gusA*, encoding a β-glucuronidase (GUS), was constructed. The reporter constructs were integrated into *A. japonicum* wild type and *A. japonicum* Δ*zur* genomes. The recombinant strains were grown in presence of various zinc concentrations before the analyses of GUS activities. Initially, GUS activities were assayed in cell based chromogenic assays. *A. japonicum* wild type containing the reporter construct solely exhibited GUS activity when grown at low zinc concentrations. In contrast, GUS activity was also visible in *A. japonicum* Δ*zur* at elevated zinc concentrations (Fig. 8B, publication 3). Quantitative

data were generated in spectrophotometric assays, subsequently. Under subinhibitory zinc concentrations, the strain representing *A. japonicum* wild type revealed GUS activity levels significantly above those of the negative controls (Fig. 8A, publication 3). Linear decreasing GUS activity was measured in the range of partially inhibitory zinc concentrations. No GUS activity was detectable in this strain when grown at zinc concentrations higher than 2 µM. In contrast, GUS activities in *A. japonicum* Δ*zur* carrying the reporter construct were measurable in presence of elevated zinc concentrations at the same level as in absence of zinc. This GUS activity was increased 4.4 fold compared to the activity in *A. japonicum* wild type carrying the reporter construct after growth in absence of zinc.

2.2.5 The *aes* genes are essential for [*S,S*]-EDDS production

To prove whether the zinc regulated *aesA-D* operon is involved in [*S,S*]-EDDS biosynthesis, the entire genomic region containing *aesA-C* was deleted. The mutant strain *A. japonicum* Δ*aesA-C* was not able to produce [*S,S*]-EDDS (Fig. 9, publication 3). To verify that the loss of [*S,S*]-EDDS production in *A. japonicum* Δ*aesA-C* is only due to the *aesABC* deletion, a genetic complementation was performed by integrating a plasmid into the *A. japonicum* Δ*aesA-C* genome which harbours the complete *aesA-D* operon downstream of its native, zinc repressed promoter. This genetically complement mutant showed restored [*S,S*]-EDDS production (Fig. 9, publication 3). Due to the transcriptional control of the integrated *aesA-D* operon by the native promoter, production of [*S,S*]-EDDS occurred solely in zinc depleted medium. The amount of [*S,S*]-EDDS produced by this recombinant strain was increased two to three times compared to *A. japonicum* wild type.

The genes *aesF*, *aesG* and *aesH* are located adjacent to *aesE* (Fig. 7, publication 3) and are predicted to encode a LysR family transcriptional regulator, a cysteine dioxygenase and an acetyltransferase, respectively. To further narrow down the [*S,S*]-EDDS biosynthetic gene cluster and to investigate the involvement of these genes in the biosynthesis of [*S,S*]-EDDS the genomic region harboring *aesE-H* was deleted. This mutant was not able to produce [*S,S*]-EDDS (Fig. S5, publication 3). However, the *aesA-D* operon was still zinc dependently transcribed in this mutant, confirming that the promoter region of *aesA* was not affected by this mutation. These results demonstrated that at least one of the *aesE-H* genes is required for the production of [*S,S*]-EDDS in addition to *aesA-C*.

2.2.6 The [*S,S*]-EDDS biosynthesis as response to zinc deficiency is phylogenetically clustered

The general microbial potential to produce [*S,S*]-EDDS was assessed by evaluating the phylogenetic abundance of the *aes* genes by computational analyses. This revealed that the occurrence of the *aesA-H* genes is restricted to certain strains of the genus *Amycolatopsis*. Of all analyzed genomes

solely these of *Amycolatopsis* sp. MJM2582, *Amycolatopsis orientalis* HCCB10007 and *Amycolatopsis lurida* DSM 43134 harbor the eight clustered genes *aesA-H* entirely with identical gene arrangement and with high sequence similarity compared to *A. japonicum* (Table S3, publication 3). *Amycolatopsis decaplanina* DSM 44594 and *Amycolatopsis alba* DSM 44262 genomes miss the terminal *aesH* homolog. Interestingly, the Zur-box is highly conserved in all discovered *aesA* 5' upstream regions (Table S4, publication 3) evidencing the common Zur mediated and zinc dependent transcriptional repression. These identified strains are all closely related to *A. japonicum* and are classified into the *Amycolatopsis* phylogentic clade A. An exception within this phylogentic clade A however is *Amycolatopsis azurea* DSM 43854, which does not show a conserved [*S,S*]-EDDS cluster. In contrast to the total *aes* gene cluster, homologs of the *aesA-D* subcluster are quite abundant in various genera of actinobacteria and proteobacteria.

To eventually correlate this genetic information to the actual capacity to produce [*S,S*]-EDDS, the phylogenetic clade A strains *A. lurida*, *A. decaplaina*, *A. alba* and *A. azurea* but also *Amycolatopsis balhimycina* DSM 5908, *Amycolatopsis nigrescens* DSM 44992 and *Amycolatopsis nigrescens* DSM 44992 as representatives of other phylogenetic clades were grown under [*S,S*]-EDDS production conditions. *A. lurida*, *A. decaplaina* and *A. alba* grown without the supplementation of zinc produced [*S,S*]-EDDS, while no production was observable after growth of these strains in presence of zinc (Fig. S7, publication 3). No [*S,S*]-EDDS production could be detected after cultivation of *A. azurea*, *A. balhimycina* DSM 5908, *A. mediterranei* DSM 43304 nor *A. nigrescens* DSM 44992.

These results show that [*S,S*]-EDDS production as an evolutionary response to zinc deficiency is likely a unique feature of the *Amycolatopsis* phylogenetic clade A.

3. Discussion

3.1 *A. japonicum* genome contains a silent gene cluster directing the biosynthesis of ristomycin A

Glycopeptides are a major type of secondary metabolites produced by the genus *Amycolatopsis*. Strains possessing the ability to produce glycopeptides tend to cluster together phylogenetically, with most, but not all, of the described producers belonging to the *Amycolatopsis* phylogenetic clade A (Everest and Meyers, 2011). Also the strain *A. japonicum*, which was known to be the producer of the chelating agent [*S,S*]-EDDS, does belong to this clade.

All previously described glycopeptide producing *Amycolatopsis* strains have been identified as producers by activity guided screening approaches. These strains do express the corresponding antibiotic gene cluster under certain culture conditions. In contrast, *A. japonicum* does not produce any bioactive compound under culture conditions usually suitable for glycopeptide production.

However, the application of a molecular genetic approach enabled the activation of glycopeptide production in the predicted producer strain *A. japonicum*. This was achieved by heterologous expression of the characterized pathway specific activator Bbr (Shawky *et al.*, 2007) of the balhimycin gene cluster of *A. balhimycina*. Bbr induced the transcription of the structural genes required for glycopeptide biosynthesis in *A. japonicum*.

The activation of a rationally predicted secondary metabolite gene cluster by overexpression of an empirical chosen transcriptional activator is a promising strategy which could be generally applied to purposefully activate various kinds of secondary metabolite classes in bacteria. The high throughput application of this strategy by activating certain secondary metabolite clusters in e.g. bacterial strain collections however may be limited by the requirement of bacterial accessibility to genetic manipulations.

In contrast to usual genome mining approaches which use the accessible genetic information as base prior to activate silent gene clusters, this approach does not necessitate availability of genetic information and its evaluation. However, the basic strategy to overexpress a transcriptional activator in order to activate a silent gene clusters is shared with various successfully conducted, classical genome mining approaches. The analysis of the *S. ambofaciens* genome for its biosynthetic potential e.g. revealed the presence of a silent PKS gene cluster and the therein encoded pathway specific activator of the LuxR protein family prior to specific cluster activation by its homologous overexpression (Laureti *et al.*, 2011).

The detailed understanding of glycopeptide biosynthesis makes it possible to reliably deduce the structure of the final product from the genetic information to a certain degree. The *in silico* analysis of the identified gene cluster in *A. japonicum* suggested the biosynthesis of a sixfold glycosylated and twice methylated heptapeptide backbone consisting of seven aromatic amino acids whose side

chains are fully cross-linked. These informations correlate to the chemical structure of the type III glycopeptide ristomycin A. Previously only the structure of ristomycin A (Fehlner *et al.*, 1972; Williams *et al.*, 1979), but not the corresponding biosynthetic gene cluster has been reported. Since there is neither any other type III glycopeptide gene cluster described, the identified *A. japonicum* gene cluster is the first reported gene cluster exemplifying this type. Isolation of the glycopeptide and subsequent structure elucidation finally revealed that the *A. japonicum* type III glycopeptide gene cluster is indeed directing the synthesis of ristomycin A. The quite reliable *in silico* prediction of the chemical structure from the genetic information encoded by the gene cluster by considering the profound knowledge of glycopetide biosynthesis shows the power of nowadays available bioinformatics tools.

The capability to produce ristomycin A however is not a unique feature of *A. japonicum* since this highly glycosylated glycopeptide was initially identified as a product of *A. lurida* (Grundy *et al.*, 1956) and recently also as a product of *Amycolatopsis* sp. MJM2582 (Truman *et al.*, 2014), two strains which are closely related to *A. japonicum*. The two strains *A. lurida* and *Amycolatopsis* sp. MJM2582 as ristomycin A producer were identified by a classical activity guided screening of culture supernatant fractions. In case of *Amycolatopsis* sp. MJM2582 a targeted two-step bioassay system specified to detect the presence of glycopeptide antibiotics was applied. This screening approach relies on the reporter strain *S. coelicolor* Δ*femX* whose genetic background necessitates the presence of a glycopeptide for viability (Truman *et al.*, 2014). This illustrates how different ways can lead to the same final goal. In contrast to the work and resource consuming activity guided screening procedures, the successfully applied molecular genetic activation of ristomycin A production in *A. japonicum* strongly facilitated the workflow leading to the isolation of the bioactive compound.

As expected, computational analysis of the recently published genome sequences of *A. lurida* (Kwun and Hong, 2014) and *Amycolatopsis* sp. MJM2582 revealed the presence of gene clusters that exhibit identical genetic organization and high similarity on nucleotide level to each other (Truman *et al.*, 2014) and also to the cluster of *A. japonicum*.

All of these gene clusters contain highly similar StrR-like transcriptional activators. However, in contrast to the *A. japonicum* gene cluster which is silent under laboratory conditions, the production of ristomycin A occurs without specific activation in *A. lurida* and *Amycolatopsis* sp. MJM2582. The silent state of the *A. japonicum* ristomycin A cluster is not due to the *ajrR* coding region itself since its *in vivo* functionality could be shown but rather due to the fact that *ajrR* is not transcribed under standardized cultivation conditions in *A. japonicum*. Therefore, we assume that there is a still unknown superior trigger required for *ajrR* activation which is either totally missing in *A. japonicum* or more probable absent under the investigated culture conditions.

The cluster border of all three described ristomycin A gene cluster are delimited by the *vanHAX* resistance cassette. The *vanHAX* resistance cassette is not an obligatory feature of glycopetide gene clusters. *vanHAX* genes are e.g. present in the gene clusters directing the biosynthesis of A47934 and teicoplanin while not in the balhimycin and chloroeremomycin gene clusters (Donadio *et al.*, 2005). The transcription of this resistant cassette is usually regulated by the two component system VanRS sensing the presence of glycopeptides. In *A. balhimycina* however the *vanHAX* regulation is independent from the *vanRS*-like two component system which is found adjacent to the balhimycin gene cluster (Schäberle *et al.*, 2011). Unlike that, no genes encoding the VanRS were identified anywhere in the *Amycolatopsis* sp. MJM2582 and *A. lurida* genomes (Truman *et al.*, 2014) nor in the *A. japonicum* genome. This implies that *vanHAX* expression is VanRS independent also in these strains. Transcriptional analysis of *vanH* in *A. japonicum* wild type revealed indeed its constitutive expression independent of ristomycin A production and coincident to the observations that the *A. japonicum* wild type strain is producing a glycopeptide resistant cell wall whereas no glycopeptide production could be detected (Schäberle *et al.*, 2011).

A paradigm of antibiotic resistance is that resistant determinants are expressed in colinearity to antibiotic production to adapt the producing strain to the presence of the own compound. Therefore *vanH* expression and synthesis of resistant cell walls in the wild type *A. japonicum* may reflect that the cluster is rather very poorly expressed than absolutely silent, meaning that there is a basal ristomycin A production which is analytically not detectable but nevertheless leading to the requirement of resistance. In this case the overexpression of the pathway specific StrR-like regulators would rather be a yield optimization approach than a genome mining approach leading to activation of a silent gene cluster.

The StrR-like independent *vanH* transcription stands in contrast to the essentiality of StrR-like protein for the expression of the structural ristomycin A genes. This is in agreement with the observation that expression of all streptomycin biosynthetic genes is StrR-dependent besides the expression of the resistant gene (Tomono *et al.*, 2005). StrR-like independent gene expression of the resistance cassette in *A. japonicum* may reflect an evolutionary adaption of the strain to the presence of other competing soil-dwelling bacteria with the potential to produce glycopeptides rather than an unidimensional protection mechanism correlating to the production of the own glycopeptide antibiotic.

Currently *A. lurida* is utilized for commercial production of ristomycin A which is needed for its application as diagnostic compound. Till date there are no described transformation protocols available to genetically manipulate *A. lurida* and *Amycolatopsis* sp. MJM2582. This seems to limit the yield optimization of ristomycin A production in these strains to classical strain development by directed evolution and to classical fermentative optimization. In contrast, several different

procedures to genetically manipulate *A. japonicum* are established (Stegmann *et al.*, 2001). These procedures are however at least not applicable for *A. lurida*. The activation of ristomycin A production in the genetically easily accessible strain *A. japonicum* now offers the possibility to optimize the production in a rational manner by metabolic engineering approaches and to increase the currently obtained ristomycin A yield of 200 mg L^{-1} significantly. Functionality of such approaches could be shown in the case of balhimycin production where productivity of *A. balhimycina* was increasable by directing metabolic fluxes to increase the availability of specific precursors (Thykaer *et al.*, 2010). The transfer of this knowledge to *A. japonicum* might lead to an optimized production strain with increased ristomycin A yield to outcompete the nowadays industrially utilized *A. lurida*.

3.2 The [*S,S*]-EDDS biosynthetic genes were identified by a novel approach exploiting knowledge in the field of zinc responsive gene regulation

3.2.1 [*S,S*]-EDDS exemplifies the rare functionally class of zinc responsive ionophores

A. japonicum produces the chelating agent [*S,S*]-EDDS as response to zinc deficiency. In contrast to zinc, other metal ions do not show any repressive effect on [*S,S*]-EDDS biosynthesis. Therefore it is considered that [*S,S*]-EDDS is an evolutionary adaptation to zinc deficiency which contributes to zinc uptake. In analogy to siderophores-mediated iron acquisition, the term zincophore was introduced for [*S,S*]-EDDS (Cebulla, 1995; Hantke, 2001a).

In general, microbial chelating agents or ionophores are classifiable into functionally classes according to their responsive metal ion, with respect to their transcriptional regulation and to specific reassociation of the metal ion ionophore complex to the cell.

To date, iron acquiring siderophores are the main group of described chelating compounds produced by microbes. The evolutionary success of siderophores suggested that microorganisms also employ analogous systems to sequester poorly accessible ions other than iron in order to enhance their assimilation. Examples describing such chelating agents however have not been given much coverage in literature though.

Considering the essentiality of iron to living cells and the predominant occurrence of iron as highly stable and insoluble ferric oxide hydrate complexes in aerobic environments, which cannot be assimilated by microorganisms (Challis, 2005), makes it very likely that the vast majority of microbial ionophores are indeed iron acquiring siderophores. On the other hand, this suggests that production of ionophores in response to metal ions other than iron may be a proportionally rare adaptive mechanism of certain specialized microbes that either have to challenge severe deficiency of certain ions in their natural environment or require a comparatively high amount of certain ions due to their metabolism. Nevertheless, many ionophores which are thought to be siderophores, have never been experimentally verified to fulfil the criteria to be classified as such. antiSMASH e.g. annotates detected NIS gene clusters automatically as siderophore gene clusters without considering predictable informations of iron responsive transcriptional regulation. Additional computational screening for known metal regulator binding sites within the corresponding gene clusters predicted to direct the synthesis of ionophores could give further insight into their physiological function and could contribute to guide isolation of more ionophores of rare or even new classes. Directed bioinformatic analyses of huge nucleotide sequence data sets by combining the understanding of ionophore biosynthesis and metal ion responsive gene regulation may lead to identification of further ionophores which function in assimilation of certain metal ions other than iron and broaden the understanding of bacterial survival strategies.

The few known examples of non-iron-ionophore systems are either zinc or copper responsive. A known zinc acquisition system, consisting of a secreted factor (Pra1) which specifically reassociates with the cell surface by a coexpressed transporter protein (Zrt1), is utilized by the major human fungal pathogen *Candida albicans* to assimilate the essential nutrient zinc from its host (Citiulo *et al.*, 2012). Another class of ionophores are the methanobactins produced by certain methanotrophic bacteria (Kim *et al.*, 2004). The methanobactins are secreted to acquire copper from the environment which is essential for these bacteria to serve as enzyme cofactor for the metabolic pathway of methane oxidation. According to the greek word for copper (chalkós) and in analogy to siderophores the methanobactins are referred to as chalkophores (Kenney and Rosenzweig, 2014).

In contrast to siderophores whose biosynthesis is mainly directed by NRPS or NIS pathways, the *C. albicans* Pra1 and the methanobactins are ribosomally synthesized peptides. Whereas Pra1 is secreted as an unaltered peptide, methanobactins derive from a prepeptide (Semrau *et al.*, 2013) which is extensively post-translationally modified (Kenney and Rosenzweig, 2014). These ribosomally synthesized chelating proteins however are no classical low molecular weight secondary metabolites but rather analogous to bacterial hemophores (Cescau *et al.*, 2007), secreted proteins capturing free heme or extract heme from hemoglobin.

A zinc responsive NRPS system which is predicted to direct the synthesis of a compound with structural features characteristic for chelating agents is described for *S. coelicolor* (Bentley *et al.*, 2002). The gene expression of this NRPS gene cluster is zinc responsively controlled by Zur (Kallifidas *et al.*, 2010). Though no product was assigned to this gene cluster yet, bioinformatical evaluation of the genetic information suggested the biosynthesis of a salicylate containing compound termed coelibactin (Bentley *et al.*, 2002). Due to the zinc responsive repression of the cluster genes it is suggested that coelibactin serves as zincophore for *S. coelicolor* (Zhao *et al.*, 2012).

The low molecular weight [*S,S*]-EDDS gives the most coherent picture as an example for an ionophore being produced in response to metal ions other than iron. However, though the strict zinc repressed production suggests a function of [*S,S*]-EDDS in specific zinc uptake, experimental proof for this hypothesis is still lacking. Till date, neither reassociation of zinc-[*S,S*]-EDDS complex with the *A. japonicum* cell surface, nor actual [*S,S*]-EDDS mediated zinc uptake into the cytoplasm was shown.

Normally, a once by the corresponding ionophore mobilized and captured metal ion gets accessible for specific cellular uptake to eventually merge into the cellular metal ion pool. Therefore, the mobilized metal has to be released from its ionophore ligand and transferred into the cytoplasm. The molecular mechanisms of this uptake have been extensively investigated for siderophore mediated iron uptake. A variety of mechanisms which are often coupled with high-affinity uptake have evolved to facilitate the removal of iron from their siderophore ligands. The iron release can either occur at the cellular surface in association with free iron uptake, or after cellular uptake of the ferric

siderophore complex (Miethke, 2013). In bacteria, the main route for siderophore-mediated iron uptake is represented by the import of ferric siderophore complexes into the cytoplasm. The entry of the ferric siderophore complexes by passive diffusion is however prevented by the cytoplasmic membrane (Beasley and Heinrichs, 2010). Thus uptake occurs by binding of the complex to a membrane associated binding protein prior to its active transport across the cytoplasmic membrane by an ABC (ATP-binding cassette) transporter system (Stintzi *et al.*, 2000; Braun, 2001; Braun and Hantke, 2011). Though, such uptake systems are usually coexpressed with the corresponding siderophore biosynthetic genes (Barona-Gomez *et al.*, 2006) no ABC-transport system is found adjacent to the [*S,S*]-EDDS biosynthetic genes.

The eventual removing of the iron from its chelator follows the same basic schemes at the cellular surface or in the cytoplasm. The iron release is either facilitated by the competition of iron coordination with ligand protonation (pH-dependent release), the hydrolysis of the siderophore backbone (hydrolytic release), or the reduction of the ferric ion center (reductive release) (Miethke, 2013). The majority of iron removal processes are non-destructive assimilatory reduction processes of ferric iron complexes. The key assumption of this process is that siderophores have high affinity for the ferric cation and much lower affinity for the ferrous cation. Ferric ion reduction is subsequently followed by the spontaneous release or competitive sequestration of the reduced species (Miethke and Marahiel, 2007).

The reduction of ferric to ferrous iron is mainly enzymatically catalyzed by oxidoreductases, like the vibriobactin utilization protein ViuB of *Vibrio cholerae* (Butterton and Calderwood, 1994). In the extracellular environment this reductive removal is often directly coupled with high-affinity uptake of the released ferrous iron species. Most likely, such a reductive release has to be excluded for the [*S,S*]-EDDS facilitated zinc uptake since the chemistry of zinc is dominated by its +2 oxidation state which is redox-inert in biologic systems (Krezel *et al.*, 2007).

The destructive hydrolytic release is only feasible for a minority of siderophores due to structural requirements such as the introduction of rather unstable ester bonds into the siderophore scaffold (Miethke, 2013). Such ferric siderophore hydrolyzing enzymes generally belong to the α/β-hydrolases superfamily exhibiting esterase activity. *E. coli* utilizes a set of three siderophore esterases consisting of the cytosolic IroD and Fes and the periplasmatic IroE to hydrolyze ferric enterobactin and its glycosylated derivatives (Lin *et al.*, 2005; Zhu *et al.*, 2005). Since [*S,S*]-EDDS does not harbor any ester bond such a α/β-hydrolases superfamily protein catalyzed degradation of the zinc loaded complex has to be ruled out.

In aqueous solution the formation of iron siderophore complexes is affected by the pH. The free protons and the iron compete for the free siderophore ligands. This coordination chemistry is exploited by the iron removal process by *Saccharomyces cerevisiae* which couples an enzymatic ferric

ion reduction with an extracellular acidification (Lesuisse *et al.*, 1995). The lowered pH leads to a partial destabilization of the ferric siderophore complex due to an increased ligand protonation (Cohen and Raymond, 2000). [*S,S*]-EDDS can complex a range of metal ions over a broad pH range with maximal chelation events occurring approximately at neutral or slightly alkaline pH (Kołodyńska, 2011). The approximate pH range which is suitable for chelation of divalent zinc ions by [*S,S*]-EDDS is between pH 5 and 12. At pH lower than 3, [*S,S*]-EDDS is present as free, not zinc bound apo form (Orama *et al.*, 2002).

The consideration of known siderophore mediated iron uptake mechanisms, of physicochemical zinc properties as inert ion and of *A. japonicum* genetics can guide further investigations on putative [*S,S*]-EDDS mediated zinc uptake. The absence of an ABC uptake system in the [*S,S*]-EDDS cluster may indicate a zinc release rather at the cellular surface in association with specific zinc uptake. A candidate uptake system linking zinc mobilization by [*S,S*]-EDDS and zinc transfer into the cytoplasm might be ZnuABC. The function of a cognate, membrane associated binding protein, recruiting the zinc [*S,S*]-EDDS complex might be performed by the predicted lipoprotein extending the ZnuABC system of *A. japonicum* which exhibits an N-terminal signal peptide with conserved lipobox (L-A-A-C). Interestingly, also the ZnuABC systems of other *Amycolatopsis* species which were shown to produce [*S,S*]-EDDS are extended by this lipoprotein while it is not found in non-producing *Amycolatopsis* species. The eventual zinc release does probably not occur by lowering the complex stability by reduction of zinc and neither by hydrolyzing [*S,S*]-EDDS by esterases. However, [*S,S*]-EDDS degradative enzymes cleaving the C-N-bond between one succinyl residue and the central Dae were already isolated (Witschel and Egli, 1998; Cokesa *et al.*, 2004). These carbon nitrogen lyases are similar to the argininosuccinate lyase ArgH (Hani and Chan, 1994), an enzyme catalyzing the last step of arginine biosynthesis. The *A. japonicum* genome encodes just one similar protein whose genetic location highly suggests its function in arginine biosynthesis rather than in [*S,S*]-EDDS hydrolysis.

3.2.2 Elucidation of the Zur mediated zinc regulation enabled the identification of the [*S,S*]-EDDS biosynthetic genes

The evaluation of the general *A. japonicum* biosynthetic potential by bioinformatic tools like antiSMASH, offering a comprehensive pipeline capable of identifying biosynthetic loci covering the whole range of known secondary metabolite compound classes (Blin *et al.*, 2013; Weber *et al.*, 2015), guided the identification of the antimicrobial compounds ristomycin A and ECO-0501 and of an iron responsive synthesized, NRPS derived siderophore.

However, a key limitation of these predictive tools is the exclusive identification of biosynthetic gene clusters of already known types. To overcome this limitation the most recent version of antiSMASH (Weber *et al.*, 2015) includes the ClusterFinder algorithm (Cimermancic *et al.*, 2014). The key

assumption of ClusterFinder is that even unknown biosynthetic pathway classes are very different from known ones, they utilize the same broad enzyme families for the catalysis of key reactions.

Therefore ClusterFinder predicts putative clusters by detecting certain PFAM domains which are located outside of a comprehensive set of known biosynthetic gene cluster types (Weber *et al.*, 2015). These biosynthetic gene cluster-like regions are suggested to putatively direct the synthesis of a secondary metabolite by a new pathway class. However, also considering this advanced detection algorithms, none of the detected orphan biosynthetic gene clusters in *A. japonicum* could be bioinformatically assigned to the characteristic structural features of [*S,S*]-EDDS. The eventually identified [*S,S*]-EDDS biosynthetic genes escape indeed detection by these approaches. This suggests a novel and unique [*S,S*]-EDDS assembly mechanism that is different from the typical NRPS or NIS pathways known for ionophore synthesis and also deviates significantly from all other previously described secondary metabolite pathways.

The failure in identifying the [*S,S*]-EDDS biosynthetic genes by using normally applied biochemical and bioinformatical strategies for the isolation of secondary metabolite gene clusters necessitated the development of a new approach which relies on the exploitation of knowledge in the field of transcriptional regulation. For the identification of the [*S,S*]-EDDS biosynthetic genes this approach relied on the characterization of the Zur mediated transcriptional zinc regulation in *A. japonicum* and the subsequent computational screening of the genome sequence for zinc repressed genes, using the deduced Zur binding site as query.

The *A. japonicum* Zur binding site was deduced by investigating the Zur mediated regulation of ZnuABC in detail. The *A. japonicum* genome contains two ABC uptake systems which exhibit high similarity to the known ZnuABC system of *S. coelicolor*. However, in contrast to *S. coelicolor*, neither of them is localized adjacent to the *zur* coding region (Shin *et al.*, 2007). In addition to the zinc responsive ZnuABC, *A. japonicum* possesses also a manganese responsive ABC transporter. This system is predicted to have manganese uptake function, similar to the MntABCD system of *B. subtilis* (Que and Helmann, 2000). Regulation of this system is probably mediated by a manganese responsive DtxR-family protein like MntR of *B. subtilis* (Glasfeld *et al.*, 2003) and TroR of *Treponema pallidum* (Posey *et al.*, 1999). *A. japonicum* possess two DtxR-family proteins, an iron responsive one, regulating e.g. siderophore synthesis and a second one exhibiting higher amino acid sequence similarity to MntR of *B.* subtilis than to corynebacterial iron responsive DtxR proteins.

Specific binding of Zur to the *znuABC* and the *aesA* promoter region of *A. japonicum* was shown by EMSAs. Though Zur was added with increasing concentrations, only a single Zur shift was observed. In contrast, *S. coelicolor* Zur forms multiple complexes with its target DNAs in dependence on increased Zur concentration (Shin *et al.*, 2007; Kallifidas *et al.*, 2010). It is thought that these multiple shifts represent independent binding events of several Zur dimers to the DNA. However, for *E. coli*

Zur no such intermediate species of protein-DNA bindings were observed. There, two Zur dimers bind to the DNA in a highly cooperative way, revealing single shifts in EMSA experiments (Gilston *et al.*, 2014), comparable to the observed single Zur shift for *A. japonicum*.

Interestingly, the predicted Zur binding site within the *aesA* promoter region is located further upstream of the *aesA* ATG start codon compared to *S. coelicolor* Zur binding sites and the predicted Zur binding site within the *A. japonicum znu* promoter, which in contrast overlap the predicted -10 and -35 promoter elements (Shin *et al.*, 2007). However, zinc dependent binding of *A. japonicum* Zur to the *aesA* promoter region does nevertheless inhibit transcriptional expression of *aesA*.

3.2.3 The biogenesis of [*S,S*]-EDDS

The proposed gene products of *aesA*, *aesB* and *aesC* share significant similarity to SbnB, SbnH and SbnA, respectively, enzymes involved in the synthesis of the NIS derived siderophore SB of *S. aureus* (Cheung *et al.*, 2009). The characteristic structural feature of SB and [*S,S*]-EDDS is a central Dae moiety. This moiety is rare in natural compounds and it was long considered that it is restricted to synthetic compounds exclusively (Bucheli-Witschel and Egli, 2001).

In *S. aureus*, SB biosynthesis starts with the formation of 2,3-diaminopropionic acid (Dap), the product of the amidation of O-phospho-serine with the aminodonor glutamic acid (Kobylarz *et al.*, 2014). This reaction is coordinately catalyzed by SbnA and SbnB. The further assembly of the single SB building blocks (2x Dap, citric acid and α-ketoglutaric acid) occurs via three distinct NIS synthetases (SbnE, SbnF and SbnC). Additionally, SbnH is required to catalyze the decarboxylation of a Dap-intermediate which leads to the Dae moiety (Cheung *et al.*, 2009) (Fig. 7, publication 3).

Paradoxically to the requirement of the TCA cycle intermediates citric acid and α-ketoglutaric acid as precursors of the siderophore SB, *S. aureus* employs an iron-sparing response in absence of iron which leads to repression of the TCA cycle and to a global metabolic reorganization, that favours energy production by the glycolysis. The enzymatic activity of SbnA and SbnB however free SB biosynthesis from this metabolic limitations imposed by the iron-sparing response. This reaction delivers both α-ketoglutaric acid and Dap from glycolysis-derived metabolites (Kobylarz *et al.*, 2014; Sheldon *et al.*, 2014).

In contrast to low iron stress, zinc starvation is not supposed to induce TCA cycle repression and is thus neither leading to limitation of TCA cycle intermediates. Though, supply of the building block Dap for [*S,S*]-EDDS biosynthesis in *A. japonicum* is suggested to occur in a similar way as in *S. aureus*.

Since feeding studies with ^{13}C isotope labeled aspartic acid suggested its transamination to oxaloacetic acid prior to its incorporation into [*S,S*]-EDDS (Cebulla, 1995) it is likely to assume that AesA and AesC use aspartic acid as amino donor for the conversion of O-phospho-serine to Dap instead of glutamic acid. This predicted AesA and AesC catalyzed reaction would thus deliver the

aproteinogenic amino acid Dap and furthermore oxaloacetic acid which is also a predicted precursor of [*S,S*]-EDDS.

In a deduced, putative [*S,S*]-EDDS biosynthesis pathway (Fig. 7, publication 3) the two precursors Dap and oxaloacetic acid are assembled by a yet unknown mechanism to form a imine intermediate. A subsequent decarboxylation of the Dap moiety, leading to the Dae moiety is suggested to be catalyzed by AesB, according to the SbnH reaction of SB biosynthesis (Cheung *et al.*, 2009). A carbonyl reaction of the Dae-intermediate and a second oxaloacetic acid molecule coupled with a subsequent reduction of the two double bonds could lead to the functional [*S,S*]-EDDS.

Two out of the three predicted [*S,S*]-EDDS building blocks are assumed to be supplied by the reaction of AesA and AesC. The supply of one molecule oxaloacetic acid by this reaction possibly relieves the TCA cycle.

Though the TCA cycle is not supposed to be repressed by zinc deficiency, its maintenance and thus adequate energy supply by membrane-bound respiration seems to have special significance for [*S,S*]-EDDS biosynthesis since its production occurs exclusively in exponential growth phase, simultaneously to biomass formation (Zwicker *et al.*, 1997). Growth dependent production is also described for siderophores like the actinomycetes desferrioxamine E (Meiwes *et al.*, 1990). This reflects that metal supply by ionophores is crucial for proliferating cells to maintain the enzymatic activity of various metalloenzymes which are required in a variety of primary metabolism pathways. This is in contrast to vast majority of secondary metabolites produced by actinomycetes whose synthesis is generally associated with low specific growth rates (Bibb, 2005; Sanchez *et al.*, 2010).

The connection of [*S,S*]-EDDS production to exponential growth phase seems not to rely on the transcriptional control of the *aesA-D* operon. *aesA-D* expression in zinc deficient conditions is also detectable in stationary growth phase opposed to [*S,S*]-EDDS production stop. Furthermore, though *aesA-D* transcription is constitutive in the Δ*zur* background [*S,S*]-EDDS production is still coupled to cell proliferation in this deletion mutant. This might indicate, that zinc responsive [*S,S*]-EDDS production is guaranteed by Zur regulated precursor supply while growth dependent production is Zur independent by e.g. posttranscriptional mechanisms or by regulation of the yet unknown assembly machinery. Consequently, an adapted [*S,S*]-EDDS production to the associated physiological conditions necessitating its presence, namely zinc deficiency and anabolic pathways in cell metabolism, seems to be guaranteed by a multifactorial regulatory network.

3.2.4 Biotechnological [*S,S*]-EDDS production

These diverse parameters influencing the [*S,S*]-EDDS biosynthesis have to be considered for the conceptual design of a biotechnological [*S,S*]-EDDS production process. The growth dependent limitation in [*S,S*]-EDDS production was already assessed previously. The development of a controlled

fed batch fermentation process with prolonged exponential growth phase led to high product yield of up to 20 g L^{-1} [S,S]-EDDS (Zwicker *et al.*, 1997). Due to the ubiquitous presence of zinc in metal fermenters, this fermentation had to be carried out in a synthetic media and in intensively treated fermenters to guarantee thorough removal of zinc ions. The zinc independent [*S,S*]-EDDS production in the genetic Δ*zur* background however solves this problem and enables the fermentative production of [*S,S*]-EDDS in untreated metal fermenters and in cheap complex media.

An *A. japonicum* strain with increased [*S,S*]-EDDS productivity was generated by complementation of Δ*aesA-C* with the entire operon *aesA-D*, leading to a duplication of *aesD*. AesD is a protein with similarity to the multidrug and toxic compound extrusion (MATE) protein family. This family is exemplified by NorM of *Vibrio parahaemolyticus* which is a sodium-driven multidrug efflux pump for various compounds such as kanamycin, ciprofloxacin, ethidium etc. (Morita *et al.*, 1998; Morita *et al.*, 2000). Accordingly, it is possible that *aesD* encodes [*S,S*]-EDDS export functions. Overexpression of exporter genes is a generally applied strategy in metabolic engineering approaches to increase production yields. For example, overexpression of the ABC transporter DrrABC in *Streptomyces peucetius* ATCC 27952 led to a 2.4-fold increased doxorubicin production (Malla *et al.*, 2010), which is in a similar range as the observed increase in [*S,S*]-EDDS production due to *aesD* duplication.

The recombinant *A. japonicum* strains characterized by zinc independent [*S,S*]-EDDS production with increased production yield now set the stage to further promote strain development for the establishment of a future fermentative production process in large-scale. As this project has a reasonable prospect of becoming commercially viable the intellectual property rights were protected by a patent application (Spohn *et al.*, 2013).

4. References

Ahn, B.E., Cha, J., Lee, E.J., Han, A.R., Thompson, C.J., and Roe, J.H. (2006) Nur, a nickel-responsive regulator of the Fur family, regulates superoxide dismutases and nickel transport in *Streptomyces coelicolor*. *Mol Microbiol* **59**, 1848-1858.

Bagg, A., and Neilands, J.B. (1987) Ferric uptake regulation protein acts as a repressor, employing iron(II) as a cofactor to bind the operator of an iron transport operon in *Escherichia coli*. *Biochemistry* **26**, 5471-5477.

Banskota, A.H., McAlpine, J.B., Sorensen, D., Ibrahim, A., Aouidate, M., Piraee, M., Alarco, A.M., Farnet, C.M., and Zazopoulos, E. (2006) Genomic analyses lead to novel secondary metabolites. Part 3. ECO-0501, a novel antibacterial of a new class. *J Antibiot (Tokyo)* **59**, 533-542.

Barona-Gomez, F., Lautru, S., Francou, F.X., Leblond, P., Pernodet, J.L., and Challis, G.L. (2006) Multiple biosynthetic and uptake systems mediate siderophore-dependent iron acquisition in *Streptomyces coelicolor* A3(2) and *Streptomyces ambofacien*s ATCC 23877. *Microbiology-Sgm* **152**, 3355-3366.

Beasley, F.C., and Heinrichs, D.E. (2010) Siderophore-mediated iron acquisition in the staphylococci. *J Inorg Biochem* **104**, 282-288.

Bentley, S.D., Chater, K.F., Cerdeno-Tarraga, A.M., Challis, G.L., Thomson, N.R., James, K.D., Harris, D.E., Quail, M.A., Kieser, H., Harper, D., Bateman, A., Brown, S., Chandra, G., Chen, C.W., Collins, M., Cronin, A., Fraser, A., Goble, A., Hidalgo, J., Hornsby, T., Howarth, S., Huang, C.H., Kieser, T., Larke, L., Murphy, L., Oliver, K., O'Neil, S., Rabbinowitsch, E., Rajandream, M.A., Rutherford, K., Rutter, S., Seeger, K., Saunders, D., Sharp, S., Squares, R., Squares, S., Taylor, K., Warren, T., Wietzorrek, A., Woodward, J., Barrell, B.G., Parkhill, J., and Hopwood, D.A. (2002) Complete genome sequence of the model actinomycete *Streptomyces coelicolor* A3(2). *Nature* **417**, 141-147.

Beyer, S., Distler, J., and Piepersberg, W. (1996) The *str* gene cluster for the biosynthesis of 5'-hydroxystreptomycin in *Streptomyces glaucescens* GLA.0 (ETH 22794): New operons and evidence for pathway specific regulation by StrR. *Molecular & General Genetics* **250**, 775-784.

Bibb, M.J. (2005) Regulation of secondary metabolism in streptomycetes. *Curr Opin Microbiol* **8**, 208-215.

Bischoff, D., Bister, B., Bertazzo, M., Pfeifer, V., Stegmann, E., Nicholson, G.J., Keller, S., Pelzer, S., Wohlleben, W., and Süssmuth, R.D. (2005) The biosynthesis of vancomycin-type glycopeptide antibiotics - a model for oxidative side-chain cross-linking by oxygenases coupled to the action of peptide synthetases. *Chembiochem* **6**, 267-272.

Blin, K., Medema, M.H., Kazempour, D., Fischbach, M.A., Breitling, R., Takano, E., and Weber, T. (2013) antiSMASH 2.0-a versatile platform for genome mining of secondary metabolite producers. *Nucleic Acids Res* **41**, W204-212.

Bode, H.B., Bethe, B., Hofs, R., and Zeeck, A. (2002) Big effects from small changes: possible ways to explore nature's chemical diversity. *Chembiochem* **3**, 619-627.

Braun, V. (2001) Iron uptake mechanisms and their regulation in pathogenic bacteria. *International Journal of Medical Microbiology* **291**, 67-79.

Braun, V., and Hantke, K. (2011) Recent insights into iron import by bacteria. *Current Opinion in Chemical Biology* **15**, 328-334.
Brigham, R.B., and Pittenger, R.C. (1956) *Streptomyces orientalis*, n. sp., the source of vancomycin. *Antibiot Chemother (Northfield)* **6**, 642-647.

Bsat, N., Herbig, A., Casillas-Martinez, L., Setlow, P., and Helmann, J.D. (1998) *Bacillus subtilis* contains multiple Fur homologues: identification of the iron uptake (Fur) and peroxide regulon (PerR) repressors. *Mol Microbiol* **29**, 189-198.

Bucheli-Witschel, M., and Egli, T. (2001) Environmental fate and microbial degradation of aminopolycarboxylic acids. *FEMS Microbiol Rev* **25**, 69-106.

Butterton, J.R., and Calderwood, S.B. (1994) Identification, cloning, and sequencing of a gene required for ferric vibriobactin utilization by *Vibrio cholerae*. *J Bacteriol* **176**, 5631-5638.

Campoy, S., Jara, M., Busquets, N., Perez De Rozas, A.M., Badiola, I., and Barbe, J. (2002) Role of the high-affinity zinc uptake *znuABC* system in *Salmonella enterica* serovar Typhimurium virulence. *Infect Immun* **70**, 4721-4725.

Cebulla, I. (1995) Gewinnung komplexbildender Substanzen mittels *Amycolatopsis orientalis*. *University of Tübingen*, Doctoral Thesis.

Cescau, S., Cwerman, H., Letoffe, S., Delepelaire, P., Wandersman, C., and Biville, F. (2007) Heme acquisition by hemophores. *Biometals* **20**, 603-613.

Challis, G.L. (2005) A widely distributed bacterial pathway for siderophore biosynthesis independent of nonribosomal peptide synthetases. *Chembiochem* **6**, 601-611.

Chen, L., Liu, T., and Ma, C. (2010) Metal complexation and biodegradation of EDTA and S,S-EDDS: a density functional theory study. *J Phys Chem A* **114**, 443-454.

Cheung, J., Beasley, F.C., Liu, S., Lajoie, G.A., and Heinrichs, D.E. (2009) Molecular characterization of staphyloferrin B biosynthesis in *Staphylococcus aureus*. *Mol Microbiol* **74**, 594-608.

Cimermancic, P., Medema, M.H., Claesen, J., Kurita, K., Brown, L.C.W., Mavrommatis, K., Pati, A., Godfrey, P.A., Koehrsen, M., Clardy, J., Birren, B.W., Takano, E., Sali, A., Linington, R.G., and Fischbach, M.A. (2014) Insights into secondary metabolism from a global analysis of prokaryotic biosynthetic gene clusters. *Cell* **158**, 412-421.

Citiulo, F., Jacobsen, I.D., Miramon, P., Schild, L., Brunke, S., Zipfel, P., Brock, M., Hube, B., and Wilson, D. (2012) *Candida albicans* scavenges host zinc via Pra1 during endothelial invasion. *Plos Pathogens* **8**.

Cohen, S.M., and Raymond, K.N. (2000) Catecholate/salicylate heteropodands: Demonstration of a catecholate to salicylate coordination change. *Inorganic Chemistry* **39**, 3624-3631.

Cokesa, Z., Lakner, S., Knackmuss, H.J., and Rieger, P.G. (2004) A stereoselective carbon-nitrogen lyase from *Ralstonia* sp SLRS7 cleaves two of three isomers of iminodisuccinate. *Biodegradation* **15**, 229-239.

Crosa, J.H., and Walsh, C.T. (2002) Genetics and assembly line enzymology of siderophore biosynthesis in bacteria. *Microbiology and Molecular Biology Reviews* **66**, 223-249.

de Lorenzo, V., and Neilands, J.B. (1986) Characterization of *iucA* and *iucC* genes of the aerobactin system of plasmid ColV-K30 in *Escherichia coli*. *J Bacteriol* **167**, 350-355.
Diaz-Mireles, E., Wexler, M., Sawers, G., Bellini, D., Todd, J.D., and Johnston, A.W.B. (2004) The Fur-like protein Mur of *Rhizobium leguminosarum* is a Mn^{2+}-responsive transcriptional regulator. *Microbiology-Sgm* **150**, 1447-1456.

Donadio, S., Sosio, M., Stegmann, E., Weber, T., and Wohlleben, W. (2005) Comparative analysis and insights into the evolution of gene clusters for glycopeptide antibiotic biosynthesis. *Molecular Genetics and Genomics* **274**, 40-50.

Dussurget, O., Rodriguez, M., and Smith, I. (1998) Protective role of the *Mycobacterium smegmatis* IdeR against reactive oxygen species and isoniazid toxicity. *Tuber Lung Dis* **79**, 99-106.

Dussurget, O., Timm, J., Gomez, M., Gold, B., Yu, S.W., Sabol, S.Z., Holmes, R.K., Jacobs, W.R., and Smith, I. (1999) Transcriptional control of the iron-responsive *fxbA* gene by the mycobacterial regulator IdeR. *J Bacteriol* **181**, 3402-3408.

Ernst, J.F., Bennett, R.L., and Rothfield, L.I. (1978) Constitutive expression of the iron-enterochelin and ferrichrome uptake systems in a mutant strain of *Salmonella typhimurium*. *J Bacteriol* **135**, 928-934.

Everest, G.J., and Meyers, P.R. (2011) Evaluation of the antibiotic biosynthetic potential of the genus *Amycolatopsis* and description of *Amycolatopsis circi* sp. nov., *Amycolatopsis equina* sp. nov. and *Amycolatopsis hippodromi* sp. nov. *J Appl Microbiol* **111**, 300-311.

Fedorenko, V., Genilloud, O., Horbal, L., Marcone, G.L., Marinelli, F., Paitan, Y., and Ron, E.Z. (2015) Antibacterial discovery and development: from gene to product and back. *Biomed Research International*.

Fehlner, J.R., Schenck, J.R., Tarbell, D.S., and Hutchins, R.E. (1972) Structure of ristocetin A. *Proc Natl Acad Sci U S A* **69**, 2420-&.

Fillat, M.F. (2014) The FUR (ferric uptake regulator) superfamily: diversity and versatility of key transcriptional regulators. *Arch Biochem Biophys* **546**, 41-52.

Frasch, H.J. (2008) Analysen zur EDDS-Biosynthese in *Amycolatopsis japonicum* MG417-C17. *University of Tübingen*, Diploma Thesis.

Gaballa, A., and Helmann, J.D. (1998) Identification of a zinc-specific metalloregulatory protein, Zur, controlling zinc transport operons in *Bacillus subtilis*. *J Bacteriol* **180**, 5815-5821.

Gehring, A.M., Mori, I., and Walsh, C.T. (1998) Reconstitution and characterization of the *Escherichia coli* enterobactin synthetase from EntB, EntE, and EntF. *Biochemistry* **37**, 2648-2659.

Gilston, B.A., Wang, S., Marcus, M.D., Canalizo-Hernandez, M.A., Swindell, E.P., Xue, Y., Mondragon, A., and O'Halloran, T.V. (2014) Structural and Mechanistic Basis of Zinc Regulation Across the *E. coli* Zur Regulon. *PLoS Biol* **12**, e1001987.

Glasfeld, A., Guedon, E., Helmann, J.D., and Brennan, R.G. (2003) Structure of the manganese-bound manganese transport regulator of *Bacillus subtilis*. *Nature Structural Biology* **10**, 652-657.

Grundy, W.E., Sinclair, A.C., Theriault, R.J., Goldstein, A.W., Rickher, C.J., Warren, H.B., Jr., Oliver, T.J., and Sylvester, J.C. (1956) Ristocetin, microbiologic properties. *Antibiot Annu*, 687-692.

Günter-Seeboth, K., and Schupp, T. (1995) Cloning and sequence-analysis of the *Corynebacterium diphtheriae dtxR* homolog from *Streptomyces lividans* and *S. pilosus* encoding a putative iron repressor protein. *Gene* **166**, 117-119.

Hadatsch, B., Butz, D., Schmiederer, T., Steudle, J., Wohlleben, W., Süssmuth, R., and Stegmann, E. (2007) The biosynthesis of teicoplanin-type glycopeptide antibiotics: assignment of P450 monooxygenases to side chain cyclizations of glycopeptide A47934. *Chem Biol* **14**, 1078-1089.

Hani, E.K., and Chan, V.L. (1994) Cloning, characterization, and nucleotide-sequence analysis of the *argH* gene from *Campylobacter jejuni* TGH9011 encoding argininosuccinate lyase. *J Bacteriol* **176**, 1865-1871.

Hantke, K. (1981) Regulation of ferric iron transport in *Escherichia coli* K12: isolation of a constitutive mutant. *Mol Gen Genet* **182**, 288-292.

Hantke, K. (2001a) Bacterial zinc transporters and regulators. *Biometals* **14**, 239-249.

Hantke, K. (2001b) Iron and metal regulation in bacteria. *Curr Opin Microbiol* **4**, 172-177.

Hough, E., Hansen, L.K., Birknes, B., Jynge, K., Hansen, S., Hordvik, A., Little, C., Dodson, E., and Derewenda, Z. (1989) High-resolution (1.5 A) crystal structure of phospholipase C from *Bacillus cereus*. *Nature* **338**, 357-360.

Hubbard, B.K., Thomas, M.G., and Walsh, C.T. (2000) Biosynthesis of L-*p*-hydroxyphenylglycine, a non-proteinogenic amino acid constituent of peptide antibiotics. *Chem Biol* **7**, 931-942.

Kallifidas, D., Pascoe, B., Owen, G.A., Strain-Damerell, C.M., Hong, H.J., and Paget, M.S. (2010) The zinc-responsive regulator Zur controls expression of the coelibactin gene cluster in *Streptomyces coelicolor*. *J Bacteriol* **192**, 608-611.

Kastner, S., Müller, S., Natesan, L., König, G., Guthke, R., and Nett, M. (2012) 4-Hydroxyphenylglycine biosynthesis in *Herpetosiphon aurantiacus*: a case of gene duplication and catalytic divergence. *Archives of Microbiology* **194**, 557-566.

Kenney, G.E., and Rosenzweig, A.C. (2014) Genome mining for methanobactins. *Journal of Biological Inorganic Chemistry* **19**, S387-S387.

Kezerian, C., and Ramsey, W.M. (1964) Bisadducts of diamines and unsaturated acids (US Patent 3,158,635).

Kim, H.J., Graham, D.W., DiSpirito, A.A., Alterman, M.A., Galeva, N., Larive, C.K., Asunskis, D., and Sherwood, P.M. (2004) Methanobactin, a copper-acquisition compound from methane-oxidizing bacteria. *Science* **305**, 1612-1615.

Kobylarz, M.J., Grigg, J.C., Takayama, S.J., Rai, D.K., Heinrichs, D.E., and Murphy, M.E. (2014) Synthesis of L-2,3-diaminopropionic acid, a siderophore and antibiotic precursor. *Chem Biol* **21**, 379-388.

Kodani, S., Komaki, H., Suzuki, M., Hemmi, H., and Ohnishi-Kameyama, M. (2015) Isolation and structure determination of new siderophore albachelin from *Amycolatopsis alba*. *Biometals* **28**, 381-389.

Kołodyńska, D. (2011) Chelating agents of a new generation as an alternative to conventional chelators for heavy metal ions removal from different waste waters. In Expanding issues in desalination, R.Y. Ning, ed. (Rijeka, Croatia: InTech), pp. 339-370.

Krezel, A., Hao, Q., and Maret, W. (2007) Zinc/thiolate redox biochemistry of metallothionein and the control of zinc ion fluctuations in cell signaling. *Arch Biochem Biophys* **463**, 188-200.

Kunstmann, M.P., Mitscher, L.A., Porter, J.N., Shay, A.J., and Darken, M.A. (1968) LL-AV290, a new antibiotic. I. Fermentation, isolation, and characterization. *Antimicrob Agents Chemother* **8**, 242-245.

Kwun, M.J., and Hong, H.J. (2014) Draft genome sequence of *Amycolatopsis lurida* NRRL 2430, producer of the glycopeptide family antibiotic ristocetin. *Genome Announc* **2**.

Labeda, D.P. (1995) *Amycolatopsis coloradensis* sp. nov., the avoparcin (LL-AV290)-producing strain. *Int J Syst Bacteriol* **45**, 124-127.

Laureti, L., Song, L., Huang, S., Corre, C., Leblond, P., Challis, G.L., and Aigle, B. (2011) Identification of a bioactive 51-membered macrolide complex by activation of a silent polyketide synthase in *Streptomyces ambofaciens*. *Proc Natl Acad Sci U S A* **108**, 6258-6263.

Lautru, S., Deeth, R.J., Bailey, L.M., and Challis, G.L. (2005) Discovery of a new peptide natural product by *Streptomyces coelicolor* genome mining. *Nat Chem Biol* **1**, 265-269.

Lei, X., Yuan, F., Shi, Y., Li, X., Wang, L., and Hong, B. (2015) Draft genome sequence of norvancomycin-producing strain *Amycolatopsis orientalis* CPCC200066. *Genome Announc* **3**.

Lesuisse, E., Casterassimon, M., and Labbe, P. (1995) Ferrireductase activity in *Saccharomyces cerevisiae* and other fungi - colorimetric assays on agar plates. *Anal Biochem* **226**, 375-377.

Lin, H., Fischbach, M.A., Liu, D.R., and Walsh, C.T. (2005) *In vitro* characterization of salmochelin and enterobactin trilactone hydrolases IroD, IroE, and Fes. *J Am Chem Soc* **127**, 11075-11084.

Liu, W.C., Fisher, S.M., Wells, J.S., Jr., Ricca, C.S., Principe, P.A., Trejo, W.H., Bonner, D.P., Gougoutos, J.Z., Toeplitz, B.K., and Sykes, R.B. (1981) Siderochelin, a new ferrous-ion chelating agent produced by *Nocardia*. *J Antibiot (Tokyo)* **34**, 791-799.

Lu, C.H., Ye, F.W., and Shen, Y.M. (2015) Siderochelins with anti-mycobacterial activity from *Amycolatopsis* sp. LZ149. *Chin J Nat Med* **13**, 69-72.

Lucarelli, D., Russo, S., Garman, E., Milano, A., Meyer-Klaucke, W., and Pohl, E. (2007) Crystal structure and function of the zinc uptake regulator FurB from *Mycobacterium tuberculosis*. *J Biol Chem* **282**, 9914-9922.

Lukezic, T., Lesnik, U., Podgorsek, A., Horvat, J., Polak, T., Sala, M., Jenko, B., Raspor, P., Herron, P.R., Hunter, I.S., and Petkovic, H. (2013) Identification of the chelocardin biosynthetic gene cluster from *Amycolatopsis sulphurea*: a platform for producing novel tetracycline antibiotics. *Microbiology* **159**, 2524-2532.

Malla, S., Niraula, N.P., Liou, K., and Sohng, J.K. (2010) Self-resistance mechanism in *Streptomyces peucetius*: overexpression of *drrA*, *drrB* and *drrC* for doxorubicin enhancement. *Microbiol Res* **165**, 259-267.

Marahiel, M.A. (1997) Protein templates for the biosynthesis of peptide antibiotics. *Chem Biol* **4**, 561-567.

Meiwes, J., Fiedler, H.P., Zähner, H., Konetschnyrapp, S., and Jung, G. (1990) Production of desferrioxamine E and new analogs by directed fermentation and feeding fermentation. *Appl Microbiol Biotechnol* **32**, 505-510.

Miethke, M. (2013) Molecular strategies of microbial iron assimilation: from high-affinity complexes to cofactor assembly systems. *Metallomics* **5**, 15-28.

Miethke, M., and Marahiel, M.A. (2007) Siderophore-based iron acquisition and pathogen control. *Microbiology and Molecular Biology Reviews* **71**, 413-451.

Moll, C. (2006) Untersuchung der EDDS-Biosynthese in *Amycolatopsis japonicum*. *University of Tübingen*, Diploma Thesis.

Monciardini, P., Iorio, M., Maffioli, S., Sosio, M., and Donadio, S. (2014) Discovering new bioactive molecules from microbial sources. *Microb Biotechnol* **7**, 209-220.

Morita, Y., Kataoka, A., Shiota, S., Mizushima, T., and Tsuchiya, T. (2000) NorM of *Vibrio parahaemolyticus* is an $Na^{(+)}$-driven multidrug efflux pump. *J Bacteriol* **182**, 6694-6697.

Morita, Y., Kodama, K., Shiota, S., Mine, T., Kataoka, A., Mizushima, T., and Tsuchiya, T. (1998) NorM, a putative multidrug efflux protein, of *Vibrio parahaemolyticus* and its homolog in *Escherichia coli*. *Antimicrob Agents Chemother* **42**, 1778-1782.

Mulyani, S., Egel, E., Kittel, C., Turkanovic, S., Wohlleben, W., Süssmuth, R.D., and van Pee, K.H. (2010) The thioesterase Bhp is involved in the formation of beta-hydroxytyrosine during balhimycin biosynthesis in *Amycolatopsis balhimycina*. *Chembiochem* **11**, 266-271.

Nadkarni, S.R., Patel, M.V., Chatterjee, S., Vijayakumar, E.K., Desikan, K.R., Blumbach, J., Ganguli, B.N., and Limbert, M. (1994) Balhimycin, a new glycopeptide antibiotic produced by *Amycolatopsis* sp. Y-86,21022. Taxonomy, production, isolation and biological activity. *J Antibiot (Tokyo)* **47**, 334-341.

Neal, J.A., and Rose, N.J. (1968) Stereospecific ligands and their complexes. I. A cobalt (III) complex of ethylenediaminedisuccinic acid. *Inorganic Chemistry* **7**, 2405-&.

Nishikiori, T., Okuyama, A., Naganawa, H., Takita, T., Hamada, M., Takeuchi, T., Aoyagi, T., and Umezawa, H. (1984) Production by actinomycetes of (S,S)-N,N'-ethylenediamine-disuccinic acid, an inhibitor of phospholipase C. *J Antibiot (Tokyo)* **37**, 426-427.

O'Brien, I.G., and Gibson, F. (1970) Structure of enterochelin and related 2,3-dihydroxyn-benzoylserine conjugates from *Escherichia coli*. *Biochim Biophys Acta* **215**, 393-&.

Orama, M., Hyvonen, H., Saarinen, H., and Aksela, R. (2002) Complexation of [S,S] and mixed stereoisomers of N,N '-ethylenediaminedisuccinic acid (EDDS) with Fe(III), Cu(II), Zn(II) and Mn(II) ions in aqueous solution. *Journal of the Chemical Society-Dalton Transactions*, 4644-4648.

Oves-Costales, D., Kadi, N., and Challis, G.L. (2009) The long-overlooked enzymology of a nonribosomal peptide synthetase-independent pathway for virulence-conferring siderophore biosynthesis. *Chem Commun (Camb)*, 6530-6541.

Owen, G.A., Pascoe, B., Kallifidas, D., and Paget, M.S. (2007) Zinc-responsive regulation of alternative ribosomal protein genes in *Streptomyces coelicolor* involves Zur and σR. *J Bacteriol* **189**, 4078-4086.

Patzer, S.I., and Hantke, K. (1998) The ZnuABC high-affinity zinc uptake system and its regulator Zur in *Escherichia coli*. *Mol Microbiol* **28**, 1199-1210.

Pawlik, M.C., Hubert, K., Joseph, B., Claus, H., Schoen, C., and Vogel, U. (2012) The zinc-responsive regulon of *Neisseria meningitidis* comprises 17 genes under control of a Zur element. *J Bacteriol* **194**, 6594-6603.

Pfeifer, V., Nicholson, G.J., Ries, J., Recktenwald, J., Schefer, A.B., Shawky, R.M., Schröder, J., Wohlleben, W., and Pelzer, S. (2001) A polyketide synthase in glycopeptide biosynthesis - The biosynthesis of the non-proteinogenic amino acid (S)-3,5-dihydroxyphenylglycine. *Journal of Biological Chemistry* **276**, 38370-38377.

Pohl, E., Holmes, R.K., and Hol, W.G.J. (1999a) Crystal structure of a cobalt-activated diphtheria toxin repressor-DNA complex reveals a metal-binding SH3-like domain. *J Mol Biol* **292**, 653-667.

Pohl, E., Holmes, R.K., and Hol, W.G.J. (1999b) Crystal structure of the iron-dependent regulator (IdeR) from *Mycobacterium tuberculosis* shows both metal binding sites fully occupied. *J Mol Biol* **285**, 1145-1156.

Pollack, J.R., and Neilands, J.B. (1970) Enterobactin, an iron transport compound from *Salmonella typhimurium*. *Biochem Biophys Res Commun* **38**, 989-992.

Posey, J.E., Hardham, J.M., Norris, S.J., and Gherardini, F.C. (1999) Characterization of a manganese-dependent regulatory protein, TroR, from *Treponema pallidum*. *Proc Natl Acad Sci U S A* **96**, 10887-10892.

Puk, O., Bischoff, D., Kittel, C., Pelzer, S., Weist, S., Stegmann, E., Süssmuth, R.D., and Wohlleben, W. (2004) Biosynthesis of chloro-beta-hydroxytyrosine, a nonproteinogenic amino acid of the peptidic backbone of glycopeptide antibiotics. *J Bacteriol* **186**, 6093-6100.

Puk, O., Huber, P., Bischoff, D., Recktenwald, J., Jung, G., Süssmuth, R.D., van Pee, K.H., Wohlleben, W., and Pelzer, S. (2002) Glycopeptide biosynthesis in *Amycolatopsis mediterranei* DSM5908: function of a halogenase and a haloperoxidase/perhydrolase. *Chem Biol* **9**, 225-235.

Qi, Z.H., Hamza, I., and O'Brian, M.R. (1999) Heme is an effector molecule for iron-dependent degradation of the bacterial iron response regulator (Irr) protein. *Proc Natl Acad Sci U S A* **96**, 13056-13061.

Que, Q., and Helmann, J.D. (2000) Manganese homeostasis in *Bacillus subtilis* is regulated by MntR, a bifunctional regulator related to the diphtheria toxin repressor family of proteins. *Mol Microbiol* **35**, 1454-1468.

Retzlaff, L., and Distler, J. (1995) The regulator of streptomycin gene expression, StrR, of *Streptomyces griseus* is a DNA binding activator protein with multiple recognition sites. *Mol Microbiol* **18**, 151-162.

Reynolds, P.E. (1989) Structure, biochemistry and mechanism of action of glycopeptide antibiotics. *Eur J Clin Microbiol Infect Dis* **8**, 943-950.

Sanchez, S., Chavez, A., Forero, A., Garcia-Huante, Y., Romero, A., Sanchez, M., Rocha, D., Sanchez, B., Avalos, M., Guzman-Trampe, S., Rodriguez-Sanoja, R., Langley, E., and Ruiz, B. (2010) Carbon source regulation of antibiotic production. *Journal of Antibiotics* **63**, 442-459.

Sarji, K.E., Stratton, R.D., Wagner, R.H., and Brinkhous, K.M. (1974) Nature of von Willebrand factor: a new assay and a specific inhibitor. *Proc Natl Acad Sci U S A* **71**, 2937-2941.

Schäberle, T.F., Vollmer, W., Frasch, H.J., Hüttel, S., Kulik, A., Röttgen, M., von Thaler, A.K., Wohlleben, W., and Stegmann, E. (2011) Self-resistance and cell wall composition in the glycopeptide producer *Amycolatopsis balhimycina*. *Antimicrob Agents Chemother* **55**, 4283-4289.

Schowanek, D., Feijtel, T.C., Perkins, C.M., Hartman, F.A., Federle, T.W., and Larson, R.J. (1997) Biodegradation of [S,S], [R,R] and mixed stereoisomers of ethylene diamine disuccinic acid (EDDS), a transition metal chelator. *Chemosphere* **34**, 2375-2391.

Semrau, J.D., Jagadevan, S., DiSpirito, A.A., Khalifa, A., Scanlan, J., Bergman, B.H., Freemeier, B.C., Baral, B.S., Bandow, N.L., Vorobev, A., Haft, D.H., Vuilleumier, S., and Murrell, J.C. (2013) Methanobactin and MmoD work in concert to act as the 'copper-switch' in methanotrophs. *Environ Microbiol* **15**, 3077-3086.

Sensi, P., Margalith, P., and Timbal, M.T. (1959) Rifomycin, a new antibiotic; preliminary report. *Farmaco Sci* **14**, 146-147.

Seyedsayamdost, M.R., Traxler, M.F., Zheng, S.L., Kolter, R., and Clardy, J. (2011) Structure and biosynthesis of amychelin, an unusual mixed-ligand siderophore from *Amycolatopsis* sp. AA4. *J Am Chem Soc* **133**, 11434-11437.

Shawky, R.M., Puk, O., Wietzorrek, A., Pelzer, S., Takano, E., Wohlleben, W., and Stegmann, E. (2007) The border sequence of the balhimycin biosynthesis gene cluster from *Amycolatopsis balhimycina* contains *bbr*, encoding a StrR-like pathway-specific regulator. *J Mol Microbiol Biotechnol* **13**, 76-88.

Sheldon, J.R., Marolda, C.L., and Heinrichs, D.E. (2014) TCA cycle activity in *Staphylococcus aureus* is essential for iron-regulated synthesis of staphyloferrin A, but not staphyloferrin B: the benefit of a second citrate synthase. *Mol Microbiol* **92**, 824-839.

Shin, J.H., Oh, S.Y., Kim, S.J., and Roe, J.H. (2007) The zinc-responsive regulator Zur controls a zinc uptake system and some ribosomal proteins in *Streptomyces coelicolor* A3(2). *J Bacteriol* **189**, 4070-4077.

Spohn, M., Kirchner, N., Kulik, A., Jochim, A., Wolf, F., Münzer, P., Borst, O., Gross, H., Wohlleben, W., and Stegmann, E. (2014) Overproduction of ristomycin A by activation of a silent gene cluster in *Amycolatopsis japonicum* MG417-CF17. *Antimicrob Agents Chemother* **58**, 6185-6196.

Spohn, M., Stegmann, E., Wohlleben, W., and Weber, T. (2013) [S,S]-EDDS Biosynthesegene und -proteine und Verfahren zur Biosynthese von [S,S]-EDDS (German Patent Application 10 2013 217 543.4).

Spohn, M., Wohlleben, W., and Stegmann, E. (2016) Elucidation of the zinc dependent regulation in *Amycolatopsis japonicum* enabled the identification of the ethylenediamine-disuccinate ([*S,S*]-EDDS) genes. *Environ Microbiol*. **18**, 1249-1263.

Stegmann, E. (1999) Molekulargenetische und biochemische Untersuchungen der EDDS-Produktion in *Amycolatopsis japonicum* MG417-CF17. *University of Tübingen*, Doctoral Thesis.

Stegmann, E., Albersmeier, A., Spohn, M., Gert, H., Weber, T., Wohlleben, W., Kalinowski, J., and Rückert, C. (2014) Complete genome sequence of the actinobacterium *Amycolatopsis japonica* MG417-CF17 (=DSM 44213T) producing (S,S)-N,N'-ethylenediaminedisuccinic acid. *J Biotechnol* **189C**, 46-47.

Stegmann, E., Frasch, H.J., and Wohlleben, W. (2010) Glycopeptide biosynthesis in the context of basic cellular functions. *Curr Opin Microbiol* **13**, 595-602.

Stegmann, E., Pelzer, S., Bischoff, D., Puk, O., Stockert, S., Butz, D., Zerbe, K., Robinson, J., Süsmuth, R.D., and Wohlleben, W. (2006) Genetic analysis of the balhimycin (vancomycin-type) oxygenase genes. *J Biotechnol* **124**, 640-653.

Stegmann, E., Pelzer, S., Wilken, K., and Wohlleben, W. (2001) Development of three different gene cloning systems for genetic investigation of the new species *Amycolatopsis japonicum* MG417-CF17, the ethylenediaminedisuccinic acid producer. *J Biotechnol* **92**, 195-204.

Stinchi, S., Carrano, L., Lazzarini, A., Feroggio, M., Grigoletto, A., Sosio, M., and Donadio, S. (2006) A derivative of the glycopeptide A40926 produced by inactivation of the beta-hydroxylase gene in *Nonomuraea* sp. ATCC39727. *FEMS Microbiol Lett* **256**, 229-235.

Stintzi, A., Barnes, C., Xu, L., and Raymond, K.N. (2000) Microbial iron transport via a siderophore shuttle: A membrane ion transport paradigm. *Proc Natl Acad Sci U S A* **97**, 10691-10696.

Takahashi, R., Fujimoto, N., Suzuki, M., and Endo, T. (1997) Biodegradabilities of ethylenediamine-N,N'-disuccinic acid (EDDS) and other chelating agents. *Biosci Biotechnol Biochem* **61**, 1957-1959.

Thykaer, J., Nielsen, J., Wohlleben, W., Weber, T., Gutknecht, M., Lantz, A.E., and Stegmann, E. (2010) Increased glycopeptide production after overexpression of shikimate pathway genes being part of the balhimycin biosynthetic gene cluster. *Metabolic Engineering* **12**, 455-461.

Tomono, A., Tsai, Y., Yamazaki, H., Ohnishi, Y., and Horinouchi, S. (2005) Transcriptional control by A-factor of *strR*, the pathway-specific transcriptional activator for streptomycin biosynthesis in *Streptomyces griseus*. *J Bacteriol* **187**, 5595-5604.

Truman, A.W., Kwun, M.J., Cheng, J., Yang, S.H., Suh, J.W., and Hong, H.J. (2014) Antibiotic resistance mechanisms inform discovery: identification and characterization of a novel *Amycolatopsis* strain producing ristocetin. *Antimicrob Agents Chemother* **58**, 5687-5695.

Tunca, S., Barreiro, C., Sola-Landa, A., Coque, J.J.R., and Martin, J.F. (2007) Transcriptional regulation of the desferrioxamine gene cluster of *Streptomyces coelicolor* is mediated by binding of DmdR1 to an iron box in the promoter of the *desA* gene. *Febs Journal* **274**, 1110-1122.

Udwary, D.W., Zeigler, L., Asolkar, R.N., Singan, V., Lapidus, A., Fenical, W., Jensen, P.R., and Moore, B.S. (2007) Genome sequencing reveals complex secondary metabolome in the marine actinomycete *Salinispora tropica*. *Proc Natl Acad Sci U S A* **104**, 10376-10381.

van Wageningen, A.M., Kirkpatrick, P.N., Williams, D.H., Harris, B.R., Kershaw, J.K., Lennard, N.J., Jones, M., Jones, S.J., and Solenberg, P.J. (1998) Sequencing and analysis of genes involved in the biosynthesis of a vancomycin group antibiotic. *Chem Biol* **5**, 155-162.

Weber, T., Blin, K., Duddela, S., Krug, D., Kim, H.U., Bruccoleri, R., Lee, S.Y., Fischbach, M.A., Muller, R., Wohlleben, W., Breitling, R., Takano, E., and Medema, M.H. (2015) antiSMASH 3.0-a

comprehensive resource for the genome mining of biosynthetic gene clusters. *Nucleic Acids Res* **43**, W237-243.

Williams, D.H., Rajananda, V., and Kalman, J.R. (1979) On the structure and mode of action of the antibiotic ristocetin A. *Journal of the Chemical Society-Perkin Transactions 1*, 787-792.

Witschel, M., and Egli, T. (1998) Purification and characterization of a lyase from the EDTA-degrading bacterial strain DSM 9103 that catalyzes the splitting of [S,S]-ethylenediaminedisuccinate, a structural isomer of EDTA (vol 8, pg 419, 1998). *Biodegradation* **9**, 389-389.

Yang, K.Q., Han, L., and Vining, L.C. (1995) Regulation of jadomycin B production in *Streptomyces venezuelae* ISP5230: involvement of a repressor gene, *jadR*$_2$. *J Bacteriol* **177**, 6111-6117.

Zerikly, M., and Challis, G.L. (2009) Strategies for the discovery of new natural products by genome mining. *Chembiochem* **10**, 625-633.

Zhao, B., Moody, S.C., Hider, R.C., Lei, L., Kelly, S.L., Waterman, M.R., and Lamb, D.C. (2012) Structural analysis of cytochrome P450 105N1 involved in the biosynthesis of the zincophore, coelibactin. *Int J Mol Sci* **13**, 8500-8513.

Zhu, M.G., Valdebenito, M., Winkelmann, G., and Hantke, K. (2005) Functions of the siderophore esterases IroD and IroE in iron-salmochelin utilization. *Microbiology-Sgm* **151**, 2363-2372.

Zwicker, N., Theobald, U., Zähner, H., and Fiedler, H.P. (1997) Optimization of fermentation conditions for the production of ethylene-diamine-disuccinic acid by *Amycolatopsis orientalis*. *J Ind Microbiol Biotechnol* **19**, 280–285.

5. Publications

5.1 Publication 1

Spohn, M., Kirchner, N., Kulik, A., Jochim, A., Wolf, F., Münzer, P., Borst, O., Gross, H., Wohlleben, W., and Stegmann, E. (2014) Overproduction of ristomycin A by activation of a silent gene cluster in *Amycolatopsis japonicum* MG417-CF17. *Antimicrobial Agents and Chemotherapy* **58**, 6185-6196.

Overproduction of Ristomycin A by Activation of a Silent Gene Cluster in *Amycolatopsis japonicum* MG417-CF17

Marius Spohn,[a] Norbert Kirchner,[b,c] Andreas Kulik,[a] Angelika Jochim,[a] Felix Wolf,[a] Patrick Muenzer,[d] Oliver Borst,[e] Harald Gross,[b,c] Wolfgang Wohlleben,[a,b] Evi Stegmann[a,b]

Interfaculty Institute of Microbiology and Infection Medicine Tuebingen, Microbiology/Biotechnology, University of Tuebingen, Tuebingen, Germany[a]; German Centre for Infection Research (DZIF), Partner Site Tuebingen, Tuebingen, Germany[b]; Pharmaceutical Institute, Department of Pharmaceutical Biology, University of Tuebingen, Tuebingen, Germany[c]; Department of Physiology I, University of Tuebingen, Tuebingen, Germany[d]; Department of Cardiology and Cardiovascular Medicine, University of Tuebingen, Tuebingen, Germany[e]

The emergence of antibiotic-resistant pathogenic bacteria within the last decades is one reason for the urgent need for new antibacterial agents. A strategy to discover new anti-infective compounds is the evaluation of the genetic capacity of secondary metabolite producers and the activation of cryptic gene clusters (genome mining). One genus known for its potential to synthesize medically important products is *Amycolatopsis*. However, *Amycolatopsis japonicum* does not produce an antibiotic under standard laboratory conditions. In contrast to most *Amycolatopsis* strains, *A. japonicum* is genetically tractable with different methods. In order to activate a possible silent glycopeptide cluster, we introduced a gene encoding the transcriptional activator of balhimycin biosynthesis, the *bbr* gene from *Amycolatopsis balhimycina* (bbr_{Aba}), into *A. japonicum*. This resulted in the production of an antibiotically active compound. Following whole-genome sequencing of *A. japonicum*, 29 cryptic gene clusters were identified by genome mining. One of these gene clusters is a putative glycopeptide biosynthesis gene cluster. Using bioinformatic tools, ristomycin (syn. ristocetin), a type III glycopeptide, which has antibacterial activity and which is used for the diagnosis of von Willebrand disease and Bernard-Soulier syndrome, was deduced as a possible product of the gene cluster. Chemical analyses by high-performance liquid chromatography and mass spectrometry (HPLC-MS), tandem mass spectrometry (MS/MS), and nuclear magnetic resonance (NMR) spectroscopy confirmed the *in silico* prediction that the recombinant *A. japonicum*/pRM4-bbr_{Aba} synthesizes ristomycin A.

The nocardioform actinomycete *Amycolatopsis japonicum* MG417-CF17 (DSM 44213) is known as the producer of the hexadentate chelating agent (*S*,*S*)-ethylenediaminedisuccinic acid [(*S*,*S*)-EDDS] (1), which is a biodegradable EDTA isomer (2) with similar properties. Though members of the genus *Amycolatopsis* are major producers of various antimicrobial compounds, such as the medically relevant rifamycin and vancomycin, no bioactive secondary metabolite has been isolated from *A. japonicum* so far.

Genome sequencing projects have revealed that the potential of actinomycetes for the production of valuable secondary metabolites is much larger than previously expected. In certain cases, more than 30 gene clusters encoding components of pathways for secondary metabolite biosynthesis have been found per actinomycete genome. For example, *Streptomyces coelicolor*, *Streptomyces avermitilis*, *Streptomyces griseus*, and *Saccharopolyspora erythraea* are each known to produce three to five secondary metabolites but actually possess more than 20 gene clusters that are predicted to encode components of biosynthetic pathways for secondary metabolites (3, 4, 5, 6). This exemplifies that a large number of these pathways are cryptic, meaning that they are expressed poorly or not at all under standardized laboratory conditions. One strategy to obtain access to this enormous genetic potential is the genome mining approach. The crucial point of genome mining is in learning how to identify, subsequently activate, and finally exploit these gene clusters, making their product accessible for evaluation as drug leads and for other biotechnological applications. The availability of hundreds of actinomycete genome sequences and the rapidly decreasing costs of genome sequencing have made genome mining the most promising tool to generate raw data for drug discovery. However, due to the biochemical heterogeneity in secondary metabolite biosynthesis and the high number of putative gene clusters, the identification, categorization, and interpretation of the information encoded within the genomes required automation. Bioinformatic tools such as antiSMASH 2.0 (7) offer a comprehensive pipeline capable of discovering and characterizing biosynthetic loci covering the whole range of described secondary metabolite compound classes.

In order to use this information, various strategies to activate cryptic secondary metabolite gene clusters have been applied. In many cases, stress conditions or variations of culture conditions led to the production of new metabolites. More-targeted approaches are the exchange of promoters or heterologous expression of all relevant genes in a suitable host (8, 9).

Previously we elucidated the biosynthesis of the glycopeptide balhimycin in detail in *Amycolatopsis balhimycina* (10). The genus *Amycolatopsis* is known to produce various glycopeptides that are important clinical emergency antibiotics. New glycopeptides might be key compounds to treat currently spreading glycopeptide-resistant pathogens, like glycopeptide-intermediate *Staphylococcus aureus* and vancomycin-resistant enterococci (VRE). A particular function is described for the highly glycosylated glycopeptide ristomycin A (also called ristocetin A), previously identified in *Amycolatopsis lurida* (11). Since ristomycin A causes thrombocytopenia and platelet agglutination, it is no longer used for the treatment of human staphylococcal infections but solely applied to assay those therapeutically unfavorable functions *in vitro* as a diagnosis compound to detect widespread hereditary genetic disorders such as von Willebrand disease and Bernard-Soulier syndrome (12).

In this study, we were able to identify and activate a new type III glycopeptide gene cluster in *A. japonicum* coding for ristomycin A production. Although ristomycin A has been in use for many years, no type III glycopeptide gene cluster has been published so far. Heterologous expression of the balhimycin pathway-specific regulator gene bbr_{Aba} (*bbr* gene from *A. balhimycina*) (13) in *A. japonicum* enabled us to activate the cryptic ristomycin gene cluster.

The activation of ristomycin A production in *A. japonicum* now offers the possibility of optimizing production of ristomycin A in a genetically accessible strain.

Received 30 May 2014 Returned for modification 15 June 2014
Accepted 27 July 2014
Published ahead of print 11 August 2014
Address correspondence to Evi Stegmann, evi.stegmann@biotech.uni-tuebingen.de.
Supplemental material for this article may be found at http://dx.doi.org/10.1128/AAC.03512-14.

doi:10.1128/AAC.03512-14

MATERIALS AND METHODS

Bacterial strains and plasmids. *Escherichia coli* XL1-Blue (14) was used for cloning purposes, and the methylation-deficient strain *E. coli* ET12567 (15) was used to obtain unmethylated DNA for *Amycolatopsis japonicum* transformations. *A. japonicum* MG417-CF17 (1) is the (*S*,*S*)-EDDS-producing wild type and was used to generate bbr_{Aba} and *ajrR* overexpression strains (this study). The overexpression plasmids pRM4-bbr_{Aba} and pRM4-*ajrR* derive from pRM4 (16), a pSET152-derived nonreplicative, ΦC31 integration vector with an integrated constitutive *ermEp** promoter, an artificial ribosomal binding site, and an apramycin resistance cassette.

Media and culture conditions. *E. coli* strains were grown in Luria broth medium (17) at 37°C and were supplemented with 100 μg ml^{-1} apramycin when necessary to maintain plasmids. Liquid cultures of *A. japonicum* were cultivated in 100 ml of R5 medium (18) in an orbital shaker (220 rpm) in 500-ml baffled Erlenmeyer flasks with steel springs at 27°C. Liquid/solid media were supplemented with 100 μg ml^{-1} apramycin to select for strains carrying integrated antibiotic resistance genes. To detect glycopeptide production, wild-type *A. japonicum* or *A. japonicum* carrying the pRM4-bbr_{Aba} or pRM4-*ajrR* plasmid, respectively, were incubated for 5 days in R5 medium without apramycin.

Construction of the integrative expression vector pRM4-bbr_{Aba}/*ajrR*. For the overexpression of bbr_{Aba} and *ajrR*, the bbr_{Aba} and *ajrR* coding regions were amplified by using the primer pair bbrAba-FP (FP stands for forward primer) and bbrAba-RP (RP stands for reverse primer) and the primer pair ajrR-FP and ajrR-RP (see Table S1 in the supplemental material), respectively. The 968-bp (bbr_{Aba}) and the 981-bp (*ajrR*) PCR products were integrated into pRM4 via the primer-attached NdeI and XbaI sites for bbr_{Aba} and NdeI and HindIII sites for *ajrR*, downstream of the *ermEp** promoter.

Direct transformation of *A. japonicum*. For transformation of *A. japonicum*, the direct transformation method of Stegmann et al. (19) was modified. Mycelia were grown in 100 ml of TSB-D (17 g Bacto tryptone, 3 g peptone 110, 5 g NaCl, 2.5 g K_2HPO_4, and 2.5 g glucose per liter Millipore H_2O) for 24 h in a 1-liter Erlenmeyer flask with 4 bottom baffles at 30°C and 220 rpm; 5-ml portions from these precultures were used to inoculate 100 ml of TSB-D, which were incubated for 36 h under the same conditions as the preculture.

Detection of ristomycin biosynthesis by HPLC-DAD. Glycopeptide production was determined by bioassays with *Bacillus subtilis* ATCC 6633 as the test organism after growth in R5 medium or by high-performance liquid chromatography (HPLC) coupled with a diode array detector (DAD). Five microliters of each sample was analyzed by HPLC with gradient elution. For gradient elution, solvent A was 0.1% phosphoric acid and solvent B was acetonitrile, and the gradient elution was performed as follows: t_0 = 0% solvent B, t_7 = 30% solvent B, t_8 to t_{10} = 100% solvent B. The flow rate was 0.85 ml min^{-1}. Gradient elution was conducted using a Nucleosil 100-C_{18} column (5 μm; 125 by 3 mm) (precolumn, 20 by 3 mm) (Dr. Maisch GmbH, Ammerbuch-Entringen, Germany). Detection was carried out at 210, 230, 260, 280, 310, 360, 400, 435, and 500 nm (1260 Infinity diode array detector; Agilent Technologies, Waldbronn, Germany).

Analytical instrumentation. Nuclear magnetic resonance (NMR) spectra were recorded on a Bruker Avance III 500 HD spectrometer, equipped with a BBFO cryo probe head. Spectra were referenced to residual protonated solvent signals with resonances at $\delta_{H/C}$ 2.50/39.5 (deuterated dimethyl sulfoxide [d_6-DMSO]). Circular dichroism (CD) spectra were measured on a Jasco J-720 spectropolarimeter. High-resolution (HR) electrospray ionization-time of flight mass spectrometry (ESI-TOF MS) data were recorded using a Bruker Daltonic maXis 4G instrument. Semipreparative HPLC was conducted using a Waters system consisting of a 600 pump, a 996 photodiode array detector, a 7725i rheodyne injector, and a PerkinElmer vacuum degasser series 200. Ristomycin monosulfate A standard was purchased from Aldrich and used without further purification for MS analyses. For NMR and CD analyses, the standard was desalted.

HPLC–ESI-MS and HPLC-MS/MS. Culture broths were prepared by centrifugation or filtration and partially purified via adsorption chromatography with Amberlite XAD16 and subsequent ethyl acetate extraction. Portions (2.5 μl) of the different fractions were analyzed by means of HPLC–ESI-MS and HPLC-MS/MS using a Nucleosil 100-C_{18} column (3 μm, 100 by 2 mm) (precolumn, 10 by 2 mm) (Dr. Maisch GmbH, Ammerbuch-Entringen, Germany) coupled to an ESI mass spectrometer. LC-MS measurements were obtained from a LC/MSD Ultra Trap system XCT 6330 (Agilent Technologies, Waldbronn, Germany). Detection of *m/z* values was conducted with Agilent DataAnalysis for 6300 series Ion Trap LC/MS 6.1 version 3.4 software (Bruker-Daltonik GmbH). Analysis was carried out at a flow rate of 0.4 ml min^{-1} with gradient elution. Solvent A was 0.1% formic acid in acetonitrile, and solvent B was 0.06% formic acid in acetonitrile. Gradient elution was performed as follows: t_0 = 0% solvent B, t_7 = 30% solvent B, t_8 to t_{10} = 100% solvent B. The flow rate was 0.4 ml min^{-1}, and the temperature was 40°C. Electrospray ionization (alternating positive and negative ionization) in Ultra Scan mode with a capillary voltage of 3.5 kV and a drying gas temperature of 350°C was used for LC-MS analysis. For tandem MS experiments, the analysis was carried out either in negative mode with an Agilent LC/MSD Ultra Trap system XCT 6330 or in positive ionization mode employing an AB SCIEX QT3200 instrument.

Scaled-up cultivation, extraction, and purification of ristomycin A. *A. japonicum*/pRM4-bbr_{Aba} was cultivated in a 20-liter fermentor (b20; Giovanola). The fermentor was inoculated with 2% (vol) of shaking cultures grown for 48 h in 500-ml Erlenmeyer flasks with one baffle and steel spring in tryptic soy broth (TSB). The fermentation was carried out at 27°C with an agitation rate of 1,000 rpm and an aeration rate of 0.5 vol/vol/min. After 50 h of fermentation, 1 liter of fermentation broth was taken, and bacterial cells were removed by centrifugation. Diaion HP-20 adsorbent resin (50 g $liter^{-1}$) was added to a portion of the supernatant (900 ml), and the mixture was agitated in a 1.5-liter Erlenmeyer flask at 120 rpm for 2 h. The HP-20 resin was then passed through a fritted funnel and washed with water, and the bound metabolites were eluted using a stepwise gradient of isopropanol-H_2O (acidified with 1% acetic acid [HOAc]) to produce five fractions (A to E). Fractions B, C, and D, eluting with 5, 10, and 15% isopropanol in acidified water, respectively, were found to potently inhibit the growth of *B. subtilis* in an agar diffusion assay. Each bioactive fraction was rechromatographed with reversed-phase HPLC (RP-HPLC). For RP-HPLC separation, a Phenomenex Syn-

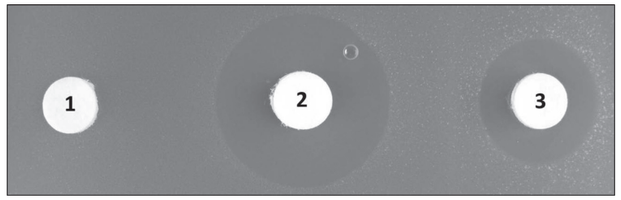

FIG 1 Bioassay after cluster activation by expression of bbr_{Aba} and *ajrR*, respectively. Wild-type *A. japonicum* (1), *A. japonicum*/pRM4-bbr_{Aba} (2), and *A. japonicum*/pRM4-*ajrR* (3) were grown for 5 days in R5 medium, and 20 μl of culture supernatant was assayed for bioactivity against *B. subtilis*.

ergi Hydro-RP 80A column (10 by 250 mm; 4 μm) in combination with a Phenomenex SecurityGuard AQ C_{18} precolumn (10 by 10 mm) was used. The flow rate was 2.0 ml min^{-1}. UV monitoring at 210 and 254 nm was performed. Elution was performed as follows: (i) isocratic elution at 20:80 acetonitrile (MeCN)-H_2O (0.1% trifluoroacetic acid [TFA]) over a period of 10 min, (ii), gradient elution from 20:80 to 40:60 MeCN-H_2O (0.1% TFA) over 10 min, (iii) gradient elution from 40:60 to 100:0 MeCN-H_2O (0.1% TFA) over 20 min, and (iv) isocratic elution at 100% MeCN for an additional 10 min. This procedure yielded collectively 33 mg of ristomycin A.

Platelet aggregation. For preparation of platelet-rich plasma (PRP), citrate-anticoagulated human blood was centrifuged at 200 × *g* for 10 min. After centrifugation, the PRP was collected in a fresh tube, and the remaining blood was centrifuged at 2,500 × *g* to obtain platelet-poor plasma (PPP). Afterwards the platelet count in the PRP was estimated with a KX21-N automatic hematology analyzer (Sysmex, Norderstedt, Germany). After adjusting the PRP to a platelet concentration of 200 × 10^5 μl^{-1} with the obtained PPP, aggregation was estimated from light transmission measurements determined with a luminoaggregometer (model 700; Chrono-Log Corp., Havertown, PA, USA). Following calibration, agonists were added at the indicated concentrations, and aggregation was measured for 10 min with a stir speed of 1,000 rpm at 37°C. The extent of aggregation was quantified as percentage of light transmission. Data analysis was performed with the aggrolink8 software (Chrono-Log). The adjusted PRP was either treated with agonists at the indicated concentrations or not treated with an agonist.

Gene expression analysis by RT-PCR. For reverse transcription-PCR (RT-PCR) experiments, the wild-type *A. japonicum* and the bbr_{Aba} and *ajrR* overexpression strains were grown in R5 medium. After 25 h, the cells were harvested and disrupted using glass beads and a Precellys homogenizer (Peqlab). RNA preparations were treated twice with DNase I (Fermentas). To exclude DNA contamination, negative controls were carried out by using total RNA as the template for a PCR using the primer pair sigB-RT-FP and sigB-RT-RP (see Table S1 in the supplemental material). cDNA from 3 mg RNA was generated with random hexameric primers, reverse transcriptase, and cofactors (Fermentas). PCRs were performed with the primers listed in Table S1. PCRs were carried out under the following conditions: (i) an initial denaturation step (94°C for 2 min); (ii) 27 cycles of PCR, with 1 cycle consisting of denaturation (95°C for 30 s), annealing (59°C for 30 s), and polymerization (72°C for 30 s); and (iii) an additional polymerization step (72°C for 1 min). Each PCR mixture (25 μl) contained a 1-μl aliquot of RT reaction product. As a positive control, cDNA was amplified from the major vegetative sigma factor (*sigB*) transcript, which is produced constitutively. The PCR products were analyzed by agarose gel electrophoresis (2.0%).

Nucleotide sequence accession number. The GenBank accession number of the genome sequence of *A. japonicum* is CP008953 (45).

RESULTS AND DISCUSSION

Activation of a cryptic glycopeptide gene cluster. Members of the genus *Amycolatopsis* are known to possess a particularly high potential for the production of secondary metabolites. They are major producers of various glycopeptides like balhimycin (*A. balhimycina*), the medically relevant vancomycin (*Amycolatopsis orientalis* NRRL 2452), and rifamycin (*Amycolatopsis mediterranei*), which is one component in the drug cocktail for the treatment of tuberculosis and inactive meningitis. However, these species are difficult to manipulate genetically because of the lack of efficient transformation systems. In contrast to these species, we were able to establish a DNA transfer protocol for *A. japonicum* (19). Although we have been working with this species in our laboratory for many years, no antibiotically active product could be identified so far. In previous work, it was shown that *A. japonicum* produces glycopeptide-resistant cell wall precursors (20) and that the genome contains an *oxyB* gene, which is involved in the production of glycopeptides (21). From these results, we assumed that *A. japonicum* may have the potential to produce a glycopeptide.

To test whether *A. japonicum* has this potential, we made use of the observation that all known glycopeptide clusters are controlled by a pathway-specific StrR-like regulator (22). Hence, we applied a new cluster activation strategy, overexpressing the gene encoding the characterized pathway-specific transcriptional regulator of the balhimycin gene cluster, bbr_{Aba} (13), in *A. japonicum* aiming to awake the cryptic glycopeptide gene cluster. Therefore, bbr_{Aba} was cloned into the integrative vector pRM4 under the control of the constitutive promoter *ermEp** and transferred into *A. japonicum* by direct transformation. The recombinant species *A. japonicum* carrying the pRM4-bbr_{Aba} plasmid was grown in R5 medium for 5 days, and the culture supernatant was analyzed in a growth inhibition assay. Whereas the supernatant from wild-type *A. japonicum* did not contain any biologically active compound, the culture supernatant from the recombinant *A. japonicum*-(pRM4-bbr_{Aba}) strongly inhibited growth of the indicator species, *B. subtilis* (Fig. 1). The metabolic profiles of the supernatants were determined by HPLC-DAD (Fig. 2). The chromatogram of the *A. japonicum*/pRM4-bbr_{Aba} supernatant revealed two peaks with glycopeptide-specific DAD spectra. These peaks were absent in the chromatogram of the wild-type *A. japonicum* supernatant (Fig. 2). From these results, we concluded that *A. japonicum* does indeed have the genetic potential to produce a glycopeptide antibiotic, which is synthesized only after transcriptional activation.

Genome mining in *A. japonicum*. In order to identify the gene cluster for biosynthesis of the new glycopeptide, its regulation, and the self-resistance mechanism and to evaluate the potential to synthesize additional secondary metabolites, the genome of *A. japonicum* was sequenced. The genome sequence of *A. japonicum* is approximately 8.96 Mb in size and contains 8,464 putative

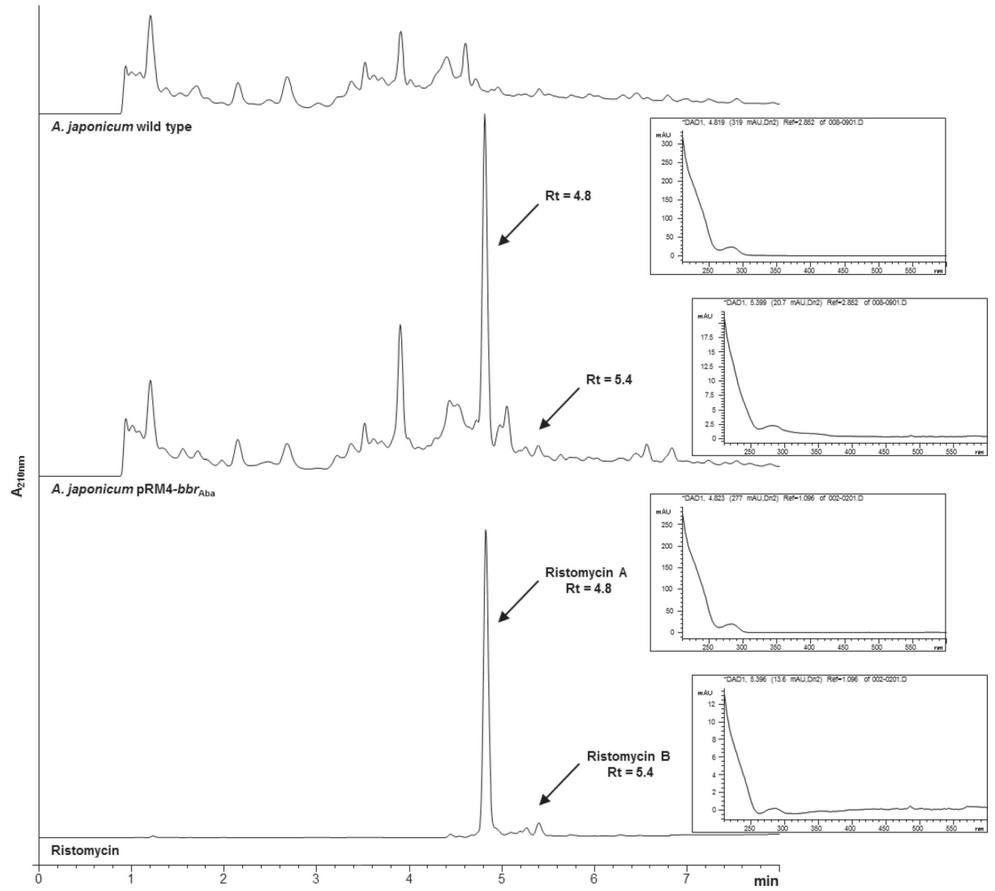

FIG 2 HPLC chromatograms of wild-type *A. japonicum* and *A. japonicum*/pRM4-bbr_{Aba} after growth for 5 days in R5 medium and ristomycin standard. The boxed regions show the corresponding DAD spectra. Rt, retention time; mAU, milliabsorbance units.

open reading frames (ORFs) (45). Extensive genome analysis using antiSMASH 2.0 (7) revealed the presence of 29 putative secondary metabolite gene clusters (see Table S2 in the supplemental material). One of the gene clusters (cluster 4) encodes the synthesis of the polyketide synthase (PKS) compound ECO-0501, which was already identified in the vancomycin producer *Amycolatopsis orientalis* ATCC 43491 by a genome-scanning technology (23). ECO-0501 defines a new structural class of the polyketide antibiotic octanoic acid glucuronide and possesses activity against Gram-positive bacteria, including methicillin-resistant *Staphylococcus aureus* (MRSA) and vancomycin-resistant enterococci (VRE) (24). However, since this cluster and the corresponding product were already known, we focused our attention on the type III PKS/nonribosomal peptide synthetase (NRPS) hybrid gene cluster (cluster 24) (Table S2) which showed high similarity to described glycopeptide gene clusters, such as the balhimycin (25), teicoplanin (26), and A47934 (27) gene clusters. Cluster 24 consists of 39 distinct ORFs (AJAP_31985 to AJAP_32175) (Fig. 3) with a total size of almost 69 kb. The putative functions of all 39 gene products were deduced by comparative amino acid sequence analysis with homologues from known glycopeptide clusters (Table 1). Cluster 24 is predicted to encode all the enzymes required for biosynthesis of a glycopeptide, comprising enzymes responsible for assembly and export of the glycopeptide, self-resistance, and gene regulation. By considering these deduced functions, the boundaries of the glycopeptide gene cluster 24 were predicted. The left border is probably delimited by *orf1*, a *dahp* homologue, involved in tyrosine precursor supply for the synthesis of the aproteinogenic amino acids (28), and the right border is most

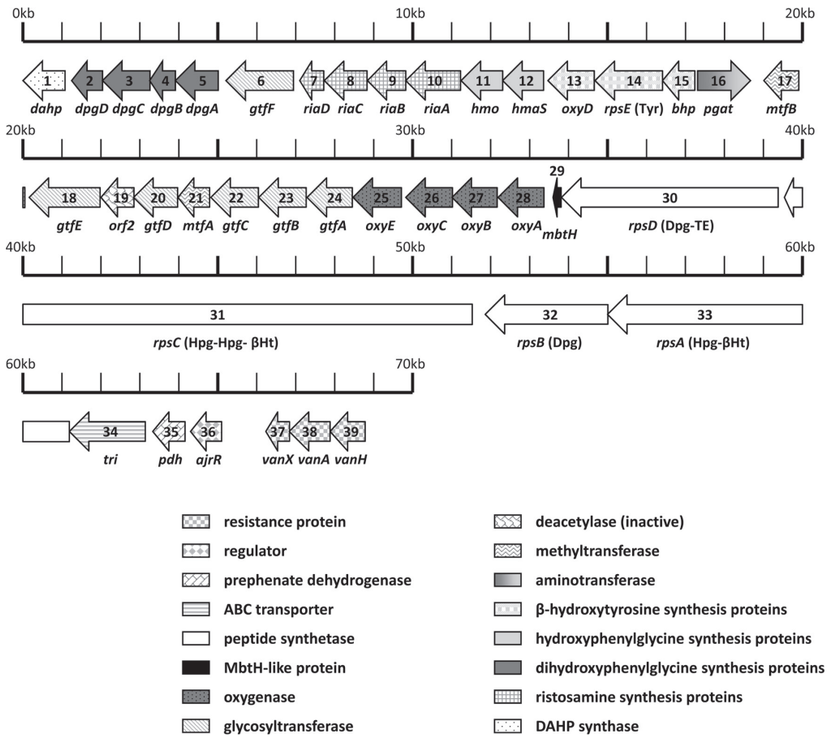

FIG 3 Genetic organization of the ristomycin A (*ris*) cluster identified in *A. japonicum*. Predicted ORFs are represented by an arrow drawn to scale and are numbered as in Table 1. Gene names are indicated underneath the corresponding ORFs. Predicted functions of genes are listed. TE, thioesterase.

likely delimited by *orf39*, a *vanH* homologue, involved in self-resistance (20) (Table 1).

Proposed glycopeptide biosynthesis in *A. japonicum*. In the last 2 decades, considerable progress has been made in understanding the genetics and biochemistry of glycopeptide biosynthesis (10, 22, 29). The profound knowledge of the individual enzymes participating in glycopeptide biosynthesis makes it possible to almost completely predict the structure of the final product.

(i) Synthesis of the nonproteinogenic amino acids. Glycopeptides consist of a heptapeptide backbone constituted mainly by aprotenogenic aromatic amino acids such as 3,5-dihydroxyphenylglycine (Dpg), *p*-hydroxyphenylglycine (Hpg), and β-hydroxytyrosine (β-Ht). Since detailed information on their biosynthesis is available (30, 31, 32, 33, 34), it is possible to conclude that most likely, *orf5* to *orf2* and *orf16* are responsible for the synthesis of Dpg, *orf11*, *orf12*, and *orf16* are responsible for Hpg synthesis, and *orf15* to *orf13* are responsible for synthesis of βHt (Fig. 3 and Table 1).

(ii) Synthesis of the aglycon. (*a*) Synthesis of the linear backbone. The amino acids are assembled by nonribosomal peptide synthetases to form a heptapeptide (35). The *A. japonicum* glycopeptide gene cluster contains four NRPS genes (*orf33* to *orf30*) that are predicted to encode the enzymes catalyzing the assembly of the heptapeptide backbone. The genetic organization and domain composition of these NRPS genes and the predicted specificity of the A domains indicate that the ORF33 protein, including module 1 and module 2, incorporates Hpg and β-Ht; ORF32, including module 3, incorporates Dpg; ORF31, including modules 4, 5, and 6, incorporates Hpg, Hpg, and β-Ht; and ORF30, including module 7, incorporates Dpg. This amino acid composition was confirmed by all three amino acid prediction tools used by antiSMASH 2.0 (7, 36). Hence, the assembled heptapeptide has the predicted amino acid sequence Hpg^1–β-Ht^2–Dpg^3–Hpg^4–Hpg^5-β-Ht^6–Dpg^7. The organization of the epimerization domains within the modules predicts a stereochemistry of L-D-L-D-D-L-L, which is consistent with the stereochemistry of teicoplanin (26), but inconsistent with L-D-D-D-D-L-D of A47934 (27) and D-D-L-D-D-L-L of balhimycin (35), respectively. *orf29*, located downstream of the NRPS genes encodes a 69-amino-acid small MbtH-like polypeptide. MbtH-like peptides are common features of NRPS biosynthesis gene clusters acting as facilitators of the peptide-assembling machineries by stimulating adenylation reac-

TABLE 1 Comparison of the *ris* cluster ORFs with ORFs from published glycopeptide clusters[a]

ris ORF[b]				Glycopeptide cluster[c]				
ORF no.	Locus tag	Gene	No. of amino acids	BAL	STA	TEI	Amino acid similarity (%)	Proposed function[d]	Biosynthetic role[e]
1	AJAP_31985	*dahp*	358	Dahp*	[-]	[-]	87	3-Deoxy-7-phosphoheptulonate synthase	Precursor supply
2	AJAP_31990	*dpgD*	263	DpgD*	DpgD	DpgD	90	Enoyl-CoA hydratase/enhances DpgA activity	Dpg formation
3	AJAP_31995	*dpgC*	404	DpgC*	DpgC	DpgC	90	3,5-Dihydroxyphenylacetyl-CoA oxidase	
4	AJAP_32000	*dpgB*	220	DpgB*	DpgB	DpgB	83	Enoyl-CoA hydratase/enhances DpgA activity	
5	AJAP_32005	*dpgA*	366	DpgA*	DpgA	DpgA	97	3,5-Dihydroxyphenylacetyl-CoA synthase (type III PKS)	
						[-]		Mannosyltransferase	Mannosyl transfer
6	AJAP_32010	*gtfF*	575	[-]	[-]	[-]	91	dTDP-4-keto-6-deoxy-glucose-5-epimerase	Sugar/ristosamine formation
7	AJAP_32015	*riaD*	205	DvaD*	[-]	[-]	94	C-3 aminotransferase	
						[-]	80	NAD-dependent epimerase/dehydratase	
						[-]	92	NDP-hexose 2,3-dehydratase	
8	AJAP_32020	*riaC*	369	DvaB*	[-]				
9	AJAP_32025	*riaB*	325	DvaE*	[-]				
10	AJAP_32030	*riaA*	469	DvaA*	[-]				
11	AJAP_32035	*hmo*	356	Hmo*	Hmo	Hmo	91	*p*-Hydroxymandelate oxidase	Hpg formation
12	AJAP_32040	*hmaS*	350	HmaS*	HmaS	HmaS	81	*p*-Hydroxymandelate synthase	
13	AJAP_32045	*oxyD*	396	OxyD*	[-]	[-]	92	P450 monooxygenase	β-Ht formation
14	AJAP_32050	*rpsE*	577	BpsB*	[-]	[-]	88	Nonribosomal peptide synthetase/adenylation domain	
						[-]	91	Hydrolase	
15	AJAP_32055	*rhp*	274	Bhp*	[-]				
16	AJAP_32060	*pgat*	453	PgaT*	HpgT	HpgT	94	*p*-Hydroxy- and 3,5-dihydroxyphenylglycine aminotransferase	Dpg/Hpg formation
						[-]	79	Methyltransferase	Methylation
17	AJAP_32065	*mtfB*	346	[-]	[-]	Orf15*		Mannosyltransferase	Mannosyl transfer
18	AJAP_32070	*gtfE*	605	[-]	[-]	Orf2/Dbv21*	78	Inactive *N*-acetylglucosamine deacetylase	Sugar addition/ deacetylation
19	AJAP_32075	*orf2*	281	Bal2	[-]				
20	AJAP_32080	*gtfD*	374	[-]	[-]	GtfA*	73	UDP-*N*-acetylglucosamine transferase	Peptide methylation
21	AJAP_32085	*mtfA*	270	[-]	[-]	[-]	70	Methyltransferase	Sugar addition
22	AJAP_32090	*gtfC*	404	BgtfC*	[-]	[-]	81	UDP-*N*-acetylglucosamine transferase	
23	AJAP_32095	*gtfB*	405	BgtfB*	[-]	GtfB	73	UDP-*N*-acetylglucosamine transferase	
24	AJAP_32100	*gtfA*	385	BgtfA*	[-]	[-]	88	P450 monooxygenase	Cross-linking (aa 5 to 7)
25	AJAP_32105	*oxyC*	413	OxyC	StaJ	OxyC*			
26	AJAP_32110	*oxyB*	398	OxyB*	StaH	OxyB	90	P450 monooxygenase	Cross-linking (aa 4 to 6)
27	AJAP_32115	*oxyE*	385	[-]	StaG*	OxyE	85	P450 monooxygenase	Cross-linking (aa 1 to 3)
28	AJAP_32120	*oxyA*	391	OxyA	StaF	OxyA*	86	P450 monooxygenase	Cross-linking (aa 2 to 4)
29	AJAP_32125	*mbtH*	69	MbtH*	StaE	MbtH	94	Adenylation, loading of NRPS	Peptide synthesis/β-Ht formation
30	AJAP_32130	*rpsD* (Dpg-TE)	1853	BspC (Dpg-TE)	StaD (Dpg-TE)	TeiD (Dpg-TE)		Nonribosomal peptide synthetase	Peptide synthesis
31	AJAP_32135	*rpsC* (Hpg-Hpg-β-Ht)	3994	OxyA	StaF	TeiC (Hpg–Hpg–β-Ht)		Nonribosomal peptide synthetase	
32	AJAP_32140	*rpsB* (Dpg)	1050	BspB (Hpg–Hpg–β-Ht)	StaB (Dpg)	TeiB (Dpg)		Nonribosomal peptide synthetase	

				Nonribosomal peptide synthetase			
StaA (Hpg-Tyr)	TeiA (Hpg-Tyr)						
StaU	Orf4		85	ABC transporter		Excretion	
Pdh	Pdh		90	Prephenate dehydrogenase		Precursor supply	
StaQ	StrR-like	*pdh*	91	StrR-like regulator		Regulation	
VanX	VanX*	*aprR*	88	D-Ala–D-Ala dipeptidase		Resistance	
VanA	VanA*	*vanX*	86	D-Ala–D-Lac ligase			
VanH	VanH*	*vanA*	88	D-Lactate dehydrogenase			
		vanH					

[a] Comparison of the *ris* ORFs with selected genes from previously published glycopeptide clusters.
[b] *ris*, ristomycin A.
[c] Homologues in other glycopeptide clusters. BAL, balhimycin, *Amycolatopsis balhimycina* DSM5908; STA, A47934, *Streptomyces toyocaensis* NRRL15009; TEI, teicoplanin, *Actinoplanes teichomyceticus* ATCC 31121. [-], absence. *, the highest score is reported. The pair responsible for the score is indicated by an asterisk.
[d] CoA, coenzyme A.
[e] aa, amino acids.

tions (37, 38, 39, 40). The predicted incorporation of aromatic amino acids into the heptapeptide revealed that the *A. japonicum* glycopeptide belongs to either the type II, type III, or type IV glycopeptides but not to the type I (vancomycin type) glycopeptides characterized by aliphatic amino acids at positions 1 and 3 (Fig. 4).

(***b***) **Cross-linking of the aromatic amino acid residues.** During peptide formation, the aromatic residues are connected due to the activity of P450 monooxygenases (Oxy) to form a rigid cup-shaped structure (41, 42) required for the interaction with their molecular target, the D-alanyl–D-alanine (D-Ala–D-Ala) terminus of bacterial cell wall precursors. The *A. japonicum* glycopeptide gene cluster contains four *oxy* genes (*orf28* to *orf25*), putatively encoding P450 monooxygenases, as within the teicoplanin, A47934, and dalbavancin gene clusters, all characterized by a fully cyclized heptapeptide backbone (22). These cross-linked glycopeptides contain three ether bridges (between amino acids 1 and 3, 2 and 4, and 4 and 6) and one C-C link (between amino acids 5 and 7). On the basis of the model proposed for the balhimycin and A47934 oxygenases (42, 43) and using amino acid sequence similarity as a criterion, it is likely that OxyA is involved in the cross-linking of the aromatic residues of amino acids 2 and 4, while OxyB is involved in the cross-linking of amino acids 4 and 6 and OxyC is involved in the cross-linking of amino acids 5 and 7. The fourth encoded oxygenase (OxyE) catalyzes the type III and type IV glycopeptide-specific cross-linking between Hpg at position 1 and Dpg at position 3 (43) (Fig. 4 and Table 1).

A backbone consisting of seven aromatic amino acids and a predicted cyclization of all of these residues is a characteristic of glycopeptide classes III and IV and excludes the classification to type II where the residues of amino acids 1 and 3 are not linked (Fig. 4).

(iii) Tailoring reactions by adding sugars and methyl groups. Structural diversity within the glycopeptide family is generated by different optionally and variably occurring glycosylation, methylation, acetylation, halogenation, and sulfation patterns. The *A. japonicum* gene cluster contains six glycosyltransferase genes (*orf24* to *orf22*, *orf20*, *orf6*, and *orf18*) presumably responsible for the decoration of the aglycon with sugar moieties. No other described glycopeptide gene cluster contains such an extended amount of glycosyltransferases. For example, the balhimycin gene cluster encodes three glycosyltransferases (BgtfA, BgtfB, and BgtfC), while the teicoplanin gene cluster encodes three glycosyltransferases (GtfA, GtfB, and one putative mannosyltransferase) (Table 1). *orf10* to *orf7* encode peptides that exhibit high similarity to the TDP-L-epivancosamine biosynthesis enzymes EvaA to EvaD (Fig. 3 and Table 1) of chloroeremomycin biosynthesis (44), suggesting that they are involved in the biosynthesis of an uncommon amino-deoxy sugar, which finally decorates the *A. japonicum* glycopeptide. Besides the glycosyltransferases, two methyltransferase homologues are encoded within the *A. japonicum* gene cluster (*orf17* and *orf21*), but the cluster does not encode further tailoring enzymes, like sulfotransferases, halogenases, or acetyltransferases. The occurrence of an acetyltransferase is a specific feature of the lipoglycopeptide class (teicoplanin type or type IV glycopeptides). The absence of an acetyltransferase gene within the identified gene cluster suggests that the *A. japonicum* glycopeptide exemplifies a type III glycopeptide (Fig. 4).

Resistance, export, regulation, and precursor supply. The seven genes of the *A. japonicum* glycopeptide gene cluster, which

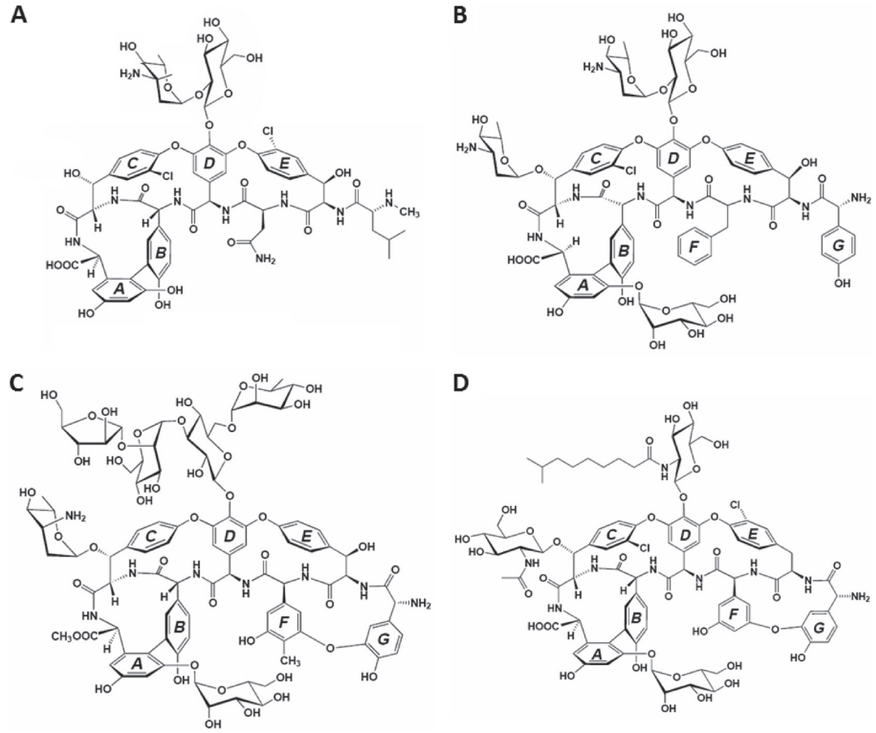

FIG 4 Classification of the glycopeptides. (A) Type I glycopeptides exemplified by vancomycin. These glycopeptides contain aliphatic chains in amino acids 1 and 3. (B) Type II glycopeptides exemplified by actinoidin A. These glycopeptides contain aromatic aliphatic chains in amino acids 1 and 3. (C) Type III glycopeptides exemplified by ristomycin A. These glycopeptides are like type II glycopeptides, and they contain an extra F-*O*-G ring system. Ring abbreviations: A, Me-L-Dpg; B, D-Hpg; C, L-β-Ht; D, D-Hpg; E, D-β-Ht; F, Me-L-Dpg; G, L-Hpg. (D) Type IV glycopeptides exemplified by teicoplanin. These glycopeptides are like type III glycopeptides plus they have aliphatic side chains on sugar.

are not directly involved in the synthesis and tailoring of the glycopeptide, are located at the left (*orf1*) and right (*orf34* to *orf39*) borders (Fig. 3). *orf39* to *orf37* encode the VanHAX-like glycopeptide resistance cassette. However, neither a *vanRS* (encoding the two-component system) nor a *vanY* (D,D-carboxypeptidase) homologue are located within the *A. japonicum* glycopeptide gene cluster. Previous cell wall precursor analyses (20) demonstrated that *A. japonicum* synthesized a glycopeptide-resistant cell wall, although no glycopeptide production could be observed, suggesting constitutive expression of the resistance genes.

The *orf34*-encoded protein is likely to specify export functions, since it is predicted to be an ABC-type transporter exhibiting high similarity to the balhimycin exporter Tba (15) (Table 1).

The *orf36* encodes a StrR-like transcriptional activator with high similarity to the balhimycin pathway-specific transcriptional activator Bbr_{Aba} (13) (see below).

Two additional genes, presumably encoding a 3-deoxy-7-phosphoheptulonate synthase (DAHP synthase) homologue (*orf1*) and a prephenate dehydrogenase homologue (*orf35*) are predicted to optimize the precursor supply of the aromatic amino acids (28). While prephenate dehydrogenase genes are encoded in all described clusters, the DAHP synthase-encoding gene is lacking in some gene clusters, like the teicoplanin and A47934 gene clusters (22).

Categorization of the *A. japonicum* glycopeptide by considering the genetic features. The *in silico* data strongly suggested that the final product of the identified gene cluster is a 6-fold-glycosylated, twice methylated, and fully cross-bridged glycopeptide. The genetic organization and domain composition of the NRPS specifies an amino acid sequence L-Hpg^1–D-β-Ht^2–L-Dpg^3–D-Hpg^4–D-Hpg^5–L-β-Ht^6–L-Dpg^7. The incorporation of aromatic amino acids at positions 1 and 3 together with the predicted complete cross-linked heptapeptide by the four oxygenases and the absence of any acyltransferase or halogenase imply that the *A. japonicum* gene cluster has the biosynthetic potential to produce a type III glycopeptide (Fig. 4). Until now, only the structure of the type III glycopeptides, exemplified by ristomycin A (produced by *A. lurida*) was known; no biosynthesis gene cluster was known. Therefore, the *A. japonicum* gene cluster identified

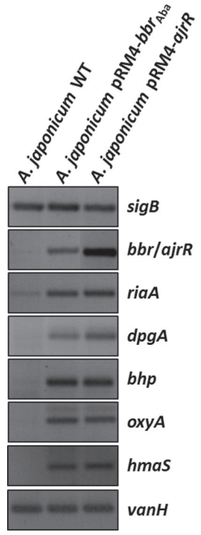

FIG 5 Transcriptional pattern of representative ristomycin biosynthesis genes. The gene names are indicated to the right of the gel. Cultures were grown in R5 medium for 25 h. *sigB* is the major sigma factor of *A. japonicum* and was used as a housekeeping gene to normalize the RNA. WT, wild type.

here is the first type III glycopeptide gene cluster described so far (Fig. 3). The amino acid sequence and stereochemistry of the glycopeptide encoded by the *A. japonicum* gene cluster are consistent with the sequence and stereochemistry of ristomycin A. Furthermore, the number and predicted function of the tailoring enzymes (six glycosyltransferases and two methyltransferases) are in agreement with the ristomycin A decorations (Fig. 4). Considering all these congruences of the described ristomycin A structure and the genetic content within the identified *A. japonicum* gene cluster, we propose that this gene cluster encodes a glycopeptide which is either ristomycin A itself or a highly similar derivative.

Expression of the *A. japonicum* StrR-like regulator AjrR. The two closely related species *A. japonicum* and *A. balhimycina* each harbor a glycopeptide gene cluster encoding the regulators AjrR and Bbr_{Aba}, respectively. These StrR-like regulators exhibit 84 and 91% amino acid identity and similarity, respectively. However, Bbr_{Aba} initiates the transcription of the glycopeptide gene cluster in *A. balhimycina*, while the *A. japonicum* gene cluster is of cryptic nature under the identical laboratory conditions.

One reason why the glycopeptide cluster in *A. japonicum* is not expressed under standard conditions could be that the regulator AjrR is not functional. To evaluate its functionality, we overexpressed *ajrR* under the control of the constitutive *ermEp** in *A. japonicum*. The supernatant of the recombinant *A. japonicum*/pRM4-*ajrR* inhibited growth of *B. subtilis*, while the supernatant of wild-type *A. japonicum* did not (Fig. 1). HPLC-DAD analyses confirmed the biosynthesis of the glycopeptide (data not shown). These results demonstrated the *in vivo* functionality of AjrR and

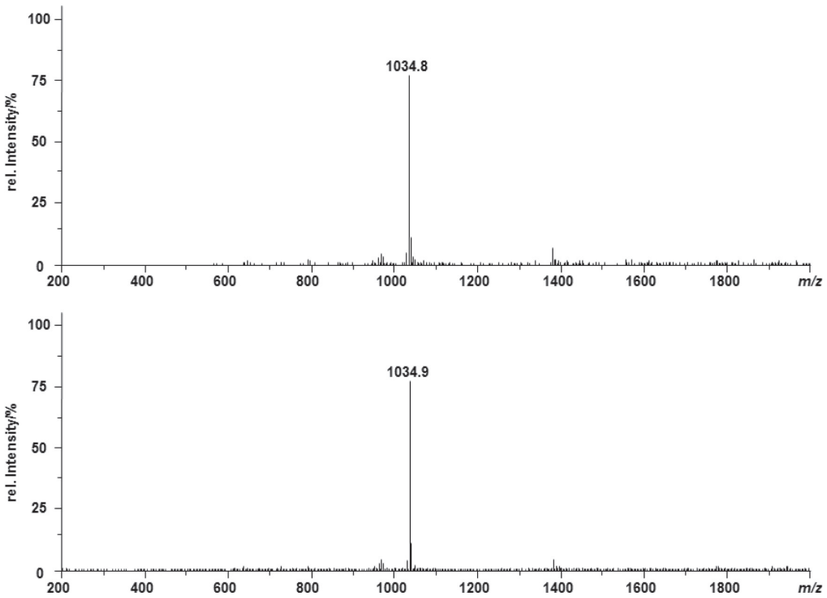

FIG 6 HPLC–ESI-MS analysis (positive mode) of *A. japonicum* glycopeptide and ristomycin A. (Top) Ristomycin A standard (0.1 mg ml^{-1}). (Bottom) *A. japonicum*/pRM4-bbr_{Aba} glycopeptide. $[M + 2H]^{2+}$ was observed at *m/z* 1,034.8 and 1,034.9. The relative intensity is shown on the *y* axes.

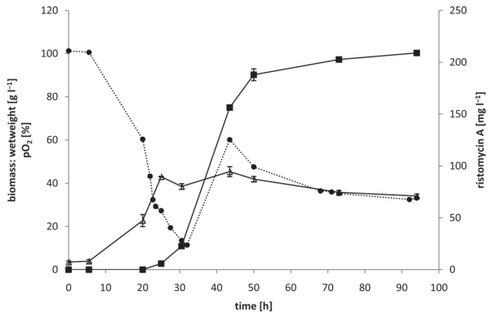

FIG 7 Batch fermentation of *A. japonicum*/pRM4-bbr_{Aba} in R5 medium. Biomass (△), ristomycin A (■), and partial O_2 pressure (pO_2) (●) are depicted. *A. japonicum*/pRM4-bbr_{Aba} reached its maximal biomass value after 44 h of incubation, decreasing afterwards slowly during 2 days of further fermentation. Metabolizing of different sugars in R5 medium (sucrose [α-1,2-glycosidic linked glucose and fructose] and glucose) is reflected by a diauxic shift (between 24 and 44 h) during cultivation, apparent in growth retardation and pO_2.

suggest that *ajrR* is not transcribed in the wild-type species. Therefore, transcriptional analyses of *ajrR* and representative biosynthetic genes (*riaA*, *dpgA*, *bhp*, *oxyA*, *hmaS*, and *vanH*) were performed after growth of wild-type *A. japonicum*, *A. japonicum*/pRM4-bbr_{Aba} and *A. japonicum*/pRM4-*ajrR* in production medium R5 (Fig. 5). In wild-type *A. japonicum*, no *ajrR* transcription was detected, and it is therefore not surprising that no other investigated biosynthetic gene was transcribed. However, in *A. japonicum*/pRM4-*ajrR* and *A. japonicum*/pRM4-bbr_{Aba}, transcription of all the investigated genes could be observed. Coincident to the observations of Schäberle et al. (20) that *A. japonicum* produces a glycopeptide-resistant cell wall, whereas no glycopeptide production could be detected, we could observe transcription of the *vanH* resistance gene in the wild type. It will be interesting to ascertain why bbr_{Aba} is transcribed under standard conditions whereas *ajrR* is not.

Isolation and spectroscopic characterization of the *A. japonicum* glycopeptide. In order to confirm the assumption deduced from the genome sequence, the chemical structure of the glycopeptide was analyzed. Initial experiments with *A. japonicum*/pRM4-bbr_{Aba} growing in shake flasks revealed a glycopeptide production with quantities up to 50 mg $liter^{-1}$. The crude extract was fractionated and analyzed for the presence of the glycopeptide (Fig. 2). A major compound with a quasimolecular ion $[M + 2H]^{2+} = m/z$ 1,034.8 (Fig. 6) and a minor compound with $[M + 2H]^{2+} = m/z$ 887.7 (data not shown) were detected. Since the masses of the major and minor components were in agreement with the masses of ristomycin A and B, the isolated glycopeptides were compared with a commercially available ristomycin standard. HPLC-DAD and HPLC–ESI-MS analyses showed that both the glycopeptides synthesized by *A. japonicum*/pRM4-bbr_{Aba} and ristomycins A and B eluted at the same time, possessed the same UV profile (Fig. 2), and showed in ESI-MS/MS analyses (positive and negative mode) an identical fragmentation pattern (see Fig. S1 to Fig. S3 in the supplemental material).

To corroborate the findings and to obtain additional information on the nature of the sugar units, the major glycopeptide synthesized by *A. japonicum*/pRM4-bbr_{Aba} was isolated in a pure form and compared with a ristomycin A standard employing NMR, CD, and high-resolution mass spectrometry. For this purpose, the initial shake flask cultivation was scaled up to a 20-liter volume using a Giovanola b20 fermentor. Glycopeptide production was detected after 24 h and reached a maximum amount up to 200 mg $liter^{-1}$ after 50 h and stayed almost constant during 2 more days of fermentation (Fig. 7). For the isolation of the glycopeptide, 1 liter of fermentation broth was taken after 50 h of fermentation and separated by centrifugation into supernatant and mycelium. Subsequent workup of the extract led to the isolation of the major glycopeptide in a highly pure form at a yield of 37 mg l^{-1}. HR-MS analysis confirmed that the isolated glycopeptide showed the same exact mass as that of the ristomycin A standard and therefore possessed the same molecular formula of $C_{95}H_{110}N_8O_{44}$ (see Fig. S4 and S5 in the supplemental material). ^1H and the ^{13}C NMR spectra of the isolated glycopeptide and the ristomycin A standard were absolutely superimposable, with the exception of additional peaks in the commercially available ristomycin standard which can be attributed to the presence of up to 10% ristomycin derivatives in the sample (Fig. S6 to S14). Further analysis of the one-dimensional (1D) and two-dimensional (2D) NMR data (Fig. S15

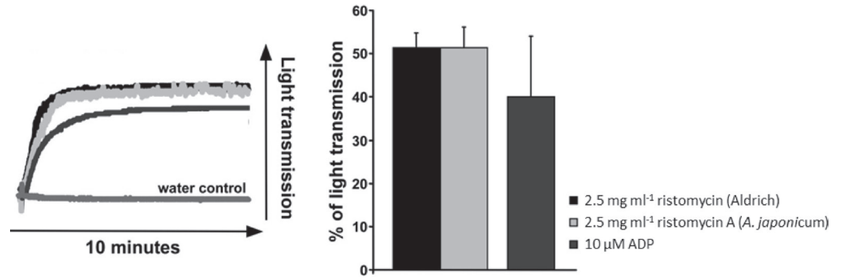

FIG 8 Ristomycin-dependent platelet aggregation. (Left) Representative tracings of aggregometry after stimulation of human platelets with 2.5 mg ml^{-1} commercial (black line) or *A. japonicum* ristomycin A (light gray line) as well as 10 μM ADP (dark gray line) and water control. (Right) Results of aggregometry after stimulation of human platelets with 2.5 mg ml^{-1} commercial or *A. japonicum* ristomycin A as well as 10 μM ADP. The values are arithmetic means plus standard errors of the means (SEM) (error bars) for four experiments.

to Fig. S20) allowed the complete assignment of all hydrogen and carbon atoms (Table S3), which supported the hypothesis that the isolated compound possessed the same planar structure and the same relative configuration as that of ristomycin A. Since the CD spectra of the isolated glycopeptide and a commercially available ristomycin A standard were consistent (Fig. S21), it was deduced that the isolated glycopeptide also possessed the same absolute configuration as that of ristomycin A. From these data, we concluded that the identified cryptic gene cluster is responsible for the production of ristomycin A.

Ristomycin A-dependent platelet aggregation. Measuring von Willebrand factor (vWF) activity is essential for the diagnosis of von Willebrand disease (vWD). A common test method is the ristomycin platelet-induced agglutination method, which allows discrimination among specific subtypes of the vWD. In a platelet aggregation assay, we could demonstrate that ristomycin A isolated from *A. japonicum* has the same *in vitro* function as the reference ristomycin (Fig. 8).

ACKNOWLEDGMENTS

We are very grateful to A. Steck, Analytical Services & Applied NMR Development, at Bruker Biospin GmbH for the generous support and NMR measurements. We also thank D. Wistuba and her team at the Mass Spectrometry Department, Institute for Organic Chemistry, University of Tuebingen, for HR-MS measurements.

This work was supported by grants from the DFG (SFB 766) to Evi Stegmann and from the BMBF (ERA-IB, GenoDrug) to Wolfgang Wohlleben.

REFERENCES

1. **Nishikiori T, Okuyama A, Naganawa H, Takita T, Hamada M, Takeuchi T, Aoyagi T, Umezawa H.** 1984. Production by actinomycetes of (S,S)-N,N′-ethylenediamine-disuccinic acid, an inhibitor of phospholipase C. J. Antibiot. (Tokyo) **37:**426–427. http://dx.doi.org/10.7164/antibiotics.37.426.
2. **Hartmann FA, Perkins CM.** November 1987. Detergent compositions containing ethylenediamine-*N,N′*-disuccinic acid. US patent 4,704,233.
3. **Bentley SD, Chater KF, Cerdeno-Tarraga AM, Challis GL, Thomson NR, James KD, Harris DE, Quail MA, Kieser H, Harper D, Bateman A, Brown S, Chandra G, Chen CW, Collins M, Cronin A, Fraser A, Goble A, Hidalgo J, Hornsby T, Howarth S, Huang CH, Kieser T, Larke L, Murphy L, Oliver K, O'Neil S, Rabbinowitsch E, Rajandream MA, Rutherford K, Rutter S, Seeger K, Saunders D, Sharp S, Squares R, Squares S, Taylor K, Warren T, Wietzorrek A, Woodward J, Barrell BG, Parkhill J, Hopwood DA.** 2002. Complete genome sequence of the model actinomycete *Streptomyces coelicolor* A3(2). Nature **417:**141–147. http://dx.doi.org/10.1038/417141a.
4. **Ikeda H, Ishikawa J, Hanamoto A, Shinose M, Kikuchi H, Shiba T, Sakaki Y, Hattori M, Omura S.** 2003. Complete genome sequence and comparative analysis of the industrial microorganism *Streptomyces avermitilis*. Nat. Biotechnol. **21:**526–531. http://dx.doi.org/10.1038/nbt820.
5. **Ohnishi Y, Ishikawa J, Hara H, Suzuki H, Ikenoya M, Ikeda H, Yamashita A, Hattori M, Horinouchi S.** 2008. Genome sequence of the streptomycin-producing microorganism *Streptomyces griseus* IFO 13350. J. Bacteriol. **190:**4050–4060. http://dx.doi.org/10.1128/JB.00204-08.
6. **Oliynyk M, Samborskyy M, Lester JB, Mironenko T, Scott N, Dickens S, Haydock SF, Leadlay PF.** 2007. Complete genome sequence of the erythromycin-producing bacterium *Saccharopolyspora erythraea* NRRL23338. Nat. Biotechnol. **25:**447–453. http://dx.doi.org/10.1038/nbt1297.
7. **Blin K, Medema MH, Kazempour D, Fischbach MA, Breitling R, Takano R, Weber T.** 2013. antiSMASH 2.0–a versatile platform for genome mining of secondary metabolite producers. Nucleic Acids Res. **41:** W204–W212. http://dx.doi.org/10.1093/nar/gkt449.
8. **Hertweck C.** 2009. Hidden biosynthetic treasures brought to light. Nat. Chem. Biol. **5:**450–452. http://dx.doi.org/10.1038/nchembio0709-450.
9. **Bachmann BO, Van Lanen SG, Baltz RH.** 2014. Microbial genome mining for accelerated natural products discovery: is a renaissance in the making? J. Ind. Microbiol. Biotechnol. **41:**175–184. http://dx.doi.org/10.1007/s10295-013-1389-9.
10. **Stegmann E, Frasch HJ, Wohlleben W.** 2010. Glycopeptide biosynthesis in the context of basic cellular functions. Curr. Opin. Microbiol. **13:**595–602. http://dx.doi.org/10.1016/j.mib.2010.08.011.
11. **Grundy WE, Sinclair AC, Theriault RJ, Goldstein AW, Rickher CJ, Warren HB, Jr, Oliver TJ, Sylvester JC.** 1956–1957. Ristocetin, microbiologic properties. Antibiot. Annu. **1956–1957:**687–692.
12. **Sarji KE, Stratton RD, Wagner RH, Brinkhous KM.** 1974. Nature of von Willebrand factor: a new assay and a specific inhibitor. Proc. Natl. Acad. Sci. U. S. A. **71:**2937–2941. http://dx.doi.org/10.1073/pnas.71.8.2937.
13. **Shawky RM, Puk O, Wietzorrek A, Pelzer S, Takano E, Wohlleben W, Stegmann E.** 2007. The border sequence of the balhimycin biosynthesis gene cluster from *Amycolatopsis balhimycina* contains *bbr*, encoding a StrR-like pathway-specific regulator. J. Mol. Microbiol. Biotechnol. **13:**76–88. http://dx.doi.org/10.1159/000103599.
14. **Bullock WO, Fernandez JM, Short JM.** 1987. Xl1-Blue: a high-efficiency plasmid transforming *recA Escherichia coli* strain with β-galactosidase selection. Biotechniques **5:**376–378.
15. **MacNeil DJ, Gewain KM, Ruby CL, Dezeny G, Gibbons PH, MacNeil T.** 1992. Analysis of *Streptomyces avermitilis* genes required for avermectin biosynthesis utilizing a novel integration vector. Gene **111:**61–68. http://dx.doi.org/10.1016/0378-1119(92)90603-M.
16. **Menges R, Muth G, Wohlleben W, Stegmann E.** 2007. The ABC transporter Tba of *Amycolatopsis balhimycina* is required for efficient export of the glycopeptide antibiotic balhimycin. Appl. Microbiol. Biotechnol. **77:**125–134. http://dx.doi.org/10.1007/s00253-007-1139-x.
17. **Sambrook J, Fritsch EF, Maniatis T.** 1989. Molecular cloning: a laboratory manual, 2nd ed. Cold Spring Harbor Laboratory, Cold Spring Harbor, NY.
18. **Kieser T, Bibb MJ, Buttner MJ, Chater KF, Hopwood DA.** 2000. Practical *Streptomyces* genetics. John Innes Foundation, Norwich, United Kingdom.
19. **Stegmann E, Pelzer S, Wilken K, Wohlleben W.** 2001. Development of three different gene cloning systems for genetic investigation of the new species *Amycolatopsis japonicum* MG417-CF17, the ethylenediaminedisuccinic acid producer. J. Biotechnol. **92:**195–204. http://dx.doi.org/10.1016/S0168-1656(01)00360-1.
20. **Schäberle TF, Vollmer W, Frasch HJ, Hüttel S, Kulik A, Röttgen M, von Thaler AK, Wohlleben W, Stegmann E.** 2011. Self-resistance and cell wall composition in the glycopeptide producer *Amycolatopsis balhimycina*. Antimicrob. Agents. Chemother. **55:**4283–4289. http://dx.doi.org/10.1128/AAC.01372-10.
21. **Everest GJ, Meyers PR.** 2011. Evaluation of the antibiotic biosynthetic potential of the genus *Amycolatopsis* and description of *Amycolatopsis circi* sp. nov., *Amycolatopsis equina* sp. nov. and *Amycolatopsis hippodromi* sp. nov. J. Appl. Microbiol. **111:**300–311. http://dx.doi.org/10.1111/j.1365-2672.2011.05058.x.
22. **Donadio S, Sosio M, Stegmann E, Weber T, Wohlleben W.** 2005. Comparative analysis and insights into the evolution of gene clusters for glycopeptide antibiotic biosynthesis. Mol. Genet. Genomics **274:**40–50. http://dx.doi.org/10.1007/s00438-005-1156-3.
23. **Shen Y, Huang H, Zhu L, Luo M, Chen D.** 2012. Type II thioesterase gene (*ECO-orf27*) from *Amycolatopsis orientalis* influences production of the polyketide antibiotic, ECO-0501 (LW01). Biotechnol. Lett. **34:**2087–2091. http://dx.doi.org/10.1007/s10529-012-1010-8.
24. **Lam KS.** 2007. New aspects of natural products in drug discovery. Trends Microbiol. **15:**279–289. http://dx.doi.org/10.1016/j.tim.2007.04.001.
25. **Pelzer S, Süssmuth RD, Heckmann D, Recktenwald J, Huber P, Jung G, Wohlleben W.** 1999. Identification and analysis of the balhimycin biosynthetic gene cluster and its use for manipulating glycopeptide biosynthesis in *Amycolatopsis mediterranei* DSM5908. Antimicrob. Agents Chemother. **43:**1565–1573.
26. **Sosio M, Kloosterman H, Bianchi A, de Vreugd P, Dijkhuizen L, Donadio S.** 2004. Organization of the teicoplanin gene cluster in *Actinoplanes teichomyceticus*. Microbiology **150:**95–102. http://dx.doi.org/10.1099/mic.0.26507-0.
27. **Pootoolal J, Thomas MG, Marshall CG, Neu JM, Hubbard BK, Walsh CT, Wright GD.** 2002. Assembling the glycopeptide antibiotic scaffold: the biosynthesis of A47934 from *Streptomyces toyocaensis* NRRL15009. Proc. Natl. Acad. Sci. U. S. A. **99:**8962–8967. http://dx.doi.org/10.1073/pnas.102285099.
28. **Thykaer J, Nielsen J, Wohlleben W, Weber T, Gutknecht M, Lantz AE, Stegmann E.** 2010. Increased glycopeptide production after overexpression of shikimate pathway genes being part of the balhimycin biosynthetic

gene cluster. Metab. Eng. **12:**455–461. http://dx.doi.org/10.1016/j.ymben.2010.05.001.
29. **Wohlleben W, Stegmann E, Süssmuth RD.** 2009. Molecular genetic approaches to analyze glycopeptide biosynthesis. Methods Enzymol. **458:**459–486. http://dx.doi.org/10.1016/S0076-6879(09)04818-6.
30. **Hubbard BK, Thomas MG, Walsh CT.** 2000. Biosynthesis of L-p-hydroxyphenylglycine, a non-proteinogenic amino acid constituent of peptide antibiotics. Chem. Biol. **7:**931–942.
31. **Kastner S, Müller S, Natesan L, König GM, Guthke R, Nett M.** 2012. 4-Hydroxyphenylglycine biosynthesis in *Herpetosiphon aurantiacus*: a case of gene duplication and catalytic divergence. Arch. Microbiol. **194:**557–566. http://dx.doi.org/10.1007/s00203-012-0789-y.
32. **Pfeifer V, Nicholson GJ, Ries J, Recktenwald J, Schefer AB, Shawky RM, Schröder J, Wohlleben W, Pelzer S.** 2001. A polyketide synthase in glycopeptide biosynthesis: the biosynthesis of the non-proteinogenic amino acid (S)-3,5-dihydroxyphenylglycine. J. Biol. Chem. **276:**38370–38377. http://dx.doi.org/10.1074/jbc.M106580200.
33. **Puk O, Bischoff D, Kittel C, Pelzer S, Weist S, Stegmann E, Süssmuth RD, Wohlleben W.** 2004. Biosynthesis of chloro-beta-hydroxytyrosine, a nonproteinogenic amino acid of the peptidic backbone of glycopeptide antibiotics. J. Bacteriol. **186:**6093–6100. http://dx.doi.org/10.1128/JB.186.18.6093-6100.2004.
34. **Mulyani S, Egel E, Kittel C, Turkanovic S, Wohlleben W, Süssmuth RD, van Pée KH.** 2010. The thioesterase Bhp is involved in the formation of beta-hydroxytyrosine during balhimycin biosynthesis in *Amycolatopsis balhimycina*. Chembiochem **11:**266–271. http://dx.doi.org/10.1002/cbic.200900600.
35. **Recktenwald J, Shawky R, Puk O, Pfennig F, Keller U, Wohlleben W, Pelzer S.** 2002. Nonribosomal biosynthesis of vancomycin-type antibiotics: a heptapeptide backbone and eight peptide synthetase modules. Microbiology **148:**1105–1118.
36. **Rausch C, Weber T, Kohlbacher O, Wohlleben W, Huson DH.** 2005. Specificity prediction of adenylation domains in nonribosomal peptide synthetases (NRPS) using transductive support vector machines (TSVMs). Nucleic Acids Res. **33:**5799–5808. http://dx.doi.org/10.1093/nar/gki885.
37. **Stegmann E, Pelzer S, Bischoff D, Puk O, Stockert S, Butz D, Zerbe K, Robinson J, Süssmuth RD, Wohlleben W.** 2006. Genetic analysis of the balhimycin (vancomycin-type) oxygenase genes. J. Biotechnol. **124:**640–653. http://dx.doi.org/10.1016/j.jbiotec.2006.04.009.
38. **Boll B, Taubitz T, Heide L.** 2011. Role of MbtH-like proteins in the adenylation of tyrosine during aminocoumarin and vancomycin biosynthesis. J. Biol. Chem. **286:**36281–36290. http://dx.doi.org/10.1074/jbc.M111.288092.
39. **Herbst DA, Boll B, Zocher G, Stehle T, Heide L.** 2013. Structural basis of the interaction of MbtH-like proteins, putative regulators of nonribosomal peptide biosynthesis, with adenylating enzymes. J. Biol. Chem. **288:**1991–2003. http://dx.doi.org/10.1074/jbc.M112.420182.
40. **Zhang W, Heemstra JR, Jr, Walsh CT, Imker HJ.** 2010. Activation of the pacidamycin PacL adenylation domain by MbtH-like proteins. Biochemistry **49:**9946–9947. http://dx.doi.org/10.1021/bi101539b.
41. **Bischoff D, Bister B, Bertazzo M, Pfeifer V, Stegmann E, Nicholson GJ, Keller S, Pelzer S, Wohlleben W, Süssmuth RD.** 2005. The biosynthesis of vancomycin-type glycopeptide antibiotics–a model for oxidative side-chain cross-linking by oxygenases coupled to the action of peptide synthetases. Chembiochem **6:**267–272. http://dx.doi.org/10.1002/cbic.200400328.
42. **Stegmann E, Rausch C, Stockert S, Burkert D, Wohlleben W.** 2006. The small MbtH-like protein encoded by an internal gene of the balhimycin biosynthetic gene cluster is not required for glycopeptide production. FEMS Microbiol. Lett. **262:**85–92. http://dx.doi.org/10.1111/j.1574-6968.2006.00368.x.
43. **Hadatsch B, Butz D, Schmiederer T, Steudle J, Wohlleben W, Süssmuth RD, Stegmann E.** 2007. The biosynthesis of teicoplanin-type glycopeptide antibiotics: assignment of p450 mono-oxygenases to side chain cyclizations of glycopeptide A47934. Chem. Biol. **14:**1078–1089. http://dx.doi.org/10.1016/j.chembiol.2007.08.014.
44. **Chen H, Thomas MG, Hubbard BK, Losey HC, Walsh CT, Burkart MD.** 2000. Deoxysugars in glycopeptide antibiotics: enzymatic synthesis of TDP-L-epivancosamine in chloroeremomycin biosynthesis. Proc. Natl. Acad. Sci. U. S. A. **97:**11942–11947. http://dx.doi.org/10.1073/pnas.210395097.
45. **Stegmann E, Albersmeier A, Spohn M, Gert H, Weber T, Wohlleben W, Kalinowski J, Rueckert C.** Complete genome sequence of the actinobacterium *Amycolatopsis japonica* MG417-CF17(T) (=DSM 44213(T)) producing (S,S)-N,N′-ethylenediaminedisuccinic acid. J. Biotechnol., in press.

Supplemental Material for

Overproduction of ristomycin A by activation of a silent gene cluster in *Amycolatopsis japonicum* MG417-CF17

Marius Spohn,[a] Norbert Kirchner,[b,c] Andreas Kulik,[a,] Angelika Jochim,[a] Felix Wolf,[a] Patrick Muenzer,[d] Oliver Borst,[e] Harald Gross,[b,c] Wolfgang Wohlleben,[a,b] Evi Stegmann,[a,b]#

Interfaculty Institute of Microbiology and Infection Medicine Tuebingen, University of Tuebingen, 72076 Tuebingen, Germany[a]
German Centre for Infection Research (DZIF), Partner Site Tuebingen, Tuebingen, Germany[b]
Pharmaceutical Institute, Department of Pharmaceutical Biology, University of Tuebingen, 72076 Tuebingen, Germany[c]
Department of Physiology I, University of Tuebingen, 72076 Tuebingen, Germany[d]
Department of Cardiology & Cardiovascular Medicine, University of Tuebingen, Germany[e]

Running title: Activation of a silent ristomycin A cluster

Address correspondence to Evi Stegmann, evi.stegmann@biotech.uni-tuebingen.de.

FIGURE AND TABLE LEGENDS

Fig. S17. 500 MHz ^{1}H-^{1}H-TOCSY NMR spectrum of the isolated glycopeptide from *A. japonicum*.

Fig. S18. 500 MHz ^{1}H-^{13}C-HMBC NMR spectrum of the isolated glycopeptide from *A. japonicum*.

Fig. S19. 500 MHz ^{1}H-^{1}H-ROESY NMR spectrum of the isolated glycopeptide from *A. japonicum*.

Figure S20. Chemical structure of ristomycin A, numbering scheme and NMR key correlations.

Table S3. NMR spectral data of isolated ristomycin A in d_6-DMSO.

Fig. S21. CD spectra of the isolated glycopeptide from *A. japonicum* and a ristomycin standard.

Table S1. List of primers used for this study.

Primer	Sequence (5'-3')	Experiment, restriction sites
bbrAba-FP	ATTCATATGGTGGATCCGACGAGAGTT	Overexpression of bbr_{Aba}, NdeI
bbrAba-RP	ATATTCTAGAGTCATCCCGCGGCCAGCTCGGT	Overexpression of bbr_{Aba}, XbaI
ajrR-FP	TAACATATGGATCCGACGAGAGTTGAC	Overexpression of *ajrR*, NdeI
ajrR-RP	AATAAGCTTTCATCGTGCGGCCAGATCG	Overexpression of *ajrR*, HindIII
strR-RT-FP	GATCCGACGAGAGTTGAC	RT-PCR of bbr_{Aba}/*ajrR*
strR-RT-RP	ATGCGTCCCGATGATCTG	RT-PCR of bbr_{Aba}/*ajrR*
riaA-RT-FP	TGAGGCCAACGTCTTCCAC	RT-PCR of *riaA*
riaA-RT-RP	GTTCCCCGGCTCCATCTTG	RT-PCR of *riaA*
dpgA-RT-FP	TTCCTGAACAGCGCCATCG	RT-PCR of *dpgA*
dpgA-RT-RP	CAGGAACCCGGTCGAGGTG	RT-PCR of *dpgA*
bhp-RT-FP	TCGTCGGCACGTCGATGG	RT-PCR of *bhp*
bhp-RT-RP	TCGTCGTCGGCGAGCGTC	RT-PCR of *bhp*
oxyA-RT-FP	CGACTTCCTCGGCATCCC	RT-PCR of *oxyA*
oxyA-RT-RP	CAGTTCCGCGTCGGTGAT	RT-PCR of *oxyA*
hmaS-RT-FP	CAGAATTTCGAGATCGACTA	RT-PCR of *hmaS*
hmaS-RT-RP	CGCTCTGGATCAGGGTGTG	RT-PCR of *hmaS*
vanH-RT-FP	GCGTAATTCCGACCATTGTG	RT-PCR of *vanH*
vanH-RT-RP	TCAGCATCAGCGTGAAATCG	RT-PCR of *vanH*

Table S2. antiSMASH 2.0 predicted gene clusters within the *A. japonicum* genome.

# cluster	type
1	ectoine
2	unknown
3	NRPS
4	type I PKS
5	unknown
6	type IV PKS
7	type I PKS
8	lanthipeptide
9	NRPS
10	lanthipeptide
11	terpene
12	unknown
13	NRPS
14	NRPS
15	NRPS
16	NRPS
17	type I PKS
18	type I PKS/NRPS
19	type I PKS/type IV PKS
20	terpene
21	bacteriocin
22	terpene
23	type I PKS
24	type III PKS/NRPS
25	type I PKS
26	aminoglycoside
27	lanthipeptide
28	terpene
29	unknown

Fig. S1. HPLC-ESI-MS/MS spectra (negative mode) of *A. japonicum* glycopeptide. Fragmentation pattern of (TOP) ristomycin A standard (0.1 mg ml^{-1}) and (BOTTOM) *A. japonicum* pRM4-*bbr*$_{Aba}$ glyopeptide.

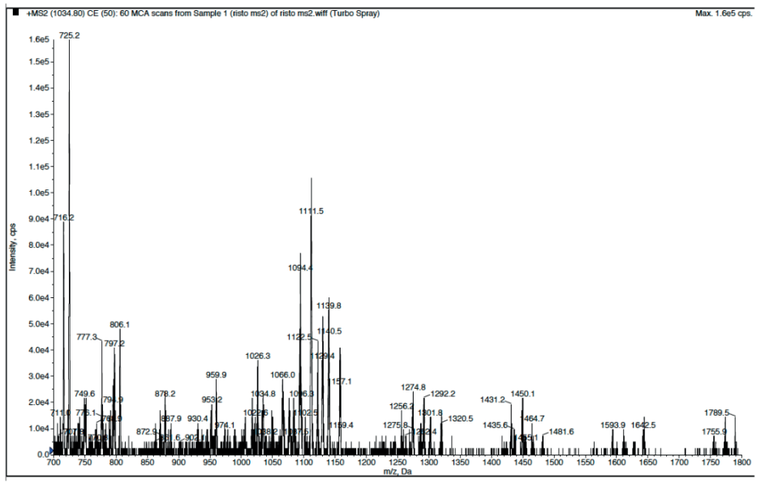

Fig. S2. HPLC-ESI-MS/MS spectra (positive mode) of *A. japonicum* glycopeptide. Fragmentation pattern of (TOP) ristomycin A standard and (BOTTOM) *A. japonicum* pRM4-*bbr*$_{Aba}$ glyopeptide. The quasimolecular ion $[M+2H]^{2+}$ = 1034 *m/z* was selected as precursor ion.

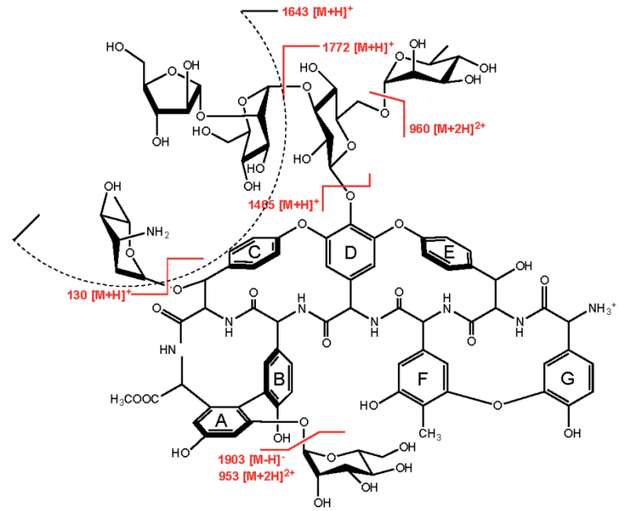

Fig. S3 Key fragment ions observed in collisionally induced ESI-MS/MS experiments with ristomycin A. The upper structural diagram shows the fragments of the regular form of ristomycin A, while the bottom structural diagram depicts the fragments derived from ristomycin A containing a dehydrated ß-hydroxy-tyrosine moiety (indicated in blue).

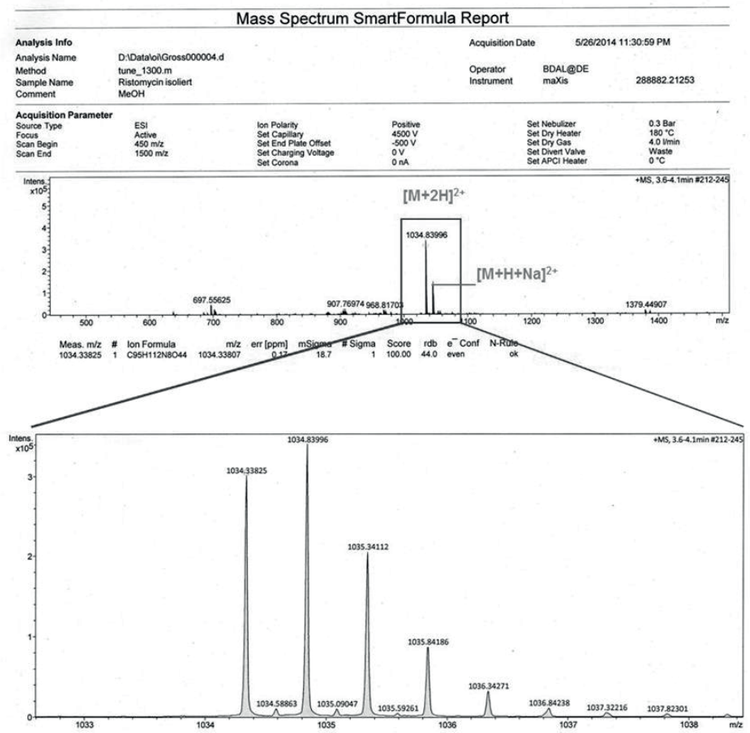

Fig. S4. HR-ESI-TOF mass spectrum of the isolated glycopeptide from *A. japonicum*. Boxed region shows details about the quasimolecular ion $[M+2H]^{2+}$.

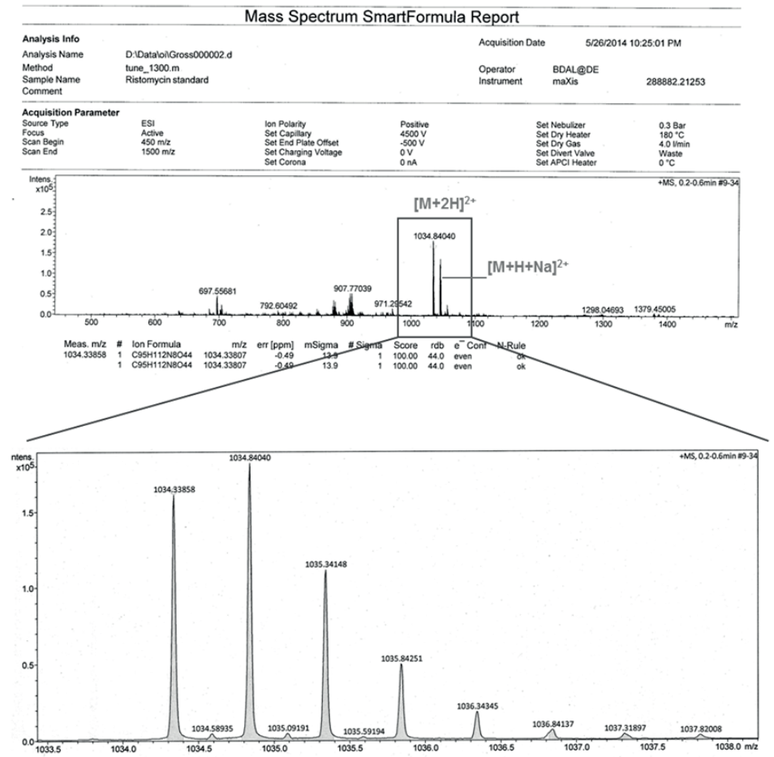

Fig. S5. HR-ESI-TOF mass spectrum of a commercially available ristomycin A monosulfate standard. Boxed region shows details about the quasimolecular ion $[M+2H]^{2+}$.

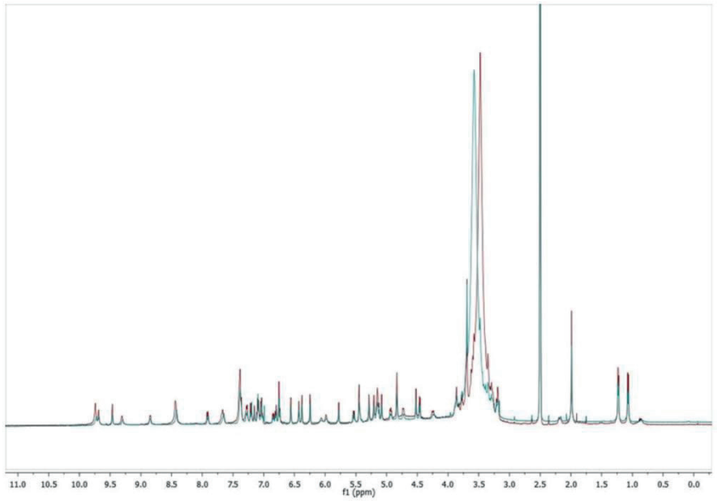

Fig. S6. Superimposed ^{1}H NMR spectra (500 MHz, d_6-DMSO) of the isolated glycopeptide from *A. japonicum* and a desalted commercially available ristomycin standard. The ristomycin standard showed an additional peak at 6.99 ppm (see detailed ^{1}H NMR regions), which can be attributed to the presence of ristomycin derivatives (up to 10%) in the commercially available standard.

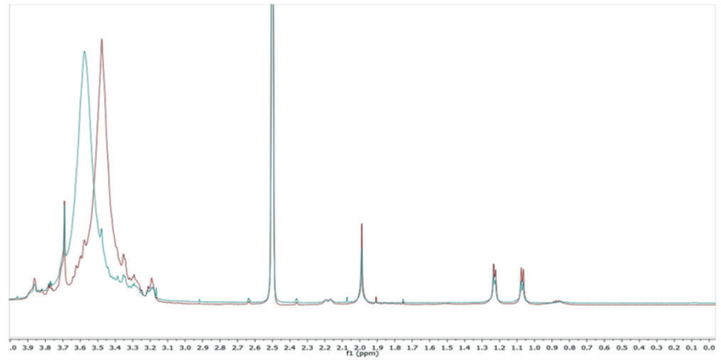

Fig. S7. Detail region (0 – 4 ppm) of the superimposed 500 MHz ^{1}H NMR spectra of the isolated glycopeptide from *A. japonicum* and a desalted commercially available ristomycin standard.

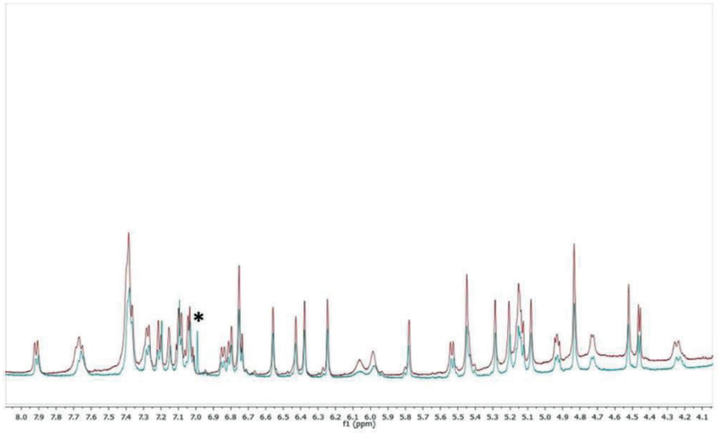

Fig. S8. Detail region (4 – 8 ppm) of the superimposed 500 MHz ^{1}H NMR spectra of the isolated glycopeptide from *A. japonicum* and a desalted commercially available ristomycin standard. The ristomycin standard showed an additional peak at 6.99 ppm (*), which can be attributed to the presence of ristomycin derivatives (up to 10%) in the commercially available standard.

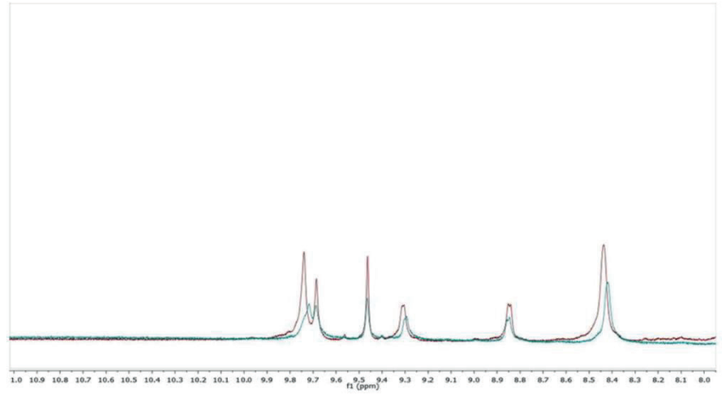

Fig. S9. Detail region (8 – 11 ppm) of the superimposed 500 MHz ^{1}H NMR spectra of the isolated glycopeptide from *A. japonicum* and a desalted commercially available ristomycin standard.

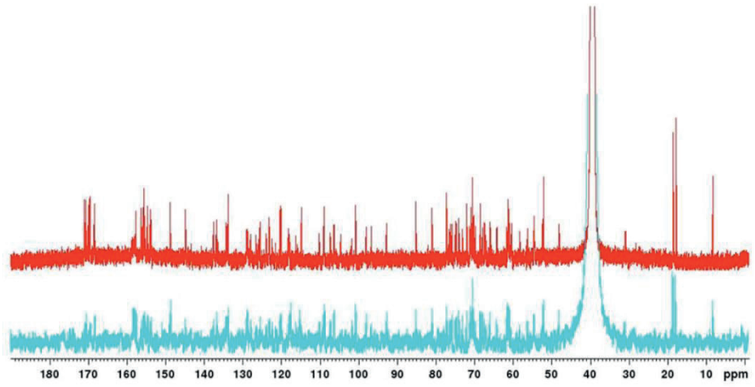

Fig. S10. Superimposed ^{13}C NMR spectra (125 MHz, d_6-DMSO) of the isolated glycopeptide from *A. japonicum* and a desalted commercially available ristomycin standard. The ristomycin standard showed additional peaks in the double bond region (see detailed ^{13}C NMR regions), which can be attributed to the presence of ristomycin derivatives (up to 10%) in the commercially available standard.

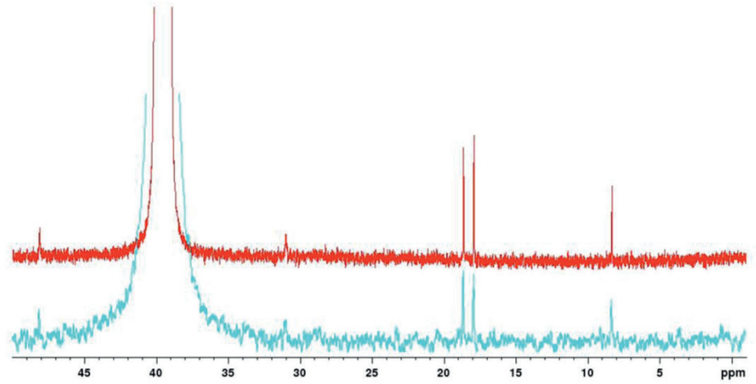

Fig. S11. Detail region (0 – 50 ppm) of the superimposed 125 MHz ^{13}C NMR spectra of the isolated glycopeptide from *A. japonicum* and a desalted commercially available ristomycin standard.

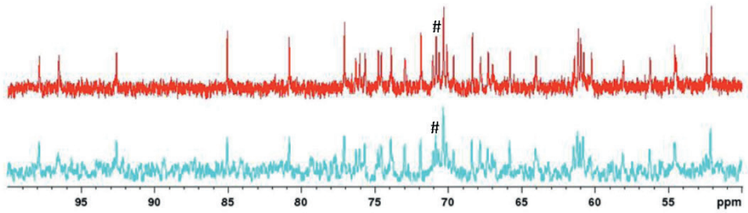

Fig. S12. Detail region (50 – 100 ppm) of the superimposed 125 MHz ^{13}C NMR spectra of the isolated glycopeptide from *A. japonicum* and a desalted commercially available ristomycin standard. Hash mark indicates a minor impurity at 70.8 ppm in both samples.

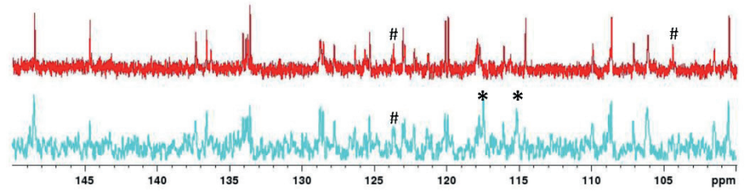

Fig. S13. Detail region (100 – 150 ppm) of the superimposed 125 MHz ^{13}C NMR spectra of the isolated glycopeptide from *A. japonicum* and a desalted commercially available ristomycin standard. The ristomycin standard showed additional peaks at 115.2 and 117.5 ppm (*). Hash marks indicate minor impurities at 104.5 and 123.7 ppm in both samples.

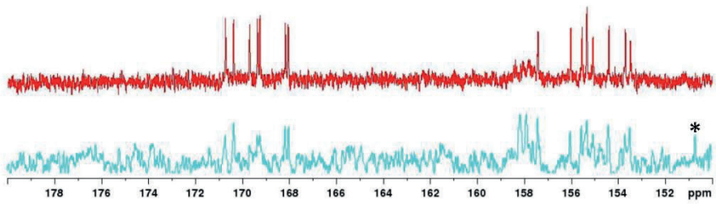

Fig. S14. Detail region (150 – 180 ppm) of the superimposed 125 MHz ^{13}C NMR spectra of the isolated glycopeptide from *A. japonicum* and a desalted commercially available ristomycin standard. The ristomycin standard showed an additional peaks at 150.7 ppm (*).

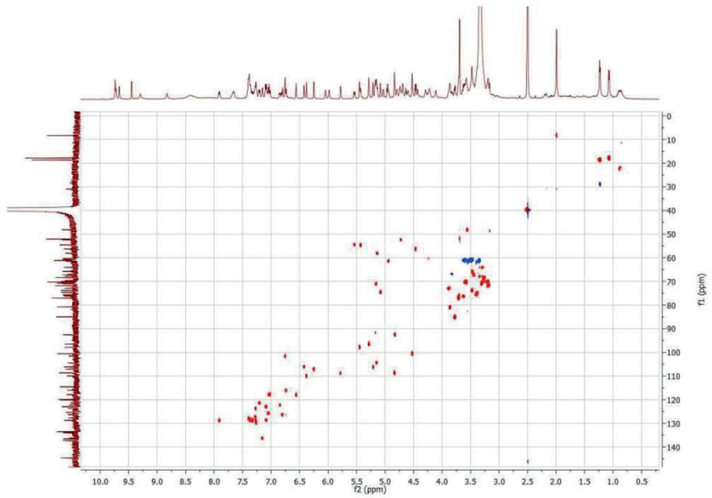

Fig. S15. 500 MHz ^{1}H-^{13}C-HSQC NMR spectrum of the isolated glycopeptide from *A. japonicum* in d_6-DMSO.

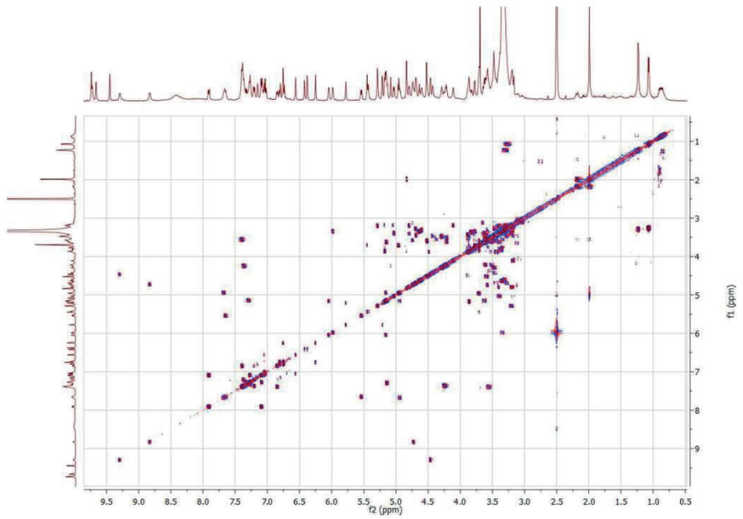

Fig. S16. 500 MHz ^{1}H-^{1}H-DQF-COSY NMR spectrum of the isolated glycopeptide from *A. japonicum* in d_6-DMSO.

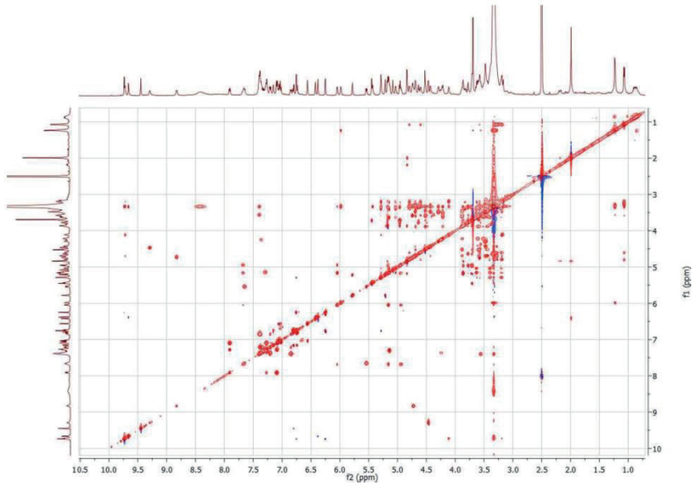

Fig. S17. 500 MHz ^{1}H-^{1}H-TOCSY NMR spectrum of the isolated glycopeptide from *A. japonicum* in d_6-DMSO.

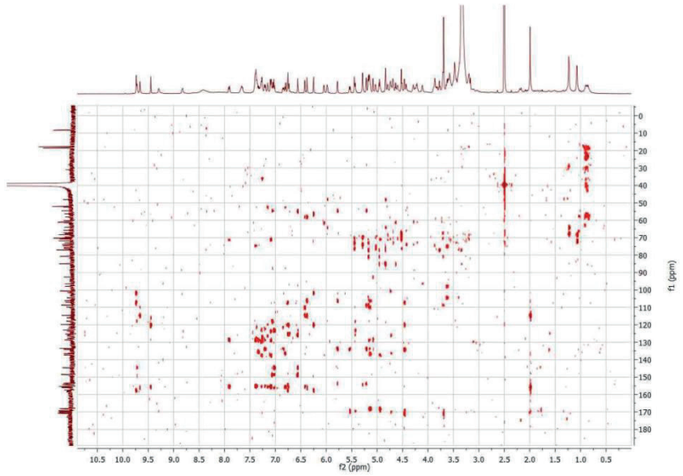

Fig. S18. 500 MHz ^{1}H-^{13}C-HMBC NMR spectrum of the isolated glycopeptide from *A. japonicum* in d_6-DMSO.

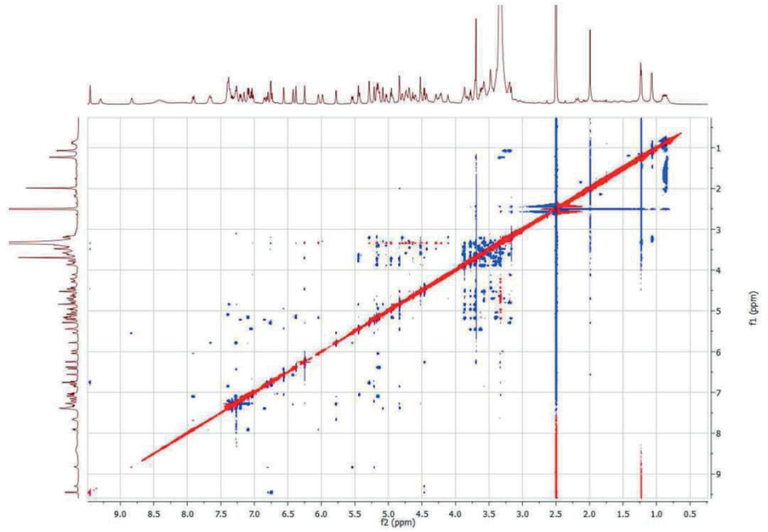

Fig. S19. 500 MHz ^{1}H-^{1}H-ROESY NMR spectrum of the isolated glycopeptide from *A. japonicum* in d_6-DMSO.

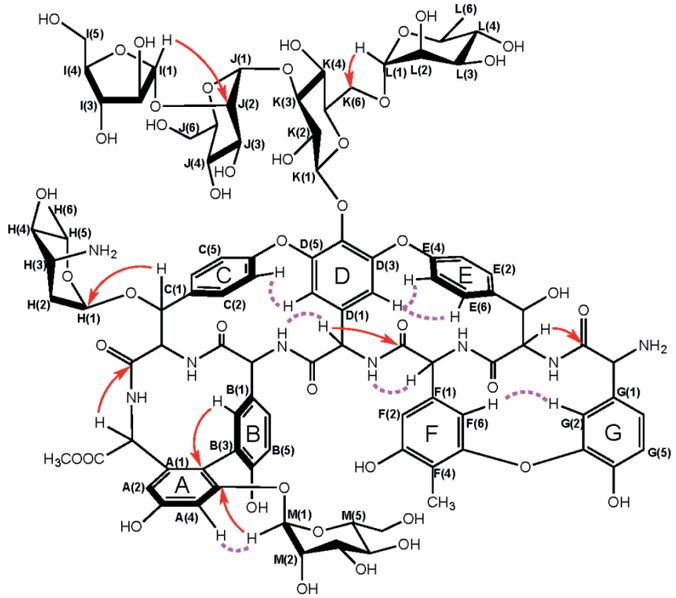

Figure S20. Chemical structure of ristomycin A, numbering scheme and ^{1}H-^{1}H-ROESY- and ^{1}H-^{13}C-HMBC NMR key correlations.

Table S3. NMR spectral data of isolated ristomycin A in d_6-DMSO, measured at 300 K (c = 22 mg/mL, δ in ppm, J in Hz).

residue	position	δ_C	δ_H	residue	position	δ_C	δ_H
Ring A:	α	56.3	4.47 d (5.5)	**Ring F:**	α	58.1	5.14
	A(1)	134.1			F(1)	136.6	
Dpg	A(2)	107.2	6.25 d (1.5)	4-Me-Dpg	F(2)	110.0	6.38 s
methyl ester	A(3)	157.4			F(3)	156.0	
	A(4)	101.6	6.76 brs		F(4)	114.6	
	A(5)	154.4			F(5)	155.4	
	A(6)	119.9			F(6)	106.1	6.42 s
	α-CO	170.7			α-CO	168.2	
	OCH_3	52.1	3.70		α-NH		7.28
	α-NH		9.30 brs		$OH^{F(3)}$		9.66 s
	$OH^{A(3)}$		9.74		$CH_3^{F(4)}$	8.4	1.99 s
Ring B:	α	52.4	4.73	**Ring G:**	α	54.6	5.43
	B(1)	125.3			G(1)	123.0	
para-Hpg	B(2)	136.3	7.16 s	3,4-di-Hpg	G(2)	117.9	6.56 s
	B(3)	120.1			G(3)	148.5	
	B(4)	155.6			G(4)	144.6	
	B(5)	116.0	6.75		G(5)	117.8	7.03
	B(6)	126.3	6.81 d (8.5)		G(6)	125.7	7.06
	α-CO	170.4			α-CO	169.3	
	α-NH		8.83 d (5.2)		α-NH_2		n.o.
	$OH^{B(4)}$		9.45 s		$OH^{G(4)}$		9.73
Ring C:	α	60.3	4.24	**Ring H:**	H(1)	92.6	4.83
	β	74.5	5.08		H(2)	31.0	2.00 & 2.19
β-Ht	C(1)	133.8		ristosamine	H(3)	48.1	3.56
	C(2)	127.8	7.39		H(4)	67.8	3.35
	C(3)	122.2	6.84 d (7.9)		H(5)	64.0	3.30
	C(4)	155.1			$OH^{H(4)}$		5.98 d (4.0)
	C(5)	121.3	7.21 d (8.2)		$CH_3^{H(5)}$	18.6	1.23 d (5.0)
	C(6)	128.7	7.37	**Ring I:**	I(1)	108.7	4.84
	α-CO	169.2			I(2)	80.8	3.86
	α-NH		7.36	arabino-	I(3)	76.3	3.63
Ring D:	α	54.5	5.54 d (7.8)	furanose	I(4)	85.0	3.78
	D(1)	133.9			I(5)	61.2	3.34
3,4,5-tri-	D(2)	108.7	5.78 brs		$OH^{I(2)}$		5.17
Hpg	D(3)	153.5			$OH^{I(3)}$		4.96
	D(4)	133.6			$OH^{I(5)}$		4.64 t (5.4)
	D(5)	153.7		**Ring J:**	J(1)	100.5	4.52
	D(6)	106.2	5.22 brs		J(2)	77.2	3.70
	α-CO	169.7		mannose	J(3)	70.3	3.58
	α-NH		7.65 d (7.8)		J(4)	67.2	3.34
Ring E:	α	61.5	4.94		J(5)	72.9	3.88
	β	71.1	5.16		J(6)	61.0	3.51 & 3.61
β-Ht	E(1)	137.3			$OH^{J(3)}$		n.o.
	E(2)	128.7	7.91 d (8.0)		$OH^{J(4)}$		4.69
	E(3)	128.6	7.09		$OH^{J(6)}$		4.21
	E(4)	155.4		**Ring K:**	K(1)	97.9	5.45
	E(5)	122.9	7.09		K(2)	76.0	3.70
	E(6)	127.2	7.28	glucose	K(3)	74.7	3.39
	α-CO	168.0			K(4)	70.2	3.20
	α-NH		7.67		K(5)	75.6	3.40
	OH(ß)		6.05 d (3.4)		K(6)	66.9	3.37 & 3.83
					$OH^{K(3)}$		5.02
					$OH^{K(4)}$		5.15

residue	position	δ_C	δ_H	residue	position	δ_C	δ_H
Ring L:	L(1)	100.5	4.52 brs	**Ring M:**	M(1)	96.5	5.29
	L(2)	70.1	3.59		M(2)	70.3	3.19
rhamnose	L(3)	70.6	3.19	mannose	M(3)	73.9	3.48
	L(4)	71.8	3.19		M(4)	65.9	3.48
	L(5)	68.3	3.26		M(5)	69.6	3.28
	$OH^{L(2)}$		n.o.		M(6)	60.8	3.33 & 3.48
	$OH^{L(3)}$		n.o.		$OH^{M(2)}$		4.11
	$OH^{L(4)}$		4.79		$OH^{M(3)}$		4.44
	$CH_3^{L(5)}$	17.9	1.07 d (6.0)		$OH^{M(4)}$		4.29
					$OH^{M(6)}$		n.o.

All shift assignments are in good agreement with former studies about ristomycins (Sztaricskai et al., 1980, Tetrahedron Lett. 21:2983-2986; Kalman and Williams, 1980, J. Am. Chem. Soc. USA 102:897-905; Williamson and Williams, 1981, J. Chem. Soc. Perkin Trans. 1: 1483-1491).
Abbreviations: Dpg = 3,5-dihydroxyphenylglycine-methyl ester; Hpg = hydroxy-phenylglycine; ß-Ht = ß-hydroxy-tyrosine; br = broad; s = singlet; d = doublet; n.o. = not observed.

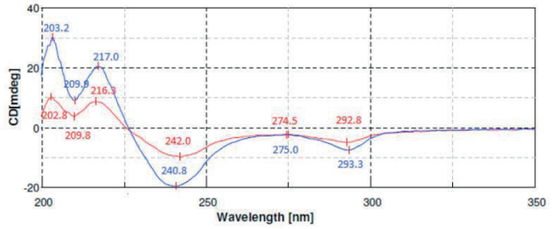

Fig. S21. CD spectra of the isolated glycopeptide from *A. japonicum* and a desalted commercially available ristomycin standard. A concentration of 0.1 mg/mL in H_2O of the isolated glycopeptide from *A. japonicum* and the commercially available standard of ristomycin A was used to generate the spectra.

5.2 Publication 2

Stegmann, E., Albersmeier, A., **Spohn, M.**, Gert, H., Weber, T., Wohlleben, W., Kalinowski, J., and Rückert, C. (2014) Complete genome sequence of the actinobacterium *Amycolatopsis japonica* MG417-CF17 (=DSM 44213T) producing (S,S)-N,N'-ethylenediaminedisuccinic acid. *Journal of Biotechnology* **189**C, 46-47.

Journal of Biotechnology 189 (2014) 46–47

Contents lists available at ScienceDirect

Journal of Biotechnology

journal homepage: www.elsevier.com/locate/jbiotec

Genome Announcement

Complete genome sequence of the actinobacterium *Amycolatopsis japonica* MG417-CF17^T (=DSM 44213T) producing (*S*,*S*)-*N*,*N*′-ethylenediaminedisuccinic acid

Evi Stegmann[a,*], Andreas Albersmeier[b], Marius Spohn[a], Helena Gert[a], Tilmann Weber[a,c], Wolfgang Wohlleben[a], Jörn Kalinowski[b], Christian Rückert[b,**]

[a] *Mikrobiologie und Biotechnologie, Interfakultäres Institut für Mikrobiologie und Infektionsmedizin/Deutsches Zentrum für Infektionsforschung, Universität Tübingen, Auf der Morgenstelle 28, 72076 Tübingen, Germany*
[b] *Technology Platform Genomics, Center for Biotechnology (CeBiTec), Bielefeld University, Sequenz 1, 33615 Bielefeld, Germany*
[c] *The Novo Nordisk Foundation Center for Biosustainability, Technical University of Denmark, Kogle Alle 6, 2970 Hørsholm, Denmark*

ARTICLE INFO

Article history:
Received 20 August 2014
Accepted 25 August 2014
Available online 3 September 2014

Keywords:
Amycolatopsis
Genome sequence
Ethylenediaminedisuccinic acid
Secondary metabolites

ABSTRACT

We report the complete genome sequence of *Amycolatopsis japonica* MG417-CF17^T (=DSM 44213^T) which was identified as the producer of (*S*,*S*)-*N*,*N*′-ethylenediaminedisuccinic acid during a screening for phospholipase C inhibitors. The genome of *A. japonica* MG417-CF17^T consists of two replicons: the chromosome (8,961,318 bp, 68.89% G + C content) and the plasmid pAmyja1 (92,539 bp, 68.23% G + C content), encoding a total of 8422 protein coding genes. Analysis of the sequence data revealed 30 clusters encoding the biosynthesis of secondary metabolites.

Introduction

The bacterial order of the *Actinomycetales* contains a large number of genera that are capable of synthesizing a wide variety of secondary metabolites (e.g., Jankowitsch et al., 2012; Myronovskyi et al., 2013; Rückert et al., 2014; Schwientek et al., 2012). The nocardioform actinomycete *Amycolatopsis japonica* MG417-CF17^T (=DSM 44213^T) is the producer of [*S*,*S*]-ethylenediaminedisuccinic acid (EDDS) which is a hexadentate chelating agent. [*S*,*S*]-EDDS is an isomer of ethylenediaminetetraacetic acid (EDTA) with comparable chelating properties. However, EDDS is in contrast to EDTA biodegradable (Schowanek et al., 1997).

The strain *A. japonica* MG417-CF17^T was discovered in a search for specific inhibitors of phospholipases (Nishikiori et al., 1984). Preliminary cultural and morphological studies indicated that the organism belonged to the family *Pseudonocardiaceae* and it was classified as *Amycolatopsis orientalis*. However, 16S rRNA analyses performed by Goodfellow et al. (1997) and a number of phenotypic properties resulted in the renaming of the strain in "*Amycolatopsis japonicum*" sp. nov., corrected to *A. japonica* upon validation (Anonymous, 1997). *A. japonica* is of great interest because the strain is genetically accessible (Stegmann et al., 2001) and has the potential to produce a wide spectrum of secondary metabolites (Spohn et al., 2014).

To obtain the complete genome sequence, data from two sequencing libraries were combined, a whole genome shotgun library and a 8 k long paired end library. Both libraries were sequenced on a 454 GS-FLX platform using the Titanium chemistry to avoid problems caused by the expected high G + C content (Schwientek et al., 2011). In total, 732,707 reads (213,725,262 bases) were assembled in two scaffolds using Newbler v2.5.3, representing the circular chromosome (51 unique contigs) and plasmid pAmyja1 (1 contig). In total 62 contigs larger than 500 bp were assembled, the average coverage of the assembled contigs was 23.6-fold. To obtain the complete sequence, gaps caused by repeats were closed using CONSED (Gordon, 2003; Gordon et al., 1998). To correct for homopolymer errors, additional data from an Illumina GA *IIx* single read run of 150 bp were used, similar to the approach for *Streptomyces collinus* (Rückert et al., 2013). A set of 2,786,834 reads was mapped on the sequence, allowing to identify and correct 31 indel errors. The polished sequences were annotated using GenDB (Meyer et al., 2003), the results are listed in Table 1.

* Corresponding author. Tel.: +49 7071 2978840.
** Corresponding author. Tel.: +49 (0)521 106 12252.
E-mail addresses: Evi.Stegmann@Biotech.Uni-Tuebingen.DE (E. Stegmann), Christian.Rueckert@CeBiTec.Uni-Bielefeld.DE (C. Rückert).

http://dx.doi.org/10.1016/j.jbiotec.2014.08.034
0168-1656/

Table 1
Genome features of *A. japonica* MG417-CF17^T.

Features	Chromosome	Plasmid pAmyja1
Length (bp)	8,961,318	92,539
DNA-coding regions (bp)	8,156,541	80,232
G + C content (%)	68.89	68.23
CDS	8298	126
rRNA genes (operons)	12 (4)	0
tRNA genes	55	0

Using the software antiSMASH 2.0 (Blin et al., 2013), in total 30 gene clusters encoding the biosynthesis of secondary metabolites were identified, a number roughly comparable to other *Pseudonocardiaceae* (Strobel et al., 2012). Among these clusters are one novel glycopeptide gene cluster (Spohn et al., 2014) as well as several clusters encoding the synthesis of polyketide, nonribosomal peptide antibiotics, and lanthipeptides.

Nucleotide sequence accession numbers

The complete genome sequence has been deposited in DDBJ/EMBL/GenBank under accession nos. CP008953 (chromosome) and CP008954 (pAmyja1).

Acknowledgements

This work was supported by grants of the BMBF (GenBioCom-0315585A, 0315585B, and 0315585J) to Wolfgang Wohlleben, Tilmann Weber, and Jörn Kalinowski, respectively.

References

Anonymous, 1997. Validation of the publication of new names and new combinations previously effectively published outside the IJSB, List No. 63. Int. J. Syst. Bacteriol. 47, 1274.
Blin, K., Medema, M.H., Kazempour, D., Fischbach, M.A., Breitling, R., Takano, E., Weber, T., 2013. antiSMASH 2.0 – a versatile platform for genome mining of secondary metabolite producers. Nucleic Acids Res. 41, W204–W212.
Goodfellow, M., Brown, A.B., Cai, J.P., Chun, J.S., Collins, M.D., 1997. *Amycolatopsis japonicum* sp. nov, an actinomycete producing (S,S)-N,N′-ethylenediaminedisuccinic acid. Syst. Appl. Microbiol. 20, 78–84.
Gordon, D., 2003. Viewing and editing assembled sequences using consed. Curr. Protoc. Bioinform., 12 (Chapter 11, Unit 11).
Gordon, D., Abajian, C., Green, P., 1998. Consed: a graphical tool for sequence finishing. Genome Res. 8, 195–202.
Jankowitsch, F., Schwarz, J., Rückert, C., Gust, B., Szczepanowski, R., Blom, J., Pelzer, S., Kalinowski, J., Mack, M., 2012. Genome sequence of the bacterium *Streptomyces davawensis* JCM 4913 and heterologous production of the unique antibiotic roseoflavin. J. Bacteriol. 194, 6818–6827.
Meyer, F., Goesmann, A., McHardy, A.C., Bartels, D., Bekel, T., Clausen, J., Kalinowski, J., Linke, B., Rupp, O., Giegerich, R., Pühler, A., 2003. GenDB – an open source genome annotation system for prokaryote genomes. Nucleic Acids Res. 31, 2187–2195.
Myronovskyi, M., Tokovenko, B., Manderscheid, N., Petzke, L., Luzhetskyy, A., 2013. Complete genome sequence of *Streptomyces fulvissimus*. J. Biotechnol. 168, 117–118.
Nishikiori, T., Okuyama, A., Naganawa, H., Takita, T., Hamada, M., Takeuchi, T., Aoyagi, T., Umezawa, H., 1984. Production by actinomycetes of (S,S)-N,N′-ethylenediamine-disuccinic acid, an inhibitor of phospholipase C. J. Antibiot. (Tokyo) 37, 426–427.
Rückert, C., Szczepanowski, R., Albersmeier, A., Goesmann, A., Fischer, N., Steinkamper, A., Pühler, A., Biener, R., Schwartz, D., Kalinowski, J., 2014. Complete genome sequence of the actinobacterium *Actinoplanes friuliensis* HAG 010964, producer of the lipopeptide antibiotic friulimycin. J. Biotechnol. 178, 41–42.
Rückert, C., Szczepanowski, R., Albersmeier, A., Goesmann, A., Iftime, D., Musiol, E.M., Blin, K., Wohlleben, W., Pühler, A., Kalinowski, J., Weber, T., 2013. Complete genome sequence of the kirromycin producer *Streptomyces collinus* Tu 365 consisting of a linear chromosome and two linear plasmids. J. Biotechnol. 168, 739–740.
Schowanek, D., Feijtel, T.C., Perkins, C.M., Hartman, F.A., Federle, T.W., Larson, R.J., 1997. Biodegradation of [S,S], [R,R] and mixed stereoisomers of ethylene diamine disuccinic acid (EDDS), a transition metal chelator. Chemosphere 34, 2375–2391.
Schwientek, P., Szczepanowski, R., Rückert, C., Kalinowski, J., Klein, A., Selber, K., Wehmeier, U.F., Stoye, J., Pühler, A., 2012. The complete genome sequence of the acarbose producer *Actinoplanes* sp. SE50/110. BMC Genomics 13, 112.
Schwientek, P., Szczepanowski, R., Rückert, C., Stoye, J., Pühler, A., 2011. Sequencing of high G + C microbial genomes using the ultrafast pyrosequencing technology. J. Biotechnol. 155, 68–77.
Spohn, M., Kirchner, N., Kulik, A., Jochim, A., Wolf, F., Muenzer, P., Borst, O., Gross, H., Wohlleben, W., Stegmann, E., 2014. Overproduction of ristomycin A by activation of a silent gene cluster in *Amycolatopsis japonicum* MG417-CF17. AAC, pii: AAC.03512-14.
Stegmann, E., Pelzer, S., Wilken, K., Wohlleben, W., 2001. Development of three different gene cloning systems for genetic investigation of the new species *Amycolatopsis japonicum* MG417-CF17, the ethylenediaminedisuccinic acid producer. J. Biotechnol. 92, 195–204.
Strobel, T., Al-Dilaimi, A., Blom, J., Gessner, A., Kalinowski, J., Luzhetska, M., Pühler, A., Szczepanowski, R., Bechthold, A., Rückert, C., 2012. Complete genome sequence of *Saccharothrix espanaensis* DSM 44229^T and comparison to the other completely sequenced Pseudonocardiaceae. BMC Genomics 13, 465.

5.3 Publication 3

Spohn, M., Wohlleben, W., and Stegmann, E. (2016) Elucidation of the zinc dependent regulation in *Amycolatopsis japonicum* enabled the identification of the ethylenediamine-disuccinate ([*S,S*]-EDDS) genes. *Environmental Microbiology* **18**, 1249-1263.

environmental microbiology

Environmental Microbiology (2016) **18**(4), 1249–1263 doi:10.1111/1462-2920.13159

Elucidation of the zinc-dependent regulation in *Amycolatopsis japonicum* enabled the identification of the ethylenediamine-disuccinate ([*S,S*]-EDDS) genes

Marius Spohn,[1] Wolfgang Wohlleben[1,2] and Evi Stegmann[1,2]*

[1]*Interfaculty Institute of Microbiology and Infection Medicine Tuebingen, Microbiology/Biotechnology, University of Tuebingen, 72076 Tuebingen, Germany.*

[2]*Partner Site Tuebingen, German Centre for Infection Research (DZIF), Tuebingen, Germany.*

Summary

The actinomycete *Amycolatopsis japonicum* produces the complexing agent ethylenediamine-disuccinate ([*S,S*]-EDDS), which is an isomer of the widely industrially applied ethylenediamine-tetraacetate (EDTA). In contrast to EDTA, [*S,S*]-EDDS is readily biodegradable and is therefore an alternative with a favourable environmental profile. Biotechnological production of [*S,S*]-EDDS, however, is not currently possible because its biosynthesis is inhibited by low-micromolar zinc concentrations. Here we illustrate the development of a new strategy for identifying a biosynthetic pathway that is based on the elucidation of transcriptional regulation and the screening for binding sites of the respective regulator that controls the [*S,S*]-EDDS biosynthesis genes. To achieve this, we identified the zinc uptake regulator Zur in *A. japonicum* and showed that it mediates the repression of the zinc uptake system $ZnuABC_{Aj}$. The Zur-binding motif, recognized by the zinc-bound Zur protein in the upstream region of $znuABC_{Aj}$, was used to screen the genome, leading to the identification of the *aes* genes. Transcriptional analysis and shift assays reveal specific zinc-responsive regulation of the *aes* genes by Zur, and gene inactivation shows their involvement in [*S,S*]-EDDS biosynthesis. Zur-mediated zinc repression of the [*S,S*]-EDDS biosynthesis genes is abolished in a Δ*zur* mutant, which offers now the opportunity to develop a biotechnological process.

Received 7 October, 2015; revised 13 November, 2015; accepted 27 November, 2015. *For correspondence. E-mail evi.stegmann@biotech.uni-tuebingen.de; Tel. +49 7071 29 78840; Fax +49 7071 29 5979.

Introduction

Ethylenediamine-disuccinate (EDDS) is an aminopolycarboxylic acid, which forms typical sixfold coordinated complexes with transient metal ions (Chen *et al.*, 2010). EDDS exhibits two asymmetric C-atoms, allowing the formation of four optical stereoisomers: [*S,S*]-, [*R,R*]-, the meso-isomers [*R,S*]- and [*S,R*]-EDDS. The [*S,S*]-configuration is the only stereoisomer readily biodegradable to complete mineralization (Schowanek *et al.*, 1997; Takahashi *et al.*, 1997).

The actinomycete strain *Amycolatopsis japonicum* MG417-CF17 (formerly described as *Amycolatopsis orientalis*; Goodfellow *et al.*, 1997) produces [*S,S*]-EDDS as a natural compound. [*S,S*]-EDDS was originally discovered during a screening for phospholipase C inhibitors (Nishikiori *et al.*, 1984) and exerts its inhibitory effect by complexing zinc ions, which are essential cofactors of this zinc-metalloenzyme (Hough *et al.*, 1989). [*S,S*]-EDDS is an ethylenediamine-tetra acetate (EDTA) isomer (Fig. 1). EDTA is used commercially in large quantities for many applications, such as in cosmetic, food and medical products as well as in the textile and paper industries or in laundry detergents. However, due to its low biodegradability, EDTA cannot be removed by conventional wastewater treatments and remains at high concentrations in aquatic environments, where it evokes constant environmental threats by undesirably mobilizing metal ions. Because [*S,S*]-EDDS exhibits similar chelating properties as EDTA, it offers a biodegradable alternative that is chemically produced from non-renewable fossil resources.

To date, siderophores are the main group of described chelating compounds produced by microbes. They are produced under iron-deficient conditions to solubilize and facilitate the uptake of iron. Also, strains of the genus *Amycolatopsis* are known siderophore producers (Meiwes *et al.*, 1990; Seyedsayamdost *et al.*, 2011). Although there are secondary metabolites that complex certain metal ions with high affinity, like the zinc-binding zincophorin (Brooks *et al.*, 1984) or the copper-binding closthioamide (Kloss *et al.*, 2013), they are neither synthesized in response to deficiency of the corresponding metal ion, nor reported to mediate its uptake.

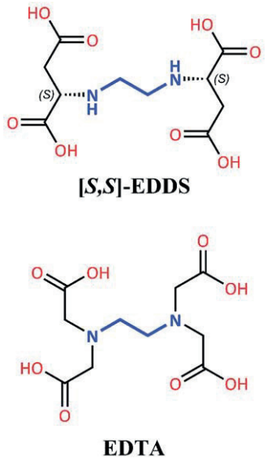

Fig. 1. Chemical structures of [*S,S*]-EDDS and EDTA.

Chelating agents (ionophores), which are predicted to function in the acquisition of transition metals other than iron, however, have been disregarded for a long time. The examples described include the zincophores, such as pyridine-2,6-bis(thiocarboxylic acid) from *Pseudomonas putida* (Leach *et al*., 2007) and coelibactin from *Streptomyces coelicolor* (Kallifidas *et al*., 2010), and the copperphore methanobactin from methane-oxidizing bacteria (Kim *et al*., 2004). Ionophores are either synthesized by non-ribosomal peptide synthetases (NRPS) (e.g. enterobactin; Pollack *et al*., 1970; Rusnak *et al*., 1991) or by NRPS-independent siderophore (NIS) synthetases (e.g. aerobactin; Gibson and Magrath, 1969; de Lorenzo and Neilands, 1986). Because [*S,S*]-EDDS production is tightly inhibited by traces of zinc, whereas iron had only a minor effect even at elevated concentrations (Cebulla, 1995; Zwicker *et al*., 1997), it is considered that [*S,S*]-EDDS is an evolutionary response to zinc deficiency, serving as a zincophore to contribute to zinc uptake.

Zinc is an essential trace element for all living cells, and it is estimated that 5–10% of all proteins contain zinc as a cofactor (Andreini *et al*., 2006). Zinc in proteins either participates directly in chemical catalysis or is important for maintaining protein structure and stability. However, highly concentrated zinc can inhibit physiological functions of proteins by blocking important thiols and by competing with other metal ions for binding sites (Kasahara and Anraku, 1974; Aagaard and Brzezinski, 2001). Hence, all cells have to maintain zinc homeostasis optimal for cell survival. In prokaryotes, this precise balance is predominantly maintained using zinc-responsive transcriptional factors, which sense zinc deficiency and zinc excess (Choi and Bird, 2014). The major prokaryotic factor regulating the expression of genes encoding zinc uptake and zinc mobilization functions is Zur (zinc uptake regulator), initially described in *Bacillus subtilis* and *Escherichia coli* (Gaballa and Helmann, 1998; Patzer and Hantke, 1998). Zur belongs to the Fur (Ferric uptake regulator) protein family of transcription regulators. Within the Fur family, there is a huge diversity in metal selectivity and biological function, including sensors of not only zinc, iron, manganese and nickel, but also of oxidative or acid stress. Fur proteins are typically transcriptional repressors that bind specifically to corresponding palindromic A/T-rich sequences found in the promoters of their DNA targets when bound to their cognate metal ion cofactors (Fillat, 2014). Under zinc-deficient conditions, Zur is inactive and has negligible affinity for the operator sequence. The inactive Zur binds only one zinc ion per monomer within a structural zinc-binding site (ZBS) to maintain its homodimeric state (Lucarelli *et al*., 2007; Ma *et al*., 2011; Shin *et al*., 2011). The increased concentration of free zinc ions leads to further binding of zinc to additional regulatory ZBSs, causing a conformational change, which gives rise to a fully active form of the repressor. Zinc-bound Zur exhibits a high affinity for its cognate DNA motifs upstream of their target genes (Choi and Bird, 2014). One of the best-investigated Zur regulators in actinomycetes, to date, is the Zur protein of *S. coelicolor*. In *S. coelicolor*, the Zur regulon includes *znuABC*, encoding an ATP-binding cassette (ABC) uptake system (Shin *et al*., 2007), an NRPS gene cluster, predicted to direct synthesis of coelibactin (Kallifidas *et al*., 2010), and a set of genes encoding alternative, zinc-free ribosomal proteins (Owen *et al*., 2007).

Because the identification of the EDDS biosynthetic genes was not possible using strategies normally applied to the isolation of secondary metabolite gene clusters, we developed a new approach to identify natural compound biosynthesis pathways by exploiting knowledge in the field of transcriptional regulation, which we termed INBEKT. Using this approach, we could elucidate the Zur_{Aj}-mediated zinc regulation in *A. japonicum* in detail. The constructed *A. japonicum* Δzur_{Aj} mutant showed elevated EDDS production, even in the presence of high zinc concentrations, revealing the EDDS biosynthesis genes as a member of the Zur_{Aj} regulon. The subsequent screening of the *A. japonicum* genome with the deduced Zur box enabled the identification of EDDS biosynthesis genes for the first time. Transcriptional analyses and gel shift experiments confirmed that they are strictly zinc repressed by Zur_{Aj}. The analysis of the phylogenetic abundance of the identified EDDS biosynthesis genes, combined with the evaluation of the capability of certain *Amycolatopsis* strains to produce EDDS, provides insight into its role as an evolutionary response to zinc deficiency and contributes to the determination of the EDDS biosynthesis gene cluster.

Results and discussion

The [S,S]-EDDS biosynthetic gene cluster cannot be identified by classical methods and stays hidden to genome-mining approaches

Amycolatopsis japonicum was described as the producer of [*S,S*]-EDDS in 1984 (Nishikiori *et al*., 1984). However, the enzymes required for [*S,S*]-EDDS biosynthesis have not yet been identified. During the pre-genomic era, different classical approaches, such as heterologous expression of an *A. japonicum* cosmid library in a non-producer strain, or comparative proteomics of cells growing in the presence or absence of zinc, have been applied unsuccessfully. In addition, a reverse genetic approach with degenerated primers did not result in the identification of any genes in the *A. japonicum* genome encoding NIS synthetases, commonly involved in ionophore biosynthesis. Access to the *A. japonicum* genome sequence (GenBank accession number CP008953) (Stegmann *et al*., 2014) allowed data analysis using bioinformatic tools such as antiSMASH 3.0 (Weber *et al*., 2015) to evaluate the biosynthetic potential of *A. japonicum*. antiSMASH 3.0 is a bioinformatic tool capable of discovering and classifying biosynthetic loci covering a wide range of known secondary metabolite compound classes. This *in silico* analysis revealed the presence of various putative gene clusters encoding the synthesis of natural products in *A. japonicum* (Spohn *et al*., 2014). Two of the identified gene clusters could be assigned to their products: ECO-0501, a polyketide synthase-derived polyene (Shen *et al*., 2012) and ristomycin A (Spohn *et al*., 2014), a glycopeptide antibiotic. However, none of the remaining clusters could be assigned to the [*S,S*]-EDDS structure, indicating a novel and unique biosynthesis mechanism different from the typical NRPS or NIS pathways known for siderophore synthesis. Therefore, the development of an alternative strategy for the identification of the [*S,S*]-EDDS biosynthesis genes was required.

Zur controls the expression of the [S,S]-EDDS biosynthesis

Because [*S,S*]-EDDS production is repressed when *A. japonicum* is grown in zinc-containing medium (>2 μM zinc), we assumed that a zinc-responsive regulator controls the [*S,S*]-EDDS biosynthesis genes. BLAST analyses of the *A. japonicum* genome using the protein sequence of Zur_{SC}, the zinc uptake regulator of *S. coelicolor* (Owen *et al*., 2007), revealed the presence of AJAP_29045 (GenBank: AIG78644) with high similarity (67% amino acid identity). All of the available Zur structures demonstrate a common homodimeric quaternary structure with each monomer consisting of an N-terminal DNA-binding domain, a C-terminal dimerization domain and an inter-domain hinge loop (Fillat, 2014). From the crystal structures of Zur from *Mycobacterium tuberculosis* (Lucarelli *et al*., 2007) and *S. coelicolor* (Shin *et al*., 2011), three ZBSs per monomer were determined. One ZBS is required to ensure the dimeric structural integrity of the proteins, whereas the other two ZBSs possess regulatory roles to modulate Zur activity (D'Autreaux *et al*., 2007; Shin *et al*., 2011). In *S. coelicolor*, it is suggested that the two regulatory ZBSs serve as an on–off switch to activate Zur and to mediate graded gene expression as a response to altered zinc concentration (Shin *et al*., 2011). In support of its potential role as a major zinc regulator, PREDZINC 1.4 (Shu *et al*., 2008) analysis and multisequence alignments revealed the presence of all three putative ZBSs in the AJAP_29045 gene product (Fig. S1), which is henceforth designated Zur_{Aj}.

To investigate the role of Zur_{Aj} as a regulator of the [*S,S*]-EDDS biosynthesis in *A. japonicum*, the entire zur_{Aj}-coding region was deleted in frame with a markerless procedure (*A. japonicum* Δ*zur*) (the deletion procedure is illustrated in Fig. S2). For this purpose, the flanking regions of zur_{Aj} were integrated into pGusA21 (Table S1, Fig. S2), which contains the *gusA* reporter gene encoding a β-glucuronidase (GUS). The gene inactivation plasmid pGusA21Δ*zur* (Table S1) was integrated into the *A. japonicum* genome via a single crossover. This event was selected by using the plasmid-encoded apramycin resistance. The integration of the plasmid was verified by polymerase chain reaction (PCR). To obtain a deletion mutant, a second homologous recombination event was provoked by stressing selected colonies using temperature shifts and protoplast formation as described previously (Puk *et al*., 2002). Protoplast regeneration was carried out on agar plates containing the GUS substrate 5-bromo-4-chloro-3-indolyl-β-d-glucuronide (X-Gluc). The loss of GUS activity (visible as white-coloured colonies) indicated the excision of the plasmid. GUS-negative colonies were selected, and the deletion of the zur_{Aj} gene was confirmed by PCR.

To study the effect of the zur_{Aj} deletion on [*S,S*]-EDDS production, *A. japonicum* Δ*zur* and *A. japonicum* wild type (WT) were grown in 12-well microtitre plates containing 3 ml of synthetic medium (SM) per well with various increasing zinc concentrations. [*S,S*]-EDDS production was quantified by high performance liquid chromatography-dioden array detector (HPLC-DAD) analyses after growth for 72 h from three biological replicates to determine the production yield in [*S,S*]-EDDS/biomass (mg g^{-1}). *A. japonicum* WT produced [*S,S*]-EDDS only with zinc concentrations lower than 2 μM (Fig. 2). In contrast, zinc independent and constant [*S,S*]-EDDS biosynthesis was observed in *A. japonicum* Δ*zur* over the total range of the applied zinc gradient (Fig. 2), an effect that was even seen at a zinc concentration of 5 mM.

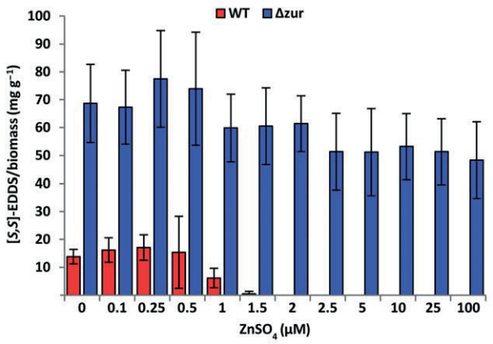

Fig. 2. Zinc-dependent production of [*S,S*]-EDDS. Strains were grown for 72 h in 12-well microtitre plates in synthetic medium (SM) supplemented with different concentrations of $ZnSO_4$. $n = 3$.

Additionally, the deletion of zur_{Aj} led to an increased total [*S,S*]-EDDS yield (4 to 4.5-fold) compared with the WT strain. To genetically complement *A. japonicum* Δ*zur*, a single-coding region of the entire zur_{Aj} gene was cloned into the integrative vector pRM4 under the control of the constitutive promoter *ermEp** and transferred into *A. japonicum* Δ*zur*. *Amycolatopsis japonicum* Δ*zur*::pRM4-*zur* showed the same phenotype as the WT; it produced [*S,S*]-EDDS exclusively in the absence of zinc (Fig. S3). [*S,S*]-EDDS production in *A. japonicum* Δ*zur* in the presence of zinc suggested that the *ajap_29045*-encoded protein is the zinc-sensing regulator Zur_{Aj} and that the [*S,S*]-EDDS biosynthesis genes are under its zinc-responsive control.

The Zur regulon of A. japonicum *contains the high-affinity zinc uptake system* znuABC

Zur regulons characterized thus far usually comprise 10–30 genes with different functions, often related to zinc homeostasis. In particular, the high-affinity zinc uptake system ZnuABC has been identified as Zur regulated in many bacteria and is widely distributed throughout the bacterial kingdom (Patzer and Hantke, 1998; Campoy *et al*., 2002; Lucarelli *et al*., 2007; Shin *et al*., 2007; Pawlik *et al*., 2012). We identified two loci in *A. japonicum* whose deduced protein sequences show high levels of similarity to the previously described ZnuABC system of *S. coelicolor* (Shin *et al*., 2007) (Fig. 3B). However, in contrast to *S. coelicolor*, neither of them is localized closely to zur_{Aj}. The two loci are encoded by *ajap_18665-80* (locus 1) and *ajap_32775-85* (locus 2), and both encode a putative ATPase, a putative membrane permease and a putative metal-binding lipoprotein. Locus 2 exhibits an identical gene arrangement to the $znuABC_{Sc}$ genes in *S. coelicolor*, whereas the gene arrangement of locus 1 deviates from that of $znuABC_{Sc}$. Moreover, locus 1 is extended by a gene (*ajap_18675*) that is predicted to encode a lipoprotein containing an N-terminal signal peptide with a conserved lipobox (L-A-A-C).

To elucidate which locus is connected to zinc uptake in *A. japonicum*, we performed qualitative reverse transcription PCR (RT-PCR). The transcriptional pattern of the two *znuABC* homologues was investigated with respect to the presence of zinc ions. Hence, cultures were grown in the presence (25 μM) and in the absence of zinc, and RNA was isolated after 10 h (early exponential phase) and 70 h (stationary phase). The presence of *ajap_32775* (locus 2) and *ajap_18670* (locus 1) transcripts were monitored with specific primer pairs (Table S2). RT-PCR analysis showed that locus 1 expression was repressed in the presence of zinc, in contrast to locus 2 whose expression was zinc independent (Fig. 3C). From these results we concluded that locus 1 encodes an ABC uptake system sensitive for zinc, and we designated it henceforth $znuABC_{Aj}$. To further specify the function of locus 2, we analysed its transcriptional pattern after growth in SM supplemented with various metal ions (Fe^{2+}, Ni^{2+}, Co^{2+} and Mn^{2+}). *ajap*_32775 expression was specifically repressed in the presence of manganese (Fig. 3C). Therefore, locus 2 was considered to encode an ABC transporter with a manganese uptake function in *A. japonicum*, similar to the *mntABCD* system of *B. subtilis* (Que and Helmann, 2000). The transcription of *znuB* (*ajap_18670*) is not repressed by any ion other than zinc, revealing the specific function of ZnuABC as a zinc acquisition system.

To assess the physiological range in which the identified zinc uptake system is required to supply the cells with zinc, *A. japonicum* WT and *A. japonicum* Δ*zur* were grown in microtitre plates in a zinc gradient. RNA isolation was performed after 72 h of growth and used for RT-PCR analyses. A $znuB_{Aj}$ transcript was only detectable in WT samples after growth with zinc concentration of ≤2.0 μM (Fig. 4). This indicates the necessity of $ZnuABC_{Aj}$ to enhance zinc uptake in an environment characterized by low zinc bioavailability (≤2.0 μM). In contrast, transcriptional analysis of $znuB_{Aj}$ in the *A. japonicum* Δ*zur* mutant occurred over the whole range of applied zinc concentrations, with detectable expression even at the most elevated zinc concentrations (100 μM) (Fig. 4).

Because $znuC_{Aj}$ and $znuB_{Aj}$ are transcribed in reverse orientation we assumed the presence of a Zur_{Aj} box in this intergenic region. To analyse whether Zur_{Aj} binds to this region in a zinc-dependent manner, electrophoretic mobility shift assays (EMSAs) were performed. His-tagged Zur_{Aj} was purified from *E. coli* BL21(DE3) pLys transformed with pET-30-*zur*. Cy5-labelled DNA, covering the region from −110 to +35 bp with respect to the $znuB_{Aj}$ GTG start codon (*iznuCB*), was used as a probe in the EMSA. The binding reaction was carried out by incubating

A

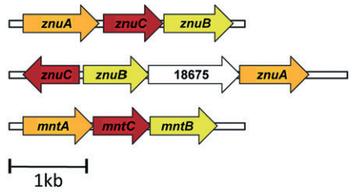

B

S. coelicolor znuABC	ZnuA	ZnuC	ZnuB
amino acids	328	256	300
GenBank-ID	NP_626745	NP_626746	NP_626747
proposed function	lipoprotein	ATPase	membrane permease

A. japonicum locus 1	AJAP_18680	AJAP_18665	AJAP_18670
amino acids	299	244	283
GenBank-ID	AIG76602	AIG76599	AIG76600
amino acids identity/similarity (%)	24/42	36/56	28/48

A. japonicum locus 2	AJAP_32775	AJAP_32780	AJAP_32785
amino acids	304	247	289
GenBank-ID	AIG79369	AIG79370	AIG79371
amino acids identity/similarity (%)	23/40	37/52	30/47

C

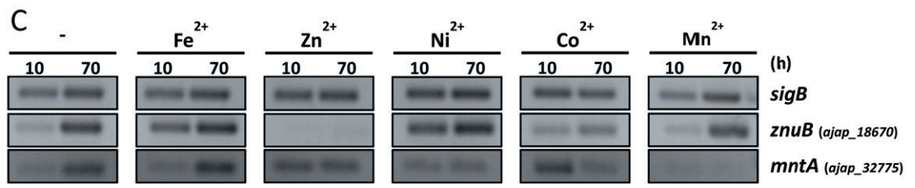

Fig. 3. Gene organization and zinc-specific regulation of *znuABC* homologues loci in *A. japonicum*.
A. Comparison of the gene organization pattern of the *znuABC* locus in *S. coelicolor* with homologues in *A. japonicum*.
B. Homology analyses using BLAST: identity/similarity of locus 1 and 2 to ZnuABC proteins of *S. coelicolor* on amino acid level.
C. Trace metal-dependent transcriptional pattern of the putative high-affinity metal uptake systems of *A. japonicum*. Cultures were grown in SM in the absence of any trace element (–) or supplemented with 25 μM Fe^{2+}, Zn^{2+}, Ni^{2+}, Co^{2+} or Mn^{2+}, and samples were taken after 10 h (exponential growth phase) and 70 h (stationary growth phase) of incubation to isolate RNA. *sigB* was used as a housekeeping gene to normalize the RNA. *znuB* (*ajap_18670*) and *mntA* (*ajap*_32775) were chosen as probes to represent the entire locus.

labelled DNA with purified Zur_{Aj} in binding buffer with or without 25 μM $ZnSO_4$. Binding of Zur_{Aj} occurred only in the presence of zinc (Fig. 5). Although Zur_{Aj} was also added in various higher concentrations, only a single Zur_{Aj} shift was observed. In contrast, *S. coelicolor* Zur forms multiple complexes with its target DNAs in dependence on increased Zur concentration (Shin *et al*., 2007; Kallifidas *et al*., 2010). It is thought that these multiple shifts represent independent binding events of several Zur dimers to the DNA. However, in *E. coli*, no such intermediate species of protein–DNA bindings were observed. There, two Zur dimers bind to the DNA in a highly cooperative

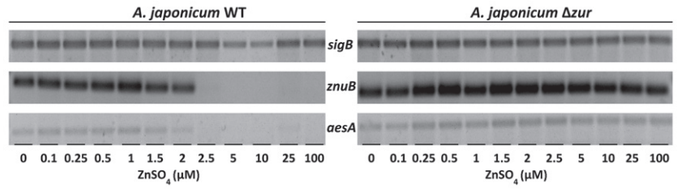

Fig. 4. Zinc-dependent gene transcription in *A. japonicum* strains. Strains were grown for 72 h in 12-well microtitre plates in synthetic medium (SM) supplemented with different concentrations of $ZnSO_4$ prior to RNA isolation. *sigB* was used as a housekeeping gene to normalize the RNA. *znuB* (*ajap_18670*) and *aesA* (*ajap*_08425) were amplified using specific primers (Table S2).

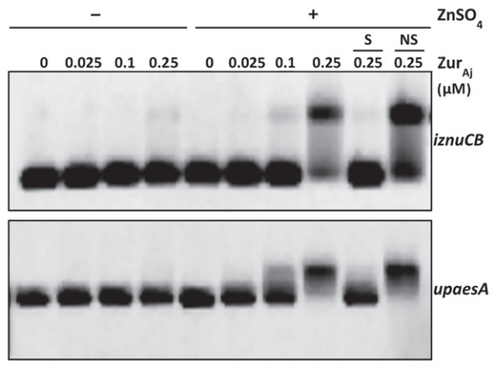

Fig. 5. Zinc-dependent binding of purified Zur_{Aj} to *znuCB* and *aesA* promoter region. Purified Zur_{Aj} was incubated with Cy5-labelled DNA fragment upstream of *znuCB* (*iznuCB*) or *aesA* (*upaesA*) (4 nM) in the absence or in the presence of 25 μM $ZnSO_4$ (indicated by – and + respectively). To confirm the specificity of the binding complexes, either an excess amount of non-specific competitors [NS; pRM4 (70 nM)] or of specific competitors [S; unlabelled fragment upstream of *znuCB* DNA (1,1 μM) or *aesA* (0.65 μM)] was added to the binding mixture.

way, revealing single shifts in EMSA experiments (Gilston *et al.*, 2014), comparable with the observed single Zur_{Aj} shift. To identify a conserved Zur_{Aj} box we used MEME, a tool for discovering motifs in a group of related DNA (Bailey *et al.*, 2009). The Zur consensus sequences of *M. tuberculosis* (Maciag *et al.*, 2007), *Corynebacterium glutamicum* (Schröder *et al.*, 2010) and *S. coelicolor* (Owen *et al.*, 2007) were aligned to the intergenic region of $znuCB_{Aj}$ to identify a conserved Zur_{Aj} box. The alignment revealed an A/T-rich palindromic sequence consisting of a 7-1-7 arrangement in the intergenic region between *znuC* and *znuB* (*iznuCB*), exhibiting high similarity to previously described Zur boxes (Fig. 6A). Using this newly identified motif, a specific *A. japonicum* Zur_{Aj} box was deduced (Fig. 6B).

The Zur_{Aj} regulon of A. japonicum *contains putative [S,S]-EDDS biosynthetic genes*

To identify further Zur_{Aj}-regulated genes, in particular the [*S,S*]-EDDS biosynthesis genes, the deduced Zur_{Aj} box was submitted to FIMO, a software tool for scanning DNA sequences with motifs described as position-specific scoring matrices (Bailey *et al.*, 2009), to screen the *A. japonicum* genome. This revealed a putative binding motif with high similarity to known Zur boxes between *ajap_08420* (*aesE*) and *ajap_08425* (*aesA*) (Fig. 6C), two genes transcribed in opposite directions (Fig. 7A). *aesE* encodes a protein belonging to the amidase signature family. Enzymes of this family catalyse the hydrolysis of amide bonds using a highly conserved Ser-Ser-Lys catalytic triad, which is also present in the predicted amino acid sequence of AesE (Ser106, Ser130 and Lys31). *ajap_08425* is the first gene of an operon consisting of four overlapping genes (*ajap_08425-40*) (Fig. 7A). The genes were designated *aesA*, *aesB*, *aesC* and *aesD* respectively. The proposed gene products of *aesA*, *aesB* and *aesC* share significant similarity to SbnB, SbnH and SbnA, respectively, enzymes involved in the synthesis of staphyloferrin B (SB) (Fig. 7B). SB is a NIS-derived siderophore of *Staphylococcus aureus* (Cheung *et al.*, 2009) containing a central 1,2-diaminoethane (Dae) moiety (Fig. 7C). Central Dae moieties are rare in natural compounds, and it was long considered that this moiety

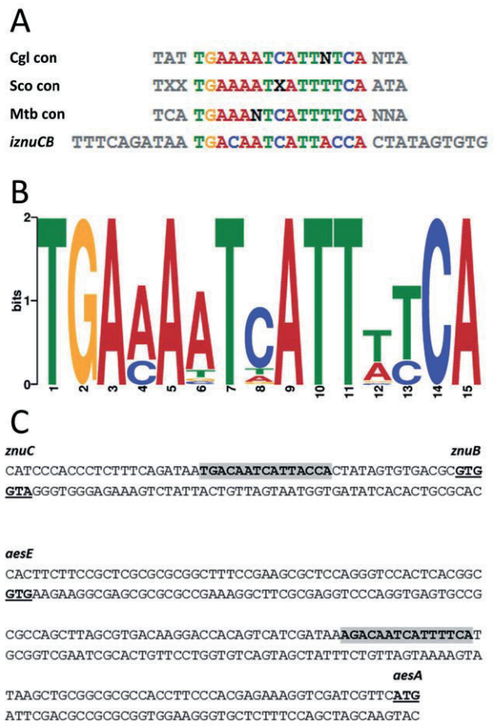

Fig. 6. MEME-FIMO analysis to screen for Zur boxes in *A. japonicum* genome.
A. MEME alignment of *znuCB* intergenic region and Zur consensus sequences of *M. tuberculosis* (Mtb con), *C. glutamicum* (Cgl con) and *S. coelicolor* (Sco con).
B. Deduced Zur box used for screening all 5′UTRs of the *A. japonicum* genome by MEME-FIMO.
C. Genetic organization and Zur box locations in the *znuCB* and *aesA* (*ajap_08425*) promoter regions. Nucleotides underlined indicate the start codons. Putative Zur boxes are indicated by grey highlighting.

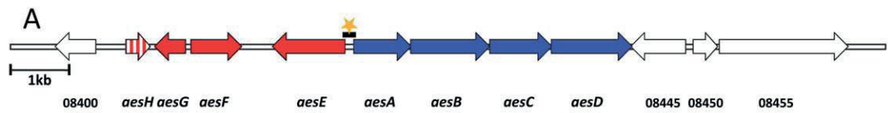

B

	SbnB	SbnH	SbnA	NorM
amino acids	336	400	326	456
strain	*S. aureus*	*S. aureus*	*S. aureus*	*Vibrio parahaemolyticus*
proposed function	ornithine cyclodeaminase	PLP-dependent decarboxylase	O-acetyl-L-serine sulfhydrylase	Na^+-driven multidrug efflux pump

A. japonicum	AesA (AJAP_08425)	AesB (AJAP_08430)	AesC (AJAP_08435)	AesD (AJAP_08440)
amino acids	327	448	352	460
GenBank-ID	AIG74588	AIG74589	AIG74590	AIG74591
amino acids identity/similarity (%)	22/42	24/35	31/50	23/44

C

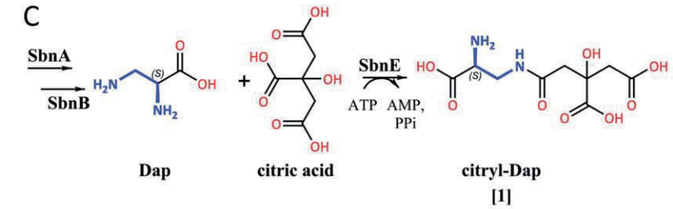

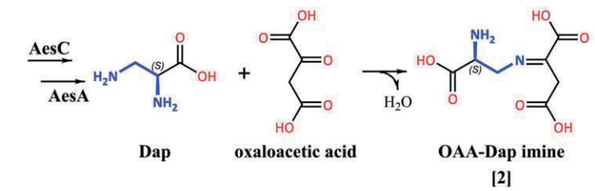

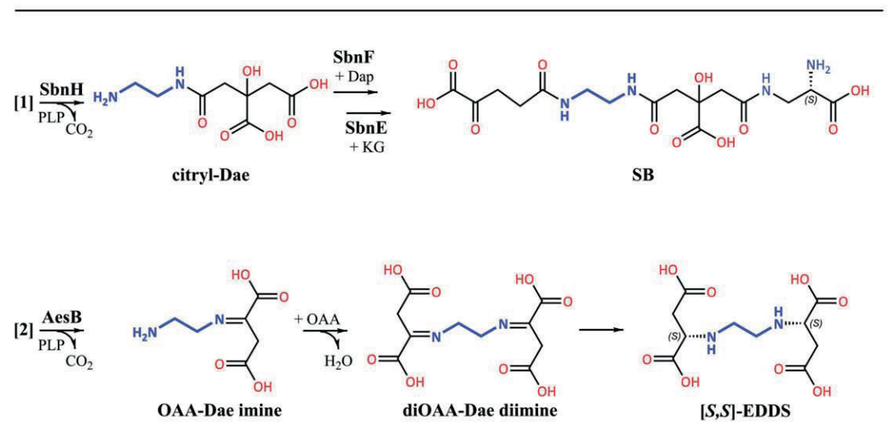

Fig. 7. Proposed [*S,S*]-EDDS biosynthesis.
A. Genetic organization of *ajap_08400-55*. The operon *aesA-D* (*ajap_08425-40*) downstream of the Zur-binding site (indicated by an orange asterisk) is highlighted in blue and *aesE-H* in red. The black bar illustrates EMSA shift fragment *upaesA* (Fig. 5).
B. Homology analyses using BLAST: identity/similarity of AesA-D to staphyloferrin (SB) biosynthesis enzymes.
C. Comparative alignment of the SB biosynthesis pathway and predicted [*S,S*]-EDDS pathway. Dae moieties are highlighted in blue.

is restricted to synthetic compounds exclusively (Bucheli-Witschel and Egli, 2001). However, the [*S,S*]-EDDS structure also harbours such a moiety. In *S. aureus*, SB biosynthesis starts with the formation of diaminopropionate (Dap), the product of the amidation of O-phospho-L-serine with the amino donor L-glutamate (Kobylarz *et al*., 2014). This reaction is coordinately catalysed by SbnA and SbnB. The further assembly of the single SB building blocks occurs via three distinct NIS synthetases (SbnE, SbnF and SbnC). Additionally, SbnH is required to catalyse the decarboxylation of a Dap intermediate, which leads to the Dae moiety (Cheung *et al*., 2009). A NIS-dependent, stepwise assembly can be excluded for [*S,S*]-EDDS biosynthesis because no NIS synthetase is encoded in the *A. japonicum* genome. Therefore, an alternative pathway has to be postulated for [*S,S*]-EDDS: we assumed that the first step, the supply of the building block Dap, occurs in a similar way and is catalysed by the SbnB and SbnA homologues AesA and AesC. A stepwise assembly of Dap with dicarboxylic acids (e.g. oxaloacetic acid) and the decarboxylation of the Dap moiety (presumably catalysed by the SbnH homologue AesB) should lead to the functional [*S,S*]-EDDS with its characteristic central Dae moiety (Fig. 7C). [*S,S*]-EDDS can then be transported over the cell membrane by AesD, a protein similar to the multidrug and toxic compound extrusion protein family (Morita *et al*., 1998; 2000). This deduced [*S,S*]-EDDS pathway does not belong to any previously described secondary metabolite pathway class, giving an explanation as to why these genes could not be identified using classical bioinformatics tools for genome mining.

The transcription of the aesA-D *operon is zinc regulated*

Because [*S,S*]-EDDS is only produced under zinc-limiting conditions, the transcriptional pattern of the identified candidate genes was determined by RT-PCR. The transcription of *aesA* was analysed with respect to the presence of various zinc concentrations. An inverse correlated transcription level of *aesA* to increased zinc concentration was observed, whereas no transcript was detected for zinc concentrations above 2 μM (Fig. 4). This result is in agreement with the observation that no [*S,S*]-EDDS production was detectable in SM with zinc concentration of ≥2 μM (Fig. 2). The zinc inhibitory effect was also seen for the genes *aesB-D* (Fig. S4). The presence of other divalent metal ions (Fe^{2+}, Ni^{2+}, Co^{2+} and Mn^{2+}) did not affect transcription. In the *A. japonicum* Δ*zur* background, however, *aesA-D* expression was zinc independent with constitutive transcription over the whole range of the applied zinc gradient (Fig. 4). This argues that Zur_{Aj} is likely the repressor that controls the operon *aesA-D*.

To quantitatively determine the transcriptional level of *aesA-D* in a zinc-dependent manner, we constructed a transcriptional fusion of the *aesA* promoter region (P*aesA*) with the *gusA* gene as a reporter system using the vector pGus (Myronovskyi *et al*., 2011). P*aesA* was amplified by PCR and fused to *gusA* by the primer-attached restriction sites, yielding pGusP*aesA* (Table S2). pGusP*aesA* was integrated into *A. japonicum* WT and *A. japonicum* Δ*zur* to generate *A. japonicum* WT:pGusP*aesA* and *A. japonicum* Δ*zur*:pGusP*aesA* respectively. Exconjugants containing unaltered pGus (*A. japonicum* WT:pGusP and *A. japonicum* Δ*zur*:pGusP) served as negative controls. The strains were grown for 72 h in microtitre plates containing SM with differing zinc concentrations. Initially, GUS activities were assayed in cell-based chromogenic assays (Fig. 8B). No X-Gluc turnover was visible in the *A. japonicum* WT and *A. japonicum* Δ*zur* strains and their corresponding recombinant strains carrying the unaltered pGus. *Amycolatopsis japonicum* WT:pGusP*aesA* exhibited GUS activity (visible as blue colour) solely when grown at low zinc concentrations, whereas GUS activity was also visible in *A. japonicum* Δ*zur* at elevated zinc concentrations (Fig. 8B). Quantitative data were generated using the soluble GUS substrate *p*-nitrophenyl-β-D-glucoronide in spectrophotometric assays (Fig. 8A). Under sub-inhibitory zinc concentrations (0–0.5 μM), *A. japonicum* WT:pGusP*aesA* revealed GUS activity levels [1.86-1.64 Miller units (MU)] significantly above those of the negative controls (0.28–0.44 MU). Linear decreasing Gus activity is seen in the range of partial inhibitory zinc concentrations of 0.5 to 2 μM, correlating to [*S,S*]-EDDS production in *A. japonicum* WT (Fig. 2). No GUS activity was detectable in this strain when grown at zinc concentrations higher than 2 μM. For *A. japonicum* Δ*zur*:pGusP*aesA*, GUS activities were determined after growth without $ZnSO_4$ and with $ZnSO_4$ at concentrations of 2 and 100 μM. The GUS activities were measurable in the presence of 2 μM (7.53 MU) and 100 μM (8.15 MU) zinc and were comparable to the GUS activity in the absence of zinc (8.24 MU) (Fig. 8). The GUS activity in *A. japonicum* Δ*zur*:pGusP*aesA* showed a 4.4 fold increase compared with the activity in *A. japonicum* WT:pGusP*aesA* after growth in the absence of zinc. This result reflects the significantly higher expression level of the *aesA-D* operon in *A. japonicum* Δ*zur*, which leads to an increased [*S,S*]-EDDS yield in this deletion mutant (Fig. 2).

To further verify the zinc-dependent repression of the operon genes (*aesA-D*), we performed gel shift assays using Zur_{Aj} and the Cy5-labelled region upstream of *aesA* (*upaesA*) including −185 to +36 bp with respect to its ATG start codon. Purified Zur_{Aj} bound specifically to the DNA probe in the presence of zinc, whereas no binding occurred in the absence of zinc (Fig. 5). This zinc-dependent binding of Zur_{Aj} to the intergenic region of *aesE-A* leads to the repression of *aesA* transcription (Fig. 4).

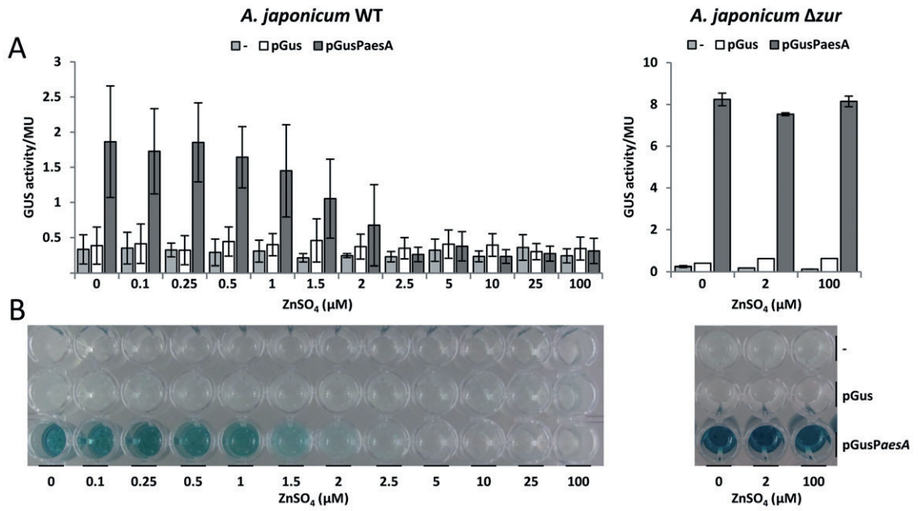

Fig. 8. Zinc-dependent GUS activity in *A. japonicum* WT and *A. japonicum* Δ*zur* containing *aesA* promoter-*gusA* fusions after growth in SM with various zinc concentrations.
A. Spectrophotometric assay using *p*-nitrophenyl-β-D-glucuronide as the substrate. Miller units are shown per milligram of cells.
B. Chromogenic assay in SM containing the substrate 5-bromo-4-chloro-3-indolyl-β-d-glucuronide (X-Gluc).

The aes *genes are essential for [*S,S*]-EDDS production*

To prove whether the zinc-regulated *aesA-D* operon is involved in [*S,S*]-EDDS biosynthesis, the in frame deletion mutant Δ*aesA-C* was constructed using pGusA21Δ*aesA-C* in analogy to the procedure described for zur_{Aj} deletion. *A. japonicum* Δ*aesA-C* and *A. japonicum* WT were grown in the absence of zinc and [*S,S*]-EDDS production was analysed by HPLC-DAD over 5 days of growth. Although the supernatant of *A. japonicum* WT contained [*S,S*]-EDDS (Fig. 9), no [*S,S*]-EDDS was detected in the supernatant of the deletion mutant, confirming the involvement of at least one of the *aesA-C* genes in [*S,S*]-EDDS biosynthesis. To verify that the loss of [*S,S*]-EDDS production in *A. japonicum* Δ*aesA-C* is due to the *aesABC* deletion and not due to any polar effects, we genetically

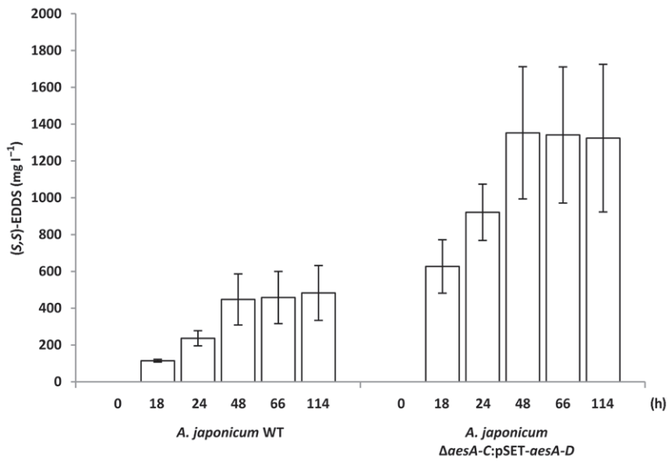

Fig. 9. Time-dependent [*S,S*]-EDDS production by *A. japonicum* WT and *A. japonicum* Δ*aesA-C*:pSET-*aesA-D*. The strains were grown in deionized flasks in zinc-deficient SM. Samples were taken directly after inoculation of the main culture (t = 0 h) and further time points of incubation and quantified by HPLC-DAD. *n* = 3.

complemented *A. japonicum* Δ*aesA-C*. Hence, we constructed the plasmid pSET152-*aesA-D*, which harbours the complete *aesA-D* operon downstream of its native, zinc-repressed promoter and applied it to complement the mutant. *Amycolatopsis japonicum* Δ*aesA-C*:pSET-*aesA-D* showed restored [*S,S*]-EDDS production (Fig. 9). Due to the transcriptional control by the native promoter, *A. japonicum* Δ*aesA-C*:pSET-*aesA-D* produces [*S,S*]-EDDS solely in zinc-depleted medium. The amount of [*S,S*]-EDDS produced by this recombinant strain was increased two to three times compared with that by *A. japonicum* WT, likely due to the presence of a second, plasmid-encoded copy of the exporter gene *aesD*. Overexpression of exporter genes is a generally applied strategy in metabolic engineering approaches to increase production yields. For example, overexpression of the ABC transporter DrrABC in *Streptomyces peucetius* ATCC 27952 led to a 2.4-fold increase of doxorubicin production (Malla *et al.*, 2010), which is in a similar range as the observed increase in [*S,S*]-EDDS production due to *aesD* overexpression. Putting these results together with the proposed biosynthetic pathway, we conclude that the whole *aesA-D* operon is involved in [*S,S*]-EDDS biosynthesis/export.

The genes *ajap_08415*, *ajap_08410* and *ajap_08405* (*aesF*, *aesG* and *aesH*) are located downstream of *aesE* and are predicted to encode a LysR family transcriptional regulator, a cysteine dioxygenase and an acetyltransferase respectively. To investigate the involvement of these genes in the biosynthesis of [*S,S*]-EDDS, we constructed the deletion mutant *A. japonicum* Δ*aesE-H*. This mutant was not able to produce [*S,S*]-EDDS (Fig. S5). However, the *aesA-D* operon was still zinc dependently transcribed in this mutant, confirming that the promoter region of *aesA* was not affected by this mutation. These results demonstrate that at least one of the *aesE-H* genes is required for the production of [*S,S*]-EDDS in addition to *aesA-D*.

*The [*S,S*]-EDDS biosynthesis as response to zinc deficiency is phylogenetically clustered*

The distribution of the genetic potential to produce [*S,S*]-EDDS in bacteria was assessed by evaluating the phylogenetic abundance of the *aes* genes by EDGAR, a software framework for comparative analysis of prokaryotic genomes (Blom *et al.*, 2009) and a combinatorial BLAST and MULTIGENEBLAST (Medema *et al.*, 2013) analysis. Computational analysis using *aesA-H* as a query sequence for searching conserved homologues in a GenBank database covering all entries revealed that the occurrence of the *aesA-H* genes is restricted to certain strains of the genus *Amycolatopsis*. Of all the analysed genomes, solely those of *Amycolatpsis* sp. MJM2582, *Amycolatpsis orientalis* HCCB10007 and *Amycolatpsis lurida* DSM 43134 harbour the eight clustered genes entirely with identical gene arrangement and with high-sequence similarity compared with *A. japonicum* (Table S3). The *Amycolatpsis decaplanina* DSM 44594 and *Amycolatpsis alba* DSM 44262 genomes exhibit a deviation in that they are both missing the terminal *aesH* homologue. Interestingly, the Zur box is highly conserved in all discovered *aesE-A* intergenic regions (Table S4), evidencing the common Zur-mediated and zinc-dependent transcriptional repressions. According to Everest and Meyers (2009), the members of the genus *Amycolatopsis* can be classified into six phylogentic clades (A–F) (Fig. S6). All strains encoding clustered *aes* genes are members of the *Amycolatopsis* phylogentic clade A. An exception, however, is *Amycolatopsis azurea* DSM 43854, which also belongs to clade A but does not show a conserved [*S,S*]-EDDS cluster. In this strain, no *aesD* homologues could be identified and the clustered putative *aesA-C* homologues show a significant drop in similarity (Table S3). Moreover, in contrast to all other clade A strains, no conserved Zur box is present upstream of the *aesA*-like gene in *A. azurea* DSM 43854 (Table S4). Interestingly, the *aes* genes could be identified exclusively in *Amycolatopsis* strains belonging to clade A. In contrast to the total *aes* gene cluster, homologues of the *aesA-D* subcluster are quite abundant in various genera of actinobacteria and proteobacteria. However, no *aesA-D* homologues could be identified, for example, in firmicutes or in any *Amycolatopsis* strain not belonging to clade A. The abundance of the *aesA-D* subcluster, when related to the biosynthesis of Dae moieties, might indicate the potential of certain strains to produce metabolites containing this building block.

To correlate the genetic information regarding the abundance of putative biosynthesis genes to the capability in producing [*S,S*]-EDDS, we cultivated the strains *A. lurida* (Lechevalier *et al.*, 1986), *A. decaplaina* (Wink *et al.*, 2004), *A. alba* (Mertz and Yao, 1993) and *A. azurea* (Henssen *et al.*, 1987) belonging to the phylogenetic clade A in SM in the absence and in the presence of zinc. Culture filtrates of *A. lurida*, *A. decaplaina* and *A. alba* grown without the supplementation of zinc showed a peak whose retention time and UV-DAD spectrum corresponded to the [*S,S*]-EDDS standard (Fig. S7). This peak was not observable after growth of these strains in the presence of zinc. As expected, no [*S,S*]-EDDS production could be detected after cultivation of *A. azurea*. Furthermore, representatives of the phylogenetic clades C and D, namely *Amycolatopsis balhimycina* DSM 5908 (Nadkarni *et al.*, 1994; Wink *et al.*, 2003), *Amycolatopsis mediterranei* DSM 43304 (Margalith and Beretta, 1960) and *Amycolatopsis nigrescens* DSM 44992 (Groth *et al.*, 2007), do not produce [*S,S*]-EDDS (Fig. S7).

Because *A. decaplaina* and *A. alba* also produce [*S,S*]-EDDS but do not encode an AesH homologue, its involvement in [*S,S*]-EDDS biosynthesis can be excluded. We therefore consider the cluster border downstream of the *aesH* coding region. The opposite border of the [*S,S*]-EDDS cluster is most probably defined by *ajap_08445*, putatively encoding a function in sporulation, and the unit *ajap_08450-55*, encoding a bifunctional catalase–peroxidase and its transcriptional regulator, which are involved in oxidative stress response. The phylogenetic analysis of the abundance of *aes* genes, combined with the capability of certain *Amycolatopsis* strains to produce [*S,S*]-EDDS confirmed the [*S,S*]-EDDS biosynthesis via the coordinated action of the enzymes encoded by the *aes* genes and contributed to assigning the cluster borders. Furthermore, these results show that [*S,S*]-EDDS production, as an evolutionary response to zinc deficiency, seems to be a quite common feature of the *Amycolatopsis* phylogenetic clade A.

Perspective

Bioinformatic tools, such as antiSMASH 3.0, are commonly used for the identification of gene clusters encoding secondary metabolites. However, the identification of clusters is limited to biosynthetic pathways of already known mechanisms. In this study, we developed a new strategy, which is INBEKT. We think that INBEKT is generally applicable to search for genes encoding zincophore, or more generally ionophore, biosynthesis and potentially other pathways consisting of unusual or novel biosynthetic steps. Our approach does not require any information regarding the structure or the biosynthesis mechanism of the compound of interest and would therefore allow the identification of totally new secondary metabolite pathways and classes. In addition, we illustrate how knowledge-based approaches can be used to increase productivity, either by deleting negatively acting regulators, or by overexpressing specific exporters. The ongoing work on the elucidation of the [*S,S*]-EDDS biosynthetic pathway will provide deeper insights into discrete biosynthetic steps and deliver additional possibilities for yield optimization. This will further promote the establishment of a biotechnological [*S,S*]-EDDS production process with a favourable environmental profile.

Experimental procedures

Strains, plasmids and oligonucleotides

The strains and plasmids used in this study are listed in Table S1. The oligonucleotides are listed in Table S2.

Media and culture conditions

E. coli and *A. japonicum* strains were cultured and manipulated as described previously (Kieser *et al.*, 2000; Stegmann *et al.*, 2001; Kołodyńska, 2011; Spohn *et al.*, 2014).

Liquid cultures of *A. japonicum* strains in 100 ml volume were grown to detect [*S,S*]-EDDS production according to Zwicker and colleagues (1997). The optimized SM consisted of glycerol (25 g l^{-1}), $MgSO_4 \times 7\ H_2O$ (1.2 g l^{-1}), Ferric (III) citrate (60 mg l^{-1}), KH_2PO_4 (8 g l^{-1}), $Na_2HPO_4 \times 2\ H_2O$ (12 g l^{-1}) and sodium glutamate monohydrate (11.3 g l^{-1}), which was used as the nitrogen source. To grow the strains in a reduced 3 ml volume, 12-well microtitre plates were used. The cultures were grown on a rotary shaker (120 r.p.m.) at 30°C. Precultures were grown in complex culture medium (glycerol (20 g l^{-1}); soybean meal (20 g l^{-1}) at pH 7.5) for 48 h. A total of 150 μl of this preculture was used to inoculate 3 ml of SM supplemented with $ZnSO_4$ to reach the final zinc concentrations of 0, 0.1, 0.25, 0.5, 1, 1.5, 2, 2.5, 5, 10, 25 and 100 μM. The cultures were grown for a further 72 h before being analysed by means of [*S,S*]-EDDS production, RT-PCR and GUS activity.

*Construction of the inactivation plasmids pGusA21Δ*zur*, pGusA21Δ*aesA-C *and pGusA21Δ*aesE-H

The upstream and downstream regions of zur_{Aj}, *aesA-C* and *aesE-H* were amplified using the primers listed in Table S2. The purified PCR products were introduced into pJet1.2 as an intermediate vector and verified by sequencing. By using the primer-attached restriction sites, the upstream and downstream fragments were consecutively cloned into the plasmid pGusA21, resulting in the inactivation plasmids pGusA21Δ*zur*, pGusA21Δ*aesA-C* and pGusA21Δ*aesE-H,* used for transformation of *A. japonicum* WT.

*Construction of the complementation plasmid pRM4-*zur

For the complementation of *A. japonicum* Δ*zur*, the entire coding region of the zur_{Aj} gene was amplified using the primer pair pzur-F and pzur-R. The 429 bp PCR product was integrated into pRM4 (Menges *et al.*, 2007) via the primer-attached restriction sites downstream of the *ermEp** promoter.

*Construction of the complementation plasmid pSET-*aesA-D

The cosmid pTWPI1-edds includes a 31 kb insert representing 1 665 131–1 696 415 bp of the *A. japonicum* genome. This genome fragment includes the entire coding regions from *ajap_08305* to *ajap_08450* and partial sequences of *ajap_08300* and *ajap_08455*. A 6545 bp fragment from the *A. japonicum* genome from 1 687 557–1 694 101 bp was isolated from the cosmid using the restriction enzymes EcoRI and BglII. This fragment contains the entire operon *aesA-D* downstream of its native promoter beside partial sequences of the genes encoded upstream (*ajap_08420*) and downstream (*ajap_08445*). The purified 6545 bp was cloned into pSET152 (Bierman *et al.*, 1992) via EcoRI and

BamHI restriction sites resulting in the recombinant pasmid pSET-*aesA-D*.

RT-PCR analysis

RNA isolation and RT-PCR analyses were performed according to Spohn and colleagues (2014) with the primer pairs listed in Table S2.

Overexpression and purification of A. japonicum *Zur in* E. coli

The coding region of the zur_{Aj} gene was amplified using the primers HIS-pzur-F and HIS-pzur-R. The 441 bp PCR fragment was cloned into pET30 Ek/LIC (Novagen) via its complementary overhangs, according to manufacturer's protocol. *Escherichia coli* BL21(DE3) pLys was transformed with the resulting plasmid pET-30-*zur*. The overexpression and purification of the His-tagged protein was performed as previously reported (Shin *et al*., 2007).

Gel mobility shift assays for DNA–Zur binding

DNA fragments containing the analysed intergenic regions were amplified from *A. japonicum* genomic DNA using the primers listed in Table S2. Fragment labelling was performed as described by Tiffert and colleagues (2008). Approximately 4 nM of the Cy5-labelled DNA fragments and purified tagged protein were incubated in reaction buffer [20 mM Tris-HCl (pH = 7,8), 50 mM KCl, 1 mM DTT, 0.1 mg of bovine serum albumin ml^{-1} and 5% glycerol] with or without 25 μM $ZnSO_4$ for 20 min at 30°C. The binding mixture was subjected to electrophoresis on a 2% TB (89 mM Trizma base, 89 mM boric acid) agarose gel in TB buffer. DNA bands were visualized by fluorescence imaging using a Typhoon (GE Healthcare) fluorescence laser scanner.

*Detection of [*S,S*]-EDDS biosynthesis using HPLC-DAD*

For the detection of [*S,S*]-EDDS, the fermentation broth was centrifuged, and 1 ml of supernatant was thoroughly mixed with 20 μl of $CuSO_4$ (100 mM) and once again centrifuged before using the supernatant for HPLC analysis. [*S,S*]-EDDS analyses were carried out on a HP1090M liquid chromatograph equipped with a thermostated autosampler, a diode-array detector and an HP Kayak XM 600 ChemStation (Agilent). A total of 10 μl of samples were injected onto a Hypersil ODS column (125 × 4 mm, 3 μm) fitted with a guard column (10 × 4 mm, 3 μm; Stagroma) and analysed by isocratic elution with solvent A – acetonitrile (96:4, v/v) at a flow rate of 1 ml min^{-1}. Solvent A consisted of 20 mM Sorensen's phosphate buffer (pH 7.2) with 5 mM tetrabutylammoniumhydrogensulfate. UV detection was performed at 253 nm. For data analysis, Chemstation LC3D software Rev. A.08.03 was used. Commercial [*S,S*]-EDDS in solution (Sigma Aldrich) was precipitated to obtain crystalline powder as previously described (Zwicker *et al*., 1997) and used as a standard.

Construction of the gusA *promoter probe plasmid pGusP*aesA

A 167 bp DNA fragment containing the complete intergenic region from *aesE* (*ajap_08420*) to *aesA* (*ajap_08425*) was PCR amplified using the primer pair PaesA-F and PaesA-R. The PCR fragment was cloned into pJet1.2 and verified by sequencing before integration into the corresponding sites of the pGus vector via XbaI and SpeI to generate pGusP*aesA*.

Spectrophotometric and chromogenic assay of GUS activity

For the quantification of expression levels, the spectrophotometric method of Myronovskyi and colleagues (2011) was modified. After cultivation for 72 h, cells were harvested and washed twice with SM before the biomass was adjusted to 200 mg ml^{-1} with SM containing glycerol. A total of 800 μl of the cell stock solutions were centrifuged and re-suspended in 1 ml of lysis buffer and incubated for 30 min at 37°C. Cell debris was removed by centrifugation and 100 μl of the cell lysate was assayed. Optical density at 405 nm was measured in a 96-well plate on a Dynamic Microplate MicroTek DS spectrophotometer (Bio-Tek Kontron instuments). Miller units were calculated as 1000× (OD_{405} of sample-OD_{405} of blank) / (time of reaction in minutes × volume of culture assayed). For the chromogenic assay, 50 μl from *A. japonicum* strain stock solutions (200 mg ml^{-1} in SM-glycerol) were mixed with 150 μl of 1.5 mg ml^{-1} X-Gluc (5-bromo-4-chloro-3-indolyl-β-d-glucuronide) and photographed after 24 h at 30°C.

Acknowledgements

This work was supported by ERA-IB GenoDrug (BMBF, FKZ 0315930) and the German Center for Infection Research (DZIF, TTU 09.802 and TTU 09.704). The authors would like to acknowledge C. Hertweck and J. Wink for the provision of *Amycolatopsis* strains, A. Luzhetskyy for the provision of pGUS, G. Muth and K. Hantke for helpful discussions, M. Schorn for proofreading the manuscript and A. Kulik for assistance in HPLC analyses.

References

Aagaard, A., and Brzezinski, P. (2001) Zinc ions inhibit oxidation of cytochrome *c* oxidase by oxygen. *FEBS Lett* **494:** 157–160.

Andreini, C., Banci, L., Bertini, I., and Rosato, A. (2006) Zinc through the three domains of life. *J Proteome Res* **5:** 3173–3178.

Bailey, T.L., Boden, M., Buske, F.A., Frith, M., Grant, C.E., Clementi, L., *et al.* (2009) MEME SUITE: tools for motif discovery and searching. *Nucleic Acids Res* **37:** W202–W208.

Bierman, M., Logan, R., O'Brien, K., Seno, E.T., Rao, R.N., and Schoner, B.E. (1992) Plasmid cloning vectors for the conjugal transfer of DNA from *Escherichia coli* to *Streptomyces* spp. *Gene* **116:** 43–49.

Blom, J., Albaum, S.P., Doppmeier, D., Pühler, A., Vorhölter, F.J., Zakrzewski, M., and Goesmann, A. (2009) EDGAR: a software framework for the comparative analysis of prokaryotic genomes. *BMC Bioinformatics* **10:** 154.

Brooks, H.A., Gardner, D., Poyser, J.P., and King, T.J. (1984) The structure and absolute stereochemistry of zincophorin (antibiotic M144255) – a monobasic carboxylic-acid ionophore having a remarkable specificity for divalent-cations. *J Antibiot* **37:** 1501–1504.

Bucheli-Witschel, M., and Egli, T. (2001) Environmental fate and microbial degradation of aminopolycarboxylic acids. *FEMS Microbiol Rev* **25:** 69–106.

Campoy, S., Jara, M., Busquets, N., Perez De Rozas, A.M., Badiola, I., and Barbe, J. (2002) Role of the high-affinity zinc uptake *znuABC* system in *Salmonella enterica* serovar Typhimurium virulence. *Infect Immun* **70:** 4721–4725.

Cebulla, I. (1995) Gewinnung komplexbildender Substanzen mittels *Amycolatopsis orientalis*. University of Tübingen, Doctoral Thesis.

Chen, L., Liu, T., and Ma, C. (2010) Metal complexation and biodegradation of EDTA and *S,S*-EDDS: a density functional theory study. *J Phys Chem A* **114:** 443–454.

Cheung, J., Beasley, F.C., Liu, S., Lajoie, G.A., and Heinrichs, D.E. (2009) Molecular characterization of staphyloferrin B biosynthesis in *Staphylococcus aureus*. *Mol Microbiol* **74:** 594–608.

Choi, S., and Bird, A.J. (2014) Zinc'ing sensibly: controlling zinc homeostasis at the transcriptional level. *Metallomics* **6:** 1198–1215.

D'Autreaux, B., Pecqueur, L., Gonzalez de Peredo, A., Diederix, R.E., Caux-Thang, C., Tabet, L., *et al.* (2007) Reversible redox- and zinc-dependent dimerization of the *Escherichia coli* Fur protein. *Biochemistry* **46:** 1329–1342.

Everest, G.J., and Meyers, P.R. (2009) The use of *gyrB* sequence analysis in the phylogeny of the genus *Amycolatopsis*. *Antonie Leeuwenhoek* **95:** 1–11.

Fillat, M.F. (2014) The FUR (ferric uptake regulator) superfamily: diversity and versatility of key transcriptional regulators. *Arch Biochem Biophys* **546:** 41–52.

Gaballa, A., and Helmann, J.D. (1998) Identification of a zinc-specific metalloregulatory protein, Zur, controlling zinc transport operons in *Bacillus subtilis*. *J Bacteriol* **180:** 5815–5821.

Gibson, F., and Magrath, D.I. (1969) The isolation and characterization of a hydroxamic acid (aerobactin) formed by *Aerobacter aerogenes* 62-I. *Biochim Biophys Acta* **192:** 175–184.

Gilston, B.A., Wang, S., Marcus, M.D., Canalizo-Hernandez, M.A., Swindell, E.P., Xue, Y., *et al.* (2014) Structural and mechanistic basis of zinc regulation across the *E. coli* Zur regulon. *PLoS Biol* **12:** e1001987.

Goodfellow, M., Brown, A.B., Cai, J., Chun, J., and Collins, D.M. (1997) *Amycolatopsis japonicum* sp. nov., an actinomycete producing (S,S)-N,N'-ethylenediamine-disuccinic acid. *Syst Appl Microbiol* **20:** 78–84.

Groth, I., Tan, G.Y.A., Gonzalez, J.M., Laiz, L., Carlsohn, M.R., Schütze, B., *et al.* (2007) *Amycolatopsis nigrescens* sp nov., an actinomycete isolated from a Roman catacomb. *Int J Syst Evol Microbiol* **57:** 513–519.

Henssen, A., Kothe, H.W., and Kroppenstedt, R.M. (1987) Transfer of *Pseudonocardia azurea* and *Pseudonocardia fastidiosa* to the genus *Amycolatopsis*, with emended species description. *Int J Syst Bacteriol* **37:** 292–295.

Hough, E., Hansen, L.K., Birknes, B., Jynge, K., Hansen, S., Hordvik, A., *et al.* (1989) High-resolution (1.5 A) crystal structure of phospholipase C from *Bacillus cereus*. *Nature* **338:** 357–360.

Kallifidas, D., Pascoe, B., Owen, G.A., Strain-Damerell, C.M., Hong, H.J., and Paget, M.S. (2010) The zinc-responsive regulator Zur controls expression of the coelibactin gene cluster in *Streptomyces coelicolor*. *J Bacteriol* **192:** 608–611.

Kasahara, M., and Anraku, Y. (1974) Succinate- and NADH oxidase systems of *Escherichia coli* membrane vesicles. Mechanism of selective inhibition of the systems by zinc ions. *J Biochem* **76:** 967–976.

Kieser, T., Bibb, M.J., Buttner, M.J., Chater, K.F., and Hopwood, D.A. (2000) *Practical* Streptomyces *Genetics*. Norwich, UK: John Innes Foundation.

Kim, H.J., Graham, D.W., DiSpirito, A.A., Alterman, M.A., Galeva, N., Larive, C.K., *et al.* (2004) Methanobactin, a copper-acquisition compound from methane-oxidizing bacteria. *Science* **305:** 1612–1615.

Kloss, F., Pidot, S., Goerls, H., Friedrich, T., and Hertweck, C. (2013) Formation of a dinuclear copper(I) complex from the *Clostridium*-derived antibiotic closthioamide. *Angew Chem Int Edit* **52:** 10745–10748.

Kobylarz, M.J., Grigg, J.C., Takayama, S.J., Rai, D.K., Heinrichs, D.E., and Murphy, M.E. (2014) Synthesis of L-2,3-diaminopropionic acid, a siderophore and antibiotic precursor. *Chem Biol* **21:** 379–388.

Kołodyńska, D. (2011) Chelating agents of a new generation as an alternative to conventional chelators for heavy metal ions removal from different waste waters. In *Expanding Issues in Desalination*. Ning, R.Y. (ed.). Rijeka/Croatia: InTech, pp. 339–370.

Leach, L.H., Morris, J.C., and Lewis, T.A. (2007) The role of the siderophore pyridine-2,6-bis (thiocarboxylic acid) (PDTC) in zinc utilization by *Pseudomonas putida* DSM 3601. *Biometals* **20:** 717–726.

Lechevalier, M.P., Prauser, H., Labeda, D.P., and Ruan, J.-S. (1986) Two new genera of nocardioform actinomycetes: *Amycolata* gen. nov. and *Amycolatopsis* gen. nov. *Int J Syst Evol Microbiol* **36:** 29–37.

de Lorenzo, V., and Neilands, J.B. (1986) Characterization of *iucA* and *iucC* genes of the aerobactin system of plasmid ColV-K30 in *Escherichia coli*. *J Bacteriol* **167:** 350–355.

Lucarelli, D., Russo, S., Garman, E., Milano, A., Meyer-Klaucke, W., and Pohl, E. (2007) Crystal structure and function of the zinc uptake regulator FurB from *Mycobacterium tuberculosis*. *J Biol Chem* **282:** 9914–9922.

Ma, Z., Gabriel, S.E., and Helmann, J.D. (2011) Sequential binding and sensing of Zn(II) by *Bacillus subtilis* Zur. *Nucleic Acids Res* **39:** 9130–9138.

Maciag, A., Dainese, E., Rodriguez, G.M., Milano, A., Provvedi, R., Pasca, M.R., *et al.* (2007) Global analysis of the *Mycobacterium tuberculosis* Zur (FurB) regulon. *J Bacteriol* **189:** 730–740.

Malla, S., Niraula, N.P., Liou, K., and Sohng, J.K. (2010) Self-resistance mechanism in *Streptomyces peucetius*: Overexpression of *drrA*, *drrB* and *drrC* for doxorubicin enhancement. *Microbiol Res* **165:** 259–267.

© 2015 Society for Applied Microbiology and John Wiley & Sons Ltd, *Environmental Microbiology*, **18,** 1249–1263

Margalith, P., and Beretta, G. (1960) Rifamycin. IX. Taxonomic study on *Streptomyces mediterranei* nov. sp. *Mycopathol Mycol Appl* **13:** 321–330.
Medema, M.H., Takano, E., and Breitling, R. (2013) Detecting sequence homology at the gene cluster level with MultiGeneBlast. *Mol Biol Evol* **30:** 1218–1223.
Meiwes, J., Fiedler, H.P., Zahner, H., Konetschnyrapp, S., and Jung, G. (1990) Production of desferrioxamine E and new analogs by directed fermentation and feeding fermentation. *Appl Microbiol Biotechnol* **32:** 505–510.
Menges, R., Muth, G., Wohlleben, W., and Stegmann, E. (2007) The ABC transporter Tba of *Amycolatopsis balhimycina* is required for efficient export of the glycopeptide antibiotic balhimycin. *Appl Microbiol Biotechnol* **77:** 125–134.
Mertz, F.P., and Yao, R.C. (1993) *Amycolatopsis alba* sp. nov., isolated from soil. *Int J Syst Bacteriol* **43:** 715–720.
Morita, Y., Kodama, K., Shiota, S., Mine, T., Kataoka, A., Mizushima, T., and Tsuchiya, T. (1998) NorM, a putative multidrug efflux protein, of *Vibrio parahaemolyticus* and its homolog in *Escherichia coli*. *Antimicrob Agents Chemother* **42:** 1778–1782.
Morita, Y., Kataoka, A., Shiota, S., Mizushima, T., and Tsuchiya, T. (2000) NorM of *Vibrio parahaemolyticus* is an $Na^{(+)}$-driven multidrug efflux pump. *J Bacteriol* **182:** 6694–6697.
Myronovskyi, M., Welle, E., Fedorenko, V., and Luzhetskyy, A. (2011) Beta-glucuronidase as a sensitive and versatile reporter in actinomycetes. *Appl Environ Microbiol* **77:** 5370–5383.
Nadkarni, S.R., Patel, M.V., Chatterjee, S., Vijayakumar, E.K., Desikan, K.R., Blumbach, J., *et al.* (1994) Balhimycin, a new glycopeptide antibiotic produced by *Amycolatopsis* sp. Y-86,21022. Taxonomy, production, isolation and biological activity. *J Antibiot (Tokyo)* **47:** 334–341.
Nishikiori, T., Okuyama, A., Naganawa, H., Takita, T., Hamada, M., Takeuchi, T., *et al.* (1984) Production by actinomycetes of (S,S)-N,N'-ethylenediamine-disuccinic acid, an inhibitor of phospholipase C. *J Antibiot (Tokyo)* **37:** 426–427.
Owen, G.A., Pascoe, B., Kallifidas, D., and Paget, M.S. (2007) Zinc-responsive regulation of alternative ribosomal protein genes in *Streptomyces coelicolor* involves Zur and σR. *J Bacteriol* **189:** 4078–4086.
Patzer, S.I., and Hantke, K. (1998) The ZnuABC high-affinity zinc uptake system and its regulator Zur in *Escherichia coli*. *Mol Microbiol* **28:** 1199–1210.
Pawlik, M.C., Hubert, K., Joseph, B., Claus, H., Schoen, C., and Vogel, U. (2012) The zinc-responsive regulon of *Neisseria meningitidis* comprises 17 genes under control of a Zur element. *J Bacteriol* **194:** 6594–6603.
Pollack, J.R., Ames, B.N., and Neilands, J.B. (1970) Iron transport in *Salmonella typhimurium*: mutants blocked in the biosynthesis of enterobactin. *J Bacteriol* **104:** 635–639.
Puk, O., Huber, P., Bischoff, D., Recktenwald, J., Jung, G., Sussmuth, R.D., *et al.* (2002) Glycopeptide biosynthesis in *Amycolatopsis mediterranei* DSM5908: function of a halogenase and a haloperoxidase/perhydrolase. *Chem Biol* **9:** 225–235.
Que, Q., and Helmann, J.D. (2000) Manganese homeostasis in *Bacillus subtilis* is regulated by MntR, a bifunctional regulator related to the diphtheria toxin repressor family of proteins. *Mol Microbiol* **35:** 1454–1468.
Rusnak, F., Sakaitani, M., Drueckhammer, D., Reichert, J., and Walsh, C.T. (1991) Biosynthesis of the *Escherichia coli* siderophore enterobactin: sequence of the *entF* gene, expression and purification of EntF, and analysis of covalent phosphopantetheine. *Biochemistry* **30:** 2916–2927.
Schowanek, D., Feijtel, T.C., Perkins, C.M., Hartman, F.A., Federle, T.W., and Larson, R.J. (1997) Biodegradation of [S,S], [R,R] and mixed stereoisomers of ethylene diamine disuccinic acid (EDDS), a transition metal chelator. *Chemosphere* **34:** 2375–2391.
Schröder, J., Jochmann, N., Rodionov, D.A., and Tauch, A. (2010) The Zur regulon of *Corynebacterium glutamicum* ATCC 13032. *BMC Genomics* **11:** 12.
Seyedsayamdost, M.R., Traxler, M.F., Zheng, S.L., Kolter, R., and Clardy, J. (2011) Structure and biosynthesis of amychelin, an unusual mixed-ligand siderophore from *Amycolatopsis* sp. AA4. *J Am Chem Soc* **133:** 11434–11437.
Shen, Y., Huang, H., Zhu, L., Luo, M., and Chen, D. (2012) Type II thioesterase gene (*ECO-orf27*) from *Amycolatopsis orientalis* influences production of the polyketide antibiotic, ECO-0501 (LW01). *Biotechnol Lett* **34:** 2087–2091.
Shin, J.H., Oh, S.Y., Kim, S.J., and Roe, J.H. (2007) The zinc-responsive regulator Zur controls a zinc uptake system and some ribosomal proteins in *Streptomyces coelicolor* A3(2). *J Bacteriol* **189:** 4070–4077.
Shin, J.H., Jung, H.J., An, Y.J., Cho, Y.B., Cha, S.S., and Roe, J.H. (2011) Graded expression of zinc-responsive genes through two regulatory zinc-binding sites in Zur. *Proc Natl Acad Sci USA* **108:** 5045–5050.
Shu, N., Zhou, T., and Hovmöller, S. (2008) Prediction of zinc-binding sites in proteins from sequence. *Bioinformatics* **24:** 775–782.
Spohn, M., Kirchner, N., Kulik, A., Jochim, A., Wolf, F., Münzer, P., *et al.* (2014) Overproduction of ristomycin A by activation of a silent gene cluster in *Amycolatopsis japonicum* MG417-CF17. *Antimicrob Agents Chemother* **58:** 6185–6196.
Stegmann, E., Pelzer, S., Wilken, K., and Wohlleben, W. (2001) Development of three different gene cloning systems for genetic investigation of the new species *Amycolatopsis japonicum* MG417-CF17, the ethylenediaminedisuccinic acid producer. *J Biotechnol* **92:** 195–204.
Stegmann, E., Albersmeier, A., Spohn, M., Gert, H., Weber, T., Wohlleben, W., *et al.* (2014) Complete genome sequence of the actinobacterium *Amycolatopsis japonica* MG417-CF17 (=DSM 44213T) producing (S,S)-N,N'-ethylenediaminedisuccinic acid. *J Biotechnol* **189C:** 46–47.
Takahashi, R., Fujimoto, N., Suzuki, M., and Endo, T. (1997) Biodegradabilities of ethylenediamine-N,N'-disuccinic acid (EDDS) and other chelating agents. *Biosci Biotechnol Biochem* **61:** 1957–1959.
Tiffert, Y., Supra, P., Wurm, R., Wohlleben, W., Wagner, R., and Reuther, J. (2008) The *Streptomyces coelicolor* GlnR regulon: identification of new GlnR targets and evidence for a central role of GlnR in nitrogen metabolism in actinomycetes. *Mol Microbiol* **67:** 861–880.
Weber, T., Blin, K., Duddela, S., Krug, D., Kim, H.U., Bruccoleri, R., *et al.* (2015) antiSMASH 3.0 – a comprehensive resource for the genome mining of biosynthetic gene clusters. *Nucleic Acids Res* **43:** W237–W243.
Wink, J., Gandhi, J., Kroppenstedt, R.M., Seibert, G., Sträubler, B., Schumann, P., and Stackebrandt, E. (2004) *Amycolatopsis decaplanina* sp. nov., a novel member of the genus with unusual morphology. *Int J Syst Evol Microbiol* **54:** 235–239.
Wink, J.M., Kroppenstedt, R.M., Ganguli, B.N., Nadkarni, S.R., Schumann, P., Seibert, G., and Stackebrandt, E. (2003) Three new antibiotic producing species of the genus *Amycolatopsis*, *Amycolatopsis balhimycina* sp. nov., *A. tolypomycina* sp. nov., *A. vancoresmycina* sp. nov., and description of *Amycolatopsis keratiniphila* subsp. *keratiniphila* subsp. nov. and *A. keratiniphila* subsp. *nogabecina* subsp. nov. *Syst Appl Microbiol* **26:** 38–46.
Zwicker, N., Theobald, U., Zähner, H., and Fiedler, H.P. (1997) Optimization of fermentation conditions for the production of ethylene-diamine-disuccinic acid by *Amycolatopsis orientalis*. *J Ind Microbiol Biotechnol* **19:** 280–285.

Supporting information

Additional Supporting Information may be found in the online version of this article at the publisher's web-site:

Fig. S1. (A) Zinc-binding site prediction by PREDZINC version 1.4 (Shu *et al.*, 2008) of Zur_{Aj} (GenBank: AIG78644). Predicted zinc-binding residues are highlighted in red. Cys, His, Asp and Glu are bolded. Residues are predicted as zinc binding if the score is ≥0.450. (B) Structure-based multiple sequence alignment of Zur from *M. tuberculosis* (Lucarelli *et al.*, 2007) and *S. coelicolor* (Shin *et al.*, 2011) with its putative orthologue from *A. japonicum*. Sequences were aligned by using CLUSTALW2. Zinc-binding sites: ■ site 1 (structural), ■ site 2, ■ site 3. Protein domains are indicated on the top. Green bar indicates the N-terminal DNA-binding domain, red bar indicates the amino acids involved in forming the inter-domain hinge loop and the blue bar indicates the C-terminal dimerization domain. Amino acid similarity is indicated at the bottom [identical (*), highly similar (:) and similar (.) respectively].
Fig. S2. The construction of the *zur* in frame deletion strain *A. japonicum* Δ*zur* using the plasmid pGusA21Δ*zur* (Table S1) via homologous recombination. First and second homologous recombinations are exemplary illustrated as succession of (first) downstream recombination and (second) upstream recombination but could also occur in opposite succession. *aac(3)-IV*, apramycin resistance gene; *gusA*, β-glucuronidase (GUS) gene. Red: upstream flanking region of *zur* amplified by using the primer pair pΔzur-US-F and pΔzur-US-R (Table S2). Yellow: downstream flanking region of *zur* amplified by using the primer pair pΔzur-DS-F and pΔzur-DS-R (Table S2). Hatched red and yellow bars illustrate the PCR-generated upstream and downstream fragments, which were integrated into pGusA21. pGusA21Δ*zur-zur* is depicted in dashed lines to illustrate that this plasmid is not replicating in *A. japonicum*. The proposed gene products *of ajap_2935 – 60* are a conserved putative-secreted protein, a HTH-type transcriptional repressor, a Fur family transcriptional regulator, a hypothetical protein, a membrane permease and a second membrane permease respectively. The deletions of *aesA-C* and *aesH-E* were performed accordingly.
Fig. S3. HPLC analysis of the zinc-dependent [*S,S*]-EDDS production. Strains were grown in deionized flasks in SM either with or without supplementation of 6 μM $ZnSO_4$. Commercial [*S,S*]-EDDS from Sigma Aldrich was used as a standard.
Fig. S4. Zinc-dependent transcriptional pattern of the putative [*S,S*]-EDDS biosynthesis genes *aesA-D* of *A. japonicum*. Cultures were grown in SM in absence of any trace element (–) or supplemented with (+) 6 μM Zn^{2+} respectively and samples were taken after 25 h of incubation to isolate RNA. *sigB* was used as housekeeping gene to normalize the RNA. Left panel shows transcription pattern in WT background, right panel in the Δ*zur* background.
Fig. S5. HPLC chromatograms of culture supernatants of *A. japonicum* strains grown in deionized flasks in SM in absence of zinc. Commercial [*S,S*]-EDDS from Sigma Aldrich was used as a standard.
Fig. S6. 16S rRNA gene phylogenetic tree for 16 members of the genus *Amycolatopsis* chosen by criteria of available genome sequence data. The tree was constructed using neighbour joining with CLUSTALW and MEGA4 software. The classification into the phylogenetic clades A–F occurred accordingly to Everest and Meyers (2009). The percentage bootstrap values of 1000 replications are shown at each node (only values above 40% are shown). The scale bar indicates 1 nucleotide substitution per 100 nucleotides. *Streptomyces scabies* was used as an out-group.
Fig. S7. HPLC chromatograms of culture supernatants of several *Amycolatopsis* strains grown in deionized flasks in SM either with or without supplementation of 25 μM $ZnSO_4$. Commercial [*S,S*]-EDDS from Sigma Aldrich was used as standard.
Table S1. Bacterial strains and plasmids used in this study.
Table S2. Oligonucleotides used in this study.
Table S3. Manual BLAST analysis of AesA-H. Comparison of *A. japonicum* AesA-H to homologues in other *Amycolatopsis* species.
Table S4. Zur boxes 5′ upstream of *aesA* homologues.

Figure legends

Fig. S1: (A) Zinc binding site prediction by PredZinc version 1.4 (Shu et al., 2008) of Zur_{Aj} (GenBank: AIG78644). Predicted zinc binding residues are highlighted in red. Cys, His, Asp and Glu are bolded. Residues are predicted as zinc binding if the score is ≥ 0.450. (B) Structure-based multiple sequence alignment of Zur from *M. tuberculosis* (Lucarelli et al ., 2007) and *S. coelicolor* (Shin et al., 2011) with its putative ortholog from *A. japonicum*. Sequences were aligned by using ClustalW2. Zinc binding sites: ▪ site 1 (structural) , ▪ site 2, ▪ site 3. Protein domains are indicated on the top. Green bar indicates the N-terminal DNA-binding domain, red bar indicates the amino acids involved in forming the inter-domain hinge loop and the blue bar indicates the C-terminal dimerization domain. Amino acid similarity is indicated at the bottom (identical (*), highly similar (:) and similar (.), respectively).

Fig. S2. Construction of the *zur* in-frame deletion strain *A. japonicum* Δ*zur* using the plasmid pGusA21Δ*zur* (Table S1) via homologous recombination. 1st and 2nd homologous recombinations are exemplary illustrated as succession of first, downstream recombination and second, upstream recombination but could also occur in opposite succession. *aac(3)-IV*, apramycin resistance gene; *gusA*, β-glucuronidase (GUS) gene. Red: upstream flanking region of *zur* amplified by using the primer pair pΔzur-US-F and pΔzur-US-R (Table S2). Yellow: downstream flanking region of *zur* amplified by using the primer pair pΔzur-DS-F and pΔzur-DS-R (Table S2). Hatched red and yellow bars illustrate the by PCR generated upstream and downstream fragments which were integrated into pGusA21. pGusA21Δ*zur-zur* is depicted in dashed lines to illustrate that this plasmid is not replicating in *A. japonicum*. The proposed gene products *of ajap_2935 – 60* are a conserved putative secreted protein, a HTH-type transcriptional repressor, a Fur family transcriptional regulator, a hypothetical protein, a membrane permease and a second membrane permease, respectively. The deletions of *aesA-C* and *aesH-E* were performed accordingly.

Fig. S3. HPLC analysis of the zinc dependent [*S,S*]-EDDS production.. Strains were grown in deionized flasks in SM either with or without supplementation of 6 µM $ZnSO_4$. Commercial [*S,S*]-EDDS from Sigma Aldrich was used as a standard.

Fig. S4. Zinc dependent transcriptional pattern of the putative [*S,S*]-EDDS biosynthesis genes *aesA-D* of *A. japonicum*. Cultures were grown in SM in absence of any trace element (-) or supplemented with (+) 6 µM Zn^{2+} respectively and samples were taken after 25 h of incubation to isolate RNA. *sigB* was used as housekeeping gene to normalize the RNA. Left panel shows transcription pattern in WT background, right panel in the Δ*zur* background.

Fig. S5. HPLC chromatograms of culture supernatants of *A. japonicum* strains grown in deionized flasks in SM in absence of zinc. Commercial [*S,S*]-EDDS from Sigma Aldrich was used as a standard.

Fig. S6. 16S rRNA gene phylogenetic tree for 16 members of the genus *Amycolatopsis* chosen by criteria of available genome sequence data. The tree was constructed using neighbor-joining with CLUSTAL W and MEGA4 software. Classification into the phylogenetic clades A-F occured accordingly to Everest and Meyers 2009. The percentage bootstrap values of 1,000 replications are shown at each node (only values above 40% are shown). The scale bar indicates 1 nucleotide substitution per 100 nucleotides. *S. scabies* was used as an outgroup.

Fig. S7. HPLC chromatograms of culture supernatants of several *Amycolatopsis* strains grown in deionized flasks in SM either with or without supplementation of 25 µM $ZnSO_4$. Commercial [*S,S*]-EDDS from Sigma Aldrich was used as a standard.

A

Query ID	Sequence with predicted ZB residues highlighted in red	List of predicted ZB residues with scores
AIG78644.1	MSPTTANSSAPVPGRRSTKQRAAVVELLKEIDDFRSAQELHDELRKRGDGIGLTTVYR TLQSLSEAGEIDVLRTDTGEAIYRRCSSHHHHHLVCRLCGSTVEVEGPAVERR WAEKIASEHGFSDISHTVEIVGTCSNH	No AA SequenceIndex Zn Score 1 HIS 126 0.972 2 CYS 94 0.896 3 HIS 90 0.877 4 CYS 97 0.871 5 HIS 91 0.861 6 HIS 88 0.860 7 HIS 87 0.755 8 GLU 109 0.747 9 GLU 102 0.728 10 HIS 89 0.723 11 HIS 41 0.654 12 CYS 134 0.587

B

```
M. tuberculosis Zur (FurB)  --------MASAAGVRSTRQRAAISTLLETLDDFRSAQELHDELRRRGEN  42
S. coelicolor Zur           ----VTTAGPPVKG-RATRQRAAVSAALQEVEEFRSAQELHDMLKHKGDA  45
A. japonicum Zur            MSPTTANSSAPVPGRRSTKQRAAVVELLKEIDDFRSAQELHDELRKRGDG  50
                                    ... * *:*:****:    *: :::********* *:::*:

M. tuberculosis Zur (FurB)  IGLTTVYRTLQSMASSGLVDTLHTDTGESVYRRCSE-HHHHHLVCRSCGS  91
S. coelicolor Zur           VGLTTVYRTLQSLADAGEVDVLRTAEGESVYRRCSTGDHHHHLVCRACGK  95
A. japonicum Zur            IGLTTVYRTLQSLSEAGEIDVLRTDTGEAIYRRCSS-HHHHHLVCRLCGS  99
                            :***********:.:* :*.*:*  **::*****  .******** **.

M. tuberculosis Zur (FurB)  TIEVGDHEVEAWAAEVATKHGFSDVSHTIEIFGTCSDCRS----  131
S. coelicolor Zur           AVEVEGPAVEKWAEAIAAEHGYVNVAHTVEIFGTCADCAGASGG  139
A. japonicum Zur            TVEVEGPAVERWAEKIASEHGFSDISHTVEIVGTCSNH------  137
                            ::** .  ** **  :*::**: :::**:**.***::
```

Fig. S1: (A) Zinc binding site prediction by PredZinc version 1.4 (Shu et al., 2008) of Zur_{Aj} (GenBank: AIG78644). Predicted zinc binding residues are highlighted in red. Cys, His, Asp and Glu are bolded. Residues are predicted as zinc binding if the score is ≥ 0.450. (B) Structure-based multiple sequence alignment of Zur from *M. tuberculosis* (Lucarelli et al ., 2007) and *S. coelicolor* (Shin et al., 2011) with its putative ortholog from *A. japonicum*. Sequences were aligned by using ClustalW2. Zinc binding sites: ▪ site 1 (structural) , ▪ site 2, ▪ site 3. Protein domains are indicated on the top. Green bar indicates the N-terminal DNA-binding domain, red bar indicates the amino acids involved in forming the inter-domain hinge loop and the blue bar indicates the C-terminal dimerization domain. Amino acid similarity is indicated at the bottom (identical (*), highly similar (:) and similar (.), respectively).

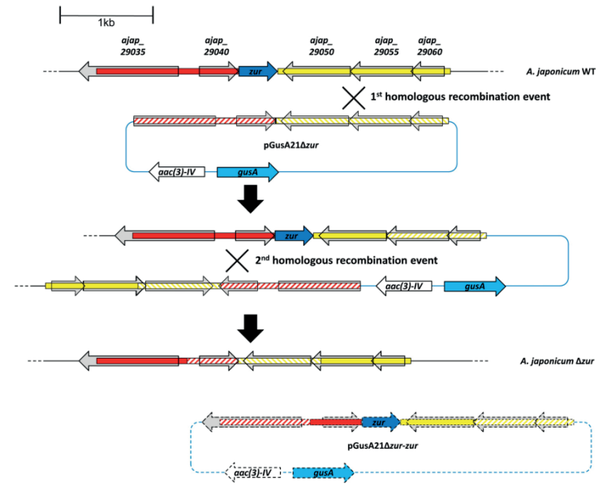

Fig. S2. Construction of the *zur* in-frame deletion strain *A. japonicum* Δ*zur* using the plasmid pGusA21Δ*zur* (Table S1) via homologous recombination. 1st and 2nd homologous recombinations are exemplary illustrated as succession of first, downstream recombination and second, upstream recombination but could also occur in opposite succession. *aac(3)-IV*, apramycin resistance gene; *gusA*, β-glucuronidase (GUS) gene. Red: upstream flanking region of *zur* amplified by using the primer pair pΔzur-US-F and pΔzur-US-R (Table S2). Yellow: downstream flanking region of *zur* amplified by using the primer pair pΔzur-DS-F and pΔzur-DS-R (Table S2). Hatched red and yellow bars illustrate the by PCR generated upstream and downstream fragments which were integrated into pGusA21. pGusA21Δ*zur-zur* is depicted in dashed lines to illustrate that this plasmid is not replicating in *A. japonicum*. The proposed gene products *of ajap_2935 – 60* are a conserved putative secreted protein, a HTH-type transcriptional repressor, a Fur family transcriptional regulator, a hypothetical protein, a membrane permease and a second membrane permease, respectively. The deletions of *aesA-C* and *aesH-E* were performed accordingly.

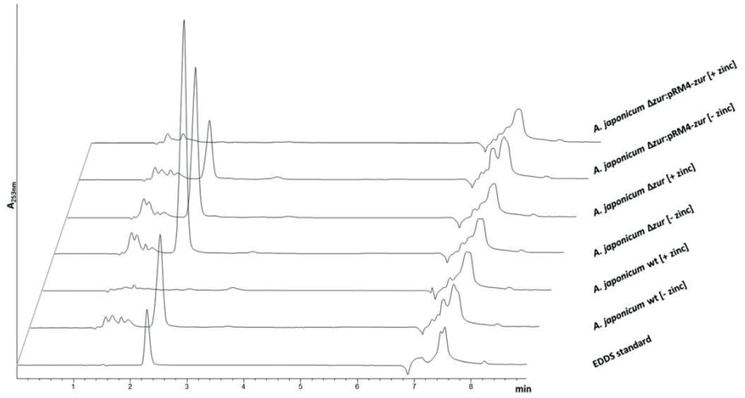

Fig. S3. HPLC analysis of the zinc dependent [*S,S*]-EDDS production. Strains were grown in deionized flasks in SM either with or without supplementation of 6 µM $ZnSO_4$. Commercial [*S,S*]-EDDS from Sigma Aldrich was used as a standard.

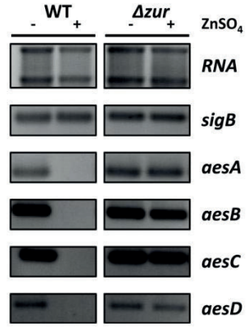

Fig. S4. Zinc dependent transcriptional pattern of the putative [*S,S*]-EDDS biosynthesis genes *aesA-D* of *A. japonicum*. Cultures were grown in SM in absence of any trace element (-) or supplemented with (+) 6 µM Zn^{2+} respectively and samples were taken after 25 h of incubation to isolate RNA. *sigB* was used as housekeeping gene to normalize the RNA. Left panel shows transcription pattern in WT background, right panel in the Δ*zur* background.

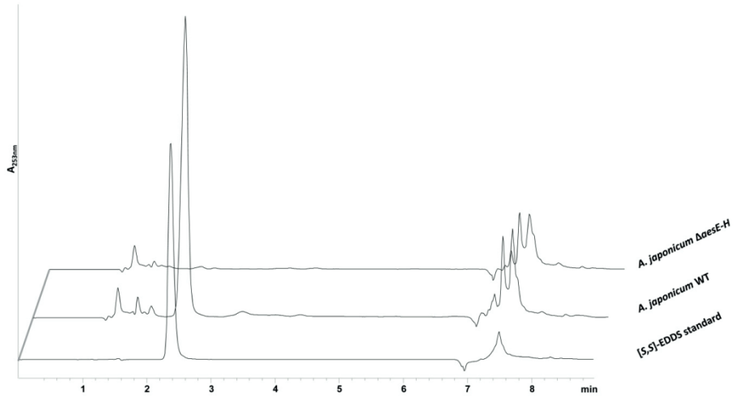

Fig. S5. HPLC chromatograms of culture supernatants of *A. japonicum* strains grown in deionized flasks in SM in absence of zinc. Commercial [*S,S*]-EDDS from Sigma Aldrich was used as a standard.

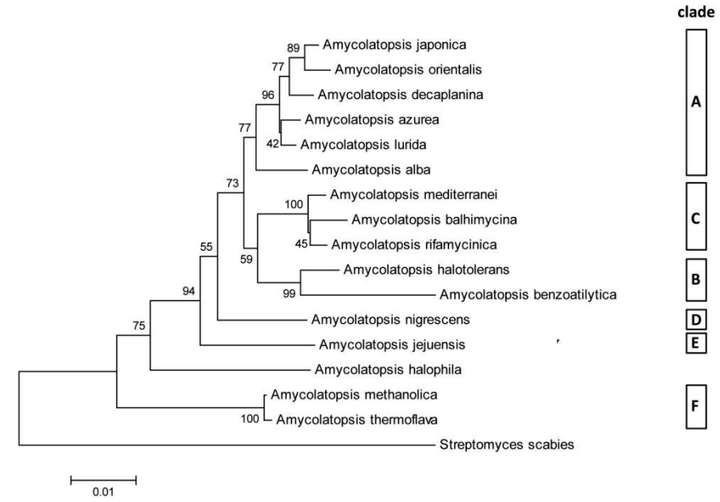

Fig. S6. 16S rRNA gene phylogenetic tree for 16 members of the genus *Amycolatopsis* chosen by criteria of available genome sequence data. The tree was constructed using neighbor-joining with CLUSTAL W and MEGA4 software. Classification into the phylogenetic clades A-F occured accordingly to Everest and Meyers 2009. The percentage bootstrap values of 1,000 replications are shown at each node (only values above 40% are shown). The scale bar indicates 1 nucleotide substitution per 100 nucleotides. *S. scabies* was used as an outgroup.

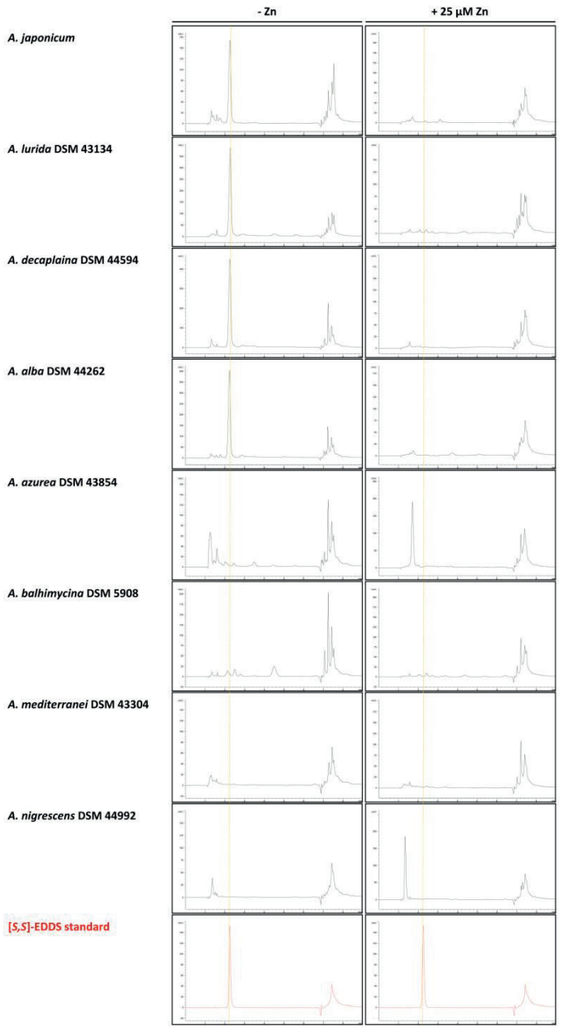

Fig. S7. HPLC chromatograms of culture supernatants of several *Amycolatopsis* strains grown in deionized flasks in SM either with or without supplementation of 25 µM $ZnSO_4$. Commercial [*S,S*]-EDDS from Sigma Aldrich was used as a standard.

Table S1: Bacterial strains and plasmids used in this study

Strain or plasmid	Relevant features[a]	Source or reference
Strains		
A. japonicum MG417-CF17	[*S,S*]-EDDS and Ristomycin A producing wild type	Nishikiori et al. 1984
A. lurida DSM 43134	Ristomycin A producing wild type	Lechevalier et al. 1984
A. decaplaina DSM 44594	Decaplain producing wild type	Wink et al. 2004
A. alba DSM 44262	Albachelin producing wild type	Mertz and Yao 1993
A. azurea DSM 43854	Azureomycin producing wild type	Henssen et al. 1987
A. balhimycina DSM 44591	Balhimycin producing wild type	Nadkarni et al. 1994, Wink et al. 2003
A. mediterranei DSM 43304	Rifamycin SV producing wild type	Margalith and Beretta 1960
A. nigrescens DSM 44992		Groth et al. 2007
Plasmids		
pJET1.2	cloning vector, Amp^R	Fermentas
pSET152	pUC replicon, Am^R, ΦC31-based Actinomycetes integrative vector	Bierman et al., 1992
pRM4	pSET152 derivative with ermEp* and artificial RBS	Menges et al., 2007
pGusA21	gene disruption plasmid. pRM4 with *gusA*, Δ*int*, Δ*attB* and MCS of pUC21	
pGusA21Δ*zur*	inactivation plasmid for zur_{AJ} (*ajap_29045*)	this study
pGusA21Δ*aesA-C*	inactivation plasmid for *aesA-C* (*ajap_08425-35*)	this study
pGusA21Δ*aesE-H*	inactivation plasmid for *aesE-H* (*ajap_08425-35*)	this study
pGus	Promoter probe vector	Myronovskyi et al., 2011
pGus*PaesA*	pGus with *aesA* promoter cloned into XbaI/SpeI site of pGus	
pTWPI1-edds	cosmid carying 31 kb insert of the *A. japonicum* genome (bp 1665131 – 1696415), including the [*S,S*]-EDDS synthesis genes	
pSET152-*aesA-D*	pSET152 carying 6545 bp insert of the *A. japonicum* genome (bp 1687557 – 1694101), including the operon *aesA-D* under the control of the native promoter	this study
pRM4-*zur*	pRM4 with zur_{AJ} gene under control of ermEp*	this study
pET-30 Ek/LIC	Expression of target proteins fused with the His-Tag and S-Tag that are cleavable with enterokinase protease	Novagen
pET-30-*zur*	pET-30 Ek/LIC with *zur* gene fused with the His-Tag and S-Tag coding sequences	this study

[a] Amp^R ampicilin resistance, Am^R apramycin resistance

Table S2: Oligonucleotides used in this study

Primer	Sequence (5'- 3')	restriction sites, features
Primers used for amplification of the A. japonicum zur (ajap_29045) flanking regions		
pΔzur-US-F	AATAAGCTTGTTTCGCGACGAAGTTCTTCGG	HindIII
pΔzur-US-R	AATCATATGGCTCACTTCCCCTCCTGAAC	NdeI
pΔzur-DS-F	AATCATATGGTCGGGACCTGCTCGAACCAC	NdeI
pΔzur-DS-R	TAATCTAGAACGGTCACCTGGCATCATC	XbaI
Primers used for amplification of the A. japonicum aesA-C (ajap_08425-35) flanking regions		
pΔaesA-US-F	AATAAGCTTCGGCATAATCACCCATTTCG	HindIII
pΔaesA-US-R	AATCATATGGAACGATCGACCTTTCTC	NdeI
pΔaesC-DS-F	AATCATATGGCACGGCGGTGACGACCCGCGGCTAC	NdeI
pΔaesC-DS-R	GCGTCTAGAGCGCTCACCTTGATCATG	XbaI
Primers used for amplification of the A. japonicum aesE-H (ajap_08420-05) flanking regions		
pΔaesH-US-F	TTAAAGCTTGCGGTGATGAGGAAATGGTC	HindIII
pΔaesH-US-R	TTTCATATGGACGGGCTTGCCTTTCTGTCATAC	NdeI
pΔaesE-US-F	TTTCATATGTTCTTCCGCTCGCGCGCGGCTTTC	NdeI
pΔaesE-US-R	AATTCTAGACCGCCTTGTTCGCCTTCTTC	XbaI
Primers used for amplification of the A. japonicum zur (ajap_29045) coding region		
pzur-F	TTACATATGAGTCCGACGACGGCCAAC	NdeI
pzur-R	ATTAAGCTTTCAGTGGTTCGAGCAGGTC	HindIII
Primers used for zur (ajap_29045) purification		
HIS-pzur-F	GACGACGACAAGATAAGTCCGACGACGGCCAAC	complementary overhang
HIS-pzur-R	GAGGAGAAGCCCGGTTCAGTGGTTCGAGCAGGTC	complementary overhang
Primers used for amplification of the A. japonicum aesA (ajap_08425) promoter region PaesA		
PaesA-F	AATTCTAGATTCTTCCGCTCGCGCGCGGC	XbaI
PaesA-R	TTTACTAGTGAACGATCGACCTTTCTC	SpeI
RT primers used for amplification of A. japonicum gene fragments		
sigB-RT-F	CCTCAACGGAATCGGCAAGACG	
sigB-RT-R	ATCAGGTCGAGCAGTGGCATCC	
znuB-RT-F	TGCGCGGTATGGCGTTCATC	
znuB-RT-R	GCATGCCGACGAACAACAGC	
mntA-RT-F	CGAATCTGCGCAAGACCGTGTG	
mntA-RT-R	GCGGCCTTCTTGATGTCGTCAG	
aesA-RT-F	TCTGCACAGCCTCGAACTCAC	
aesA-RT-R	TTGGCGGTAGCTCGTCTTGAAC	
aesB-RT-F	TGGTCCATCCGGCCACTTTC	
aesB-RT-R	AAAGGAGGCCGTCGGGTTTG	
aesC-RT-F	CATCCCGATCAGCACAACCATCC	
aesC-RT-R	AAGATGATCGAGCCGACAGGTTC	
aesD-RT-F	TCGCCGGTCCGATGATGTTC	
aesD-RT-R	AGATGAAGGCGGCGTTGAG	
Primers used for amplification of A. japonicum upstream regions		
iznuCB-EMSA-F	AGCCAGTGGCGATAAGTCGCGGGAGCCGTAATGGG	used for Cy5 PCR labelling
iznuCB-EMSA-R	AACGACACCTCGAAGGGGATCAG	
upaesA-EMSA-F	AGCCAGTGGCGATAAGCGGCGACGTGGATGTTGTCCTTGACC	used for Cy5 PCR labelling
upaesA-EMSA-R	GCGCGTGAGTACGTGCAGCGAG	

Table S3: Manual BLAST analysis of AesA-H. Comparison of *A. japonicum* AesA-H to homologs in other *Amycolatopsis* species.

***Amycolatopsis japonicum* MG417-CF17**	**AesH (AJAP_08405)**	**AesG (AJAP_08410)**	**AesF (AJAP_08415)**	**AesE (AJAP_08420)**	**AesA (AJAP_08425)**	**AesB (AJAP_08430)**	**AesC (AJAP_08435)**	**AesD (AJAP_08440)**
GenBank-ID	AIG74584	AIG74585	AIG74586	AIG74587	AIG74588	AIG74589	AIG74590	AIG74591
Amycolatopsis sp. MJM2582	KFZ80361	KFZ80362	KFZ80363	KFZ80364	KFZ80365	KFZ80366	KFZ80367	KFZ80368
	96%	97%	99%	97%	99%	98%	99%	98%
Amycolatopsis orientalis HCCB10007	AGM08784	AGM08783	AGM08782	AGM08781	AGM08780	AGM08779	AGM08778	AGM08777
	95%	93%	98%	95%	99%	97%	98%	97%
Amycolatopsis lurida DSM 43134	AJK59034	AJK59035	AJK59036	AJK59037	AJK59038	AJK59039	AJK59040	AJK59041
	92%	86%	95%	85%	97%	93%	93%	94%
Amycolatopsis decaplanina DSM 44594	x	EME58574	EME58573	EME58572	EME58571	EME58570	EME58569	EME58568
	x	92%	98%	85%	96%	94%	95%	95%
Amycolatopsis alba DSM 44262	x	WP_020630846	WP_020630847	WP_020630846	WP_020630845	WP_020630844	WP_020630843	WP_020630842
	x	82%	93%	78%	95%	92%	95%	93%
Amycolatopsis azurea DSM 43854	x	EMD25756	EMD25755	EMD25754	EMD28638	EMD28637	EMD28640	x
	x	85%	92%	80%	39%	40%	49%	x
Next best HIT	*Lechevalieria aeracolonigenes*	*Streptosporangium roseum*	*Actinomadura madurae*	*Dasania marina*	*Kibdelosporangium sp. MJ126-NF4*	*Kibdelosporangium sp. MJ126-NF4*	*Kibdelosporangium sp. MJ126-NF4*	*Kibdelosporangium sp. MJ126-NF4*
GenBank-ID	WP_045310026	WP_031162391	WP_021596002	WP_035802097	WP_042178415	WP_042178413	WP_042178411	WP_042178409
	76%	52%	70%	48%	88%	78%	83%	82
% amino acid identity								

Table S4: Zur-boxes 5‘ upstream of *aesA* homologues

***Amycolatopsis japonicum* MG417-CF17**	**AGACAAT-C-ATTTTCA**
Amycolatopsis sp. MJM2582	AGACAAT-C-ATTTTCA
Amycolatopsis orientalis HCCB10007	AGACAAT-C-ATTTTCA
Amycolatopsis lurida DSM 43134	AGACAAT-C-ATTTTCA
Amycolatopsis decaplanina DSM 44594	AGACAAT-C-ATTTTCA
Amycolatopsis alba DSM 44262	GGACAAT-C-ATTTTCA
Amycolatopsis azurea DSM 43854	x